ATLAS and CMS latest results on ttH and tH

Thomas Strebler

Centre de Physique
des Particules de Marseille
Aix-Marseille Univ. / CNRS-IN2P3

on behalf of the ATLAS and CMS collaborations

SM@LHC2021
April 27th, 2021

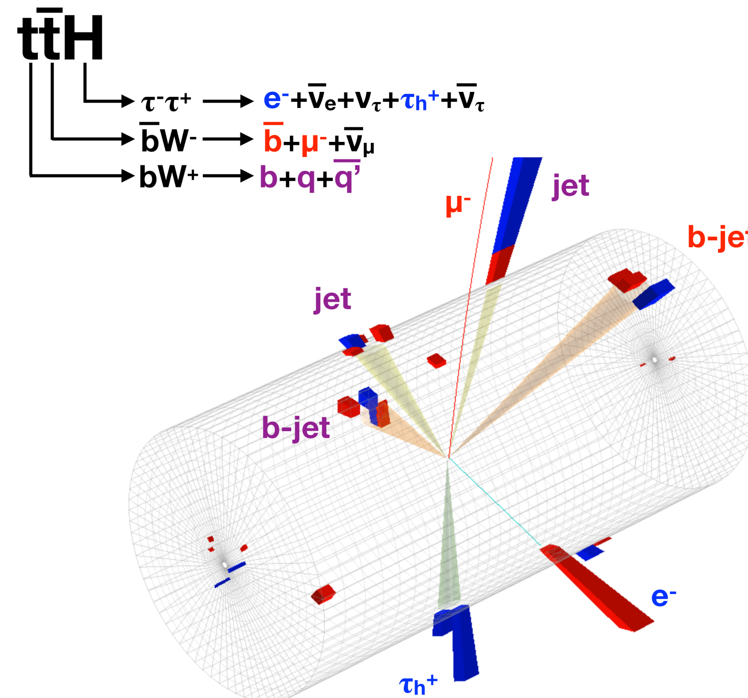

Introduction

- **Higgs boson observation with LHC Run 1 data:** unambiguous evidence for **Higgs boson coupling to gauge bosons**

- Run 2 dataset offered possibility to probe in more details **Higgs couplings to 3rd-generation fermions**

- In particular, **first observation by ATLAS and CMS of Higgs+top associated production** in Spring 2018 with partial Run 2 datasets

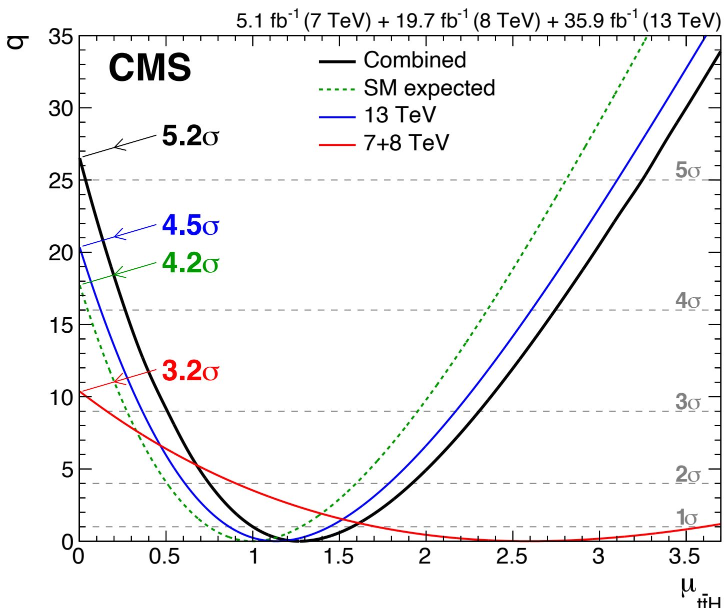

Phys. Rev. Lett. 120 (2018) 231801
arXiv:1804.02610 **[hep-ex]**

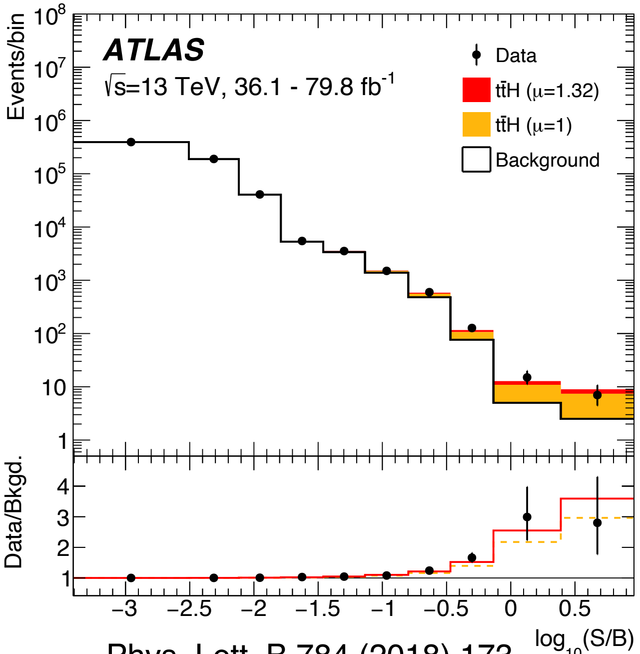

Phys. Lett. B 784 (2018) 173
arXiv:1806.00425 **[hep-ex]**

Motivation

- In SM, top-Higgs coupling (Y_t) **very large wrt other fermions:** good opportunity to study Higgs Yukawa couplings to fermions

- Access to Y_t with **ggF + H→$\gamma\gamma$ decay**

- **Model-dependent constraints on Y_t,** assuming no BSM particles in the loop

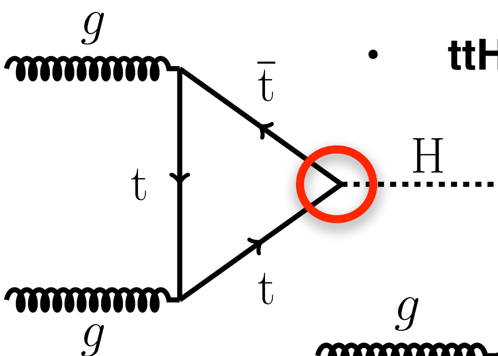

- **ttH and tH => direct probes to study Y_t**

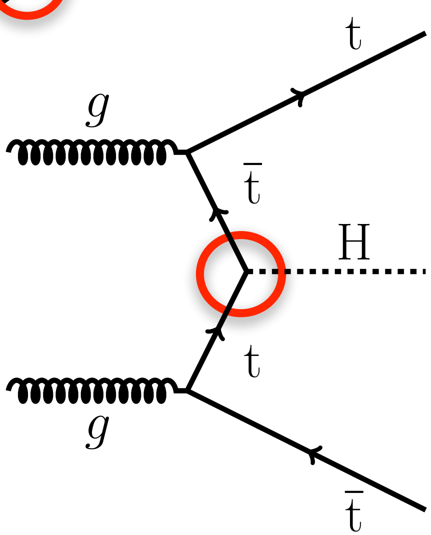

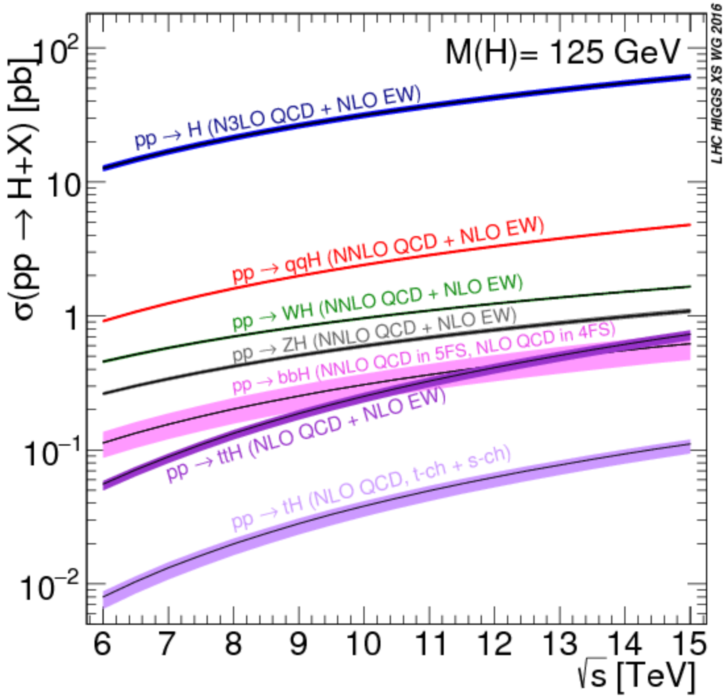

- **Target as many decay modes as possible** for top + Higgs to optimally exploit small cross-section (0.5 fb, ~1% ggF)

- **Single top + Higgs cross-section even one order of magnitude lower than ttH:** very challenging SM process to observe…

Motivation

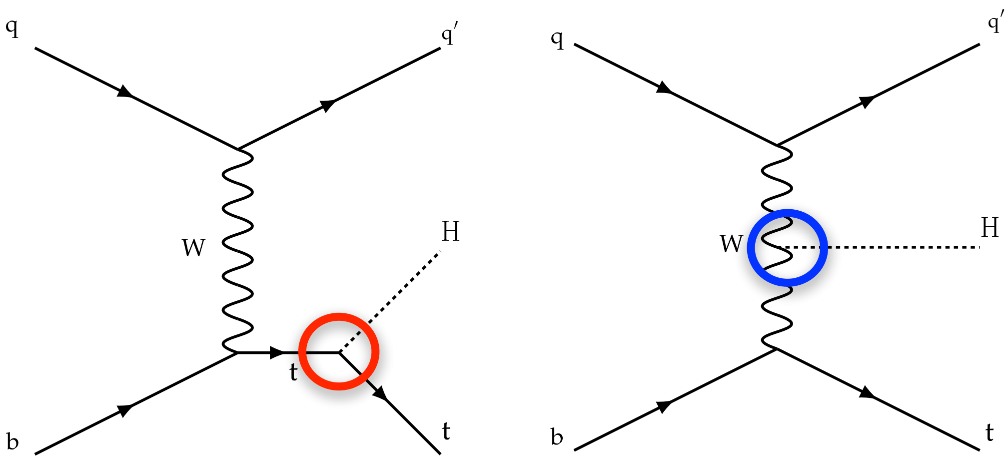

- **Single-top + Higgs production** involves **interfering diagrams** with **top-Higgs and W-Higgs couplings**
- **In SM destructive interference** but if Y_t=-Y_t(SM) **tH cross-section can be enhanced** by one order of magnitude

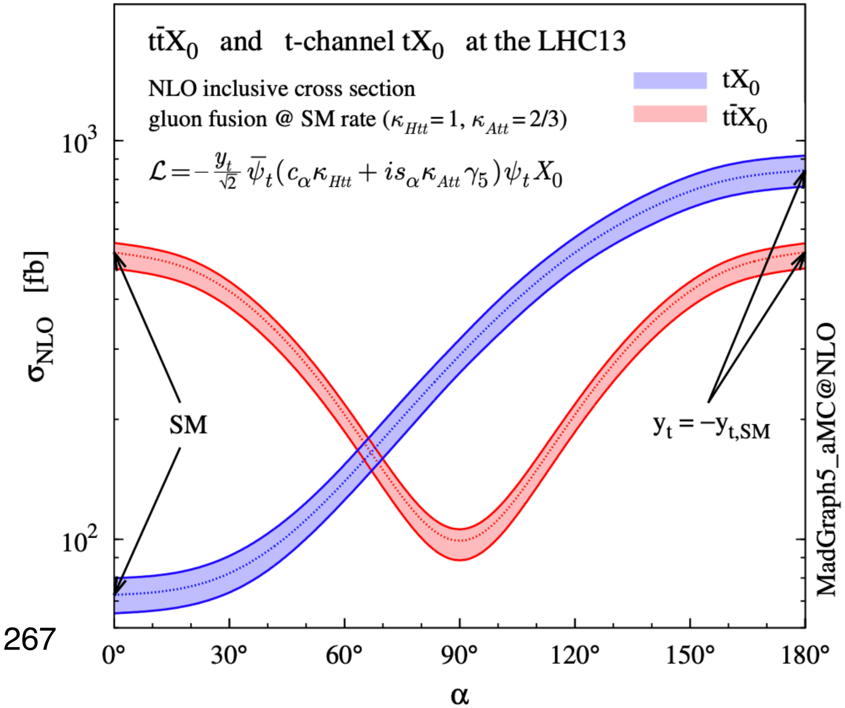

- In general, not only $|Y_t|$ can be probed with ttH process but also the **CP-structure of the top-Higgs coupling** (CP-mixing angle **α**)

  => impacts cross-section and kinematics of top + Higgs

- **Combined analysis of ttH + tH processes** can be used to **lift degeneracy between α and 180°-α** hypotheses

Eur. Phys. J. C 75 (2015) 6, 267
arXiv:1504.00611 **[hep-ex]**

Searches for ttH@LHC

- **ttH H→bb**: ATLAS 139 fb^{-1} / CMS 77.4 fb^{-1} — Full Run 2 dataset / Partial Run 2 dataset
  ATLAS-CONF-2020-058 / CMS-PAS-HIG-18-030
  Largest branching ratio
  Low purity + combinatorics + large theoretical uncertainties on irreducible tt+bb background

- **ttH H→WW / ZZ / $\tau\tau$**: ATLAS 80 fb^{-1} / CMS 137 fb^{-1}
  ATLAS-CONF-2019-045 / CMS-HIG-19-008 (accepted by EPJC)
  Clean final state with leptons + moderate irreducible backgrounds
  Challenging modelling of ttW and reducible backgrounds w/ non-prompt leptons + jets faking τ_h

- **ttH H→$\gamma\gamma$**: ATLAS 139 fb^{-1} / CMS 137 fb^{-1}
  ATLAS-HIGG-2019-01 Phys. Rev. Lett. 125 (2020) 061802 / ATLAS-CONF-2020-026
  CMS-HIG-19-013 Phys. Rev. Lett. 125 (2020) 061801 / CMS-HIG-19-015 (submitted to JHEP)
  Clean signature + possible to reconstruct all Higgs decay products + S/B~1
  Low branching ratio

- **ttH H→ZZ→4l**: ATLAS 139 fb^{-1} / CMS 137 fb^{-1}
  ATLAS-HIGG-2018-28 Eur. Phys. J. C 80 (2020) 957 / CMS-HIG-19-001 (submitted to EPJC)
  Very clean signature + possible to reconstruct all Higgs decay products + very high purity
  Very low branching ratio, only a handful of events expected
  => in back-up slides

ttH H→bb

CMS-PAS-HIG-18-030

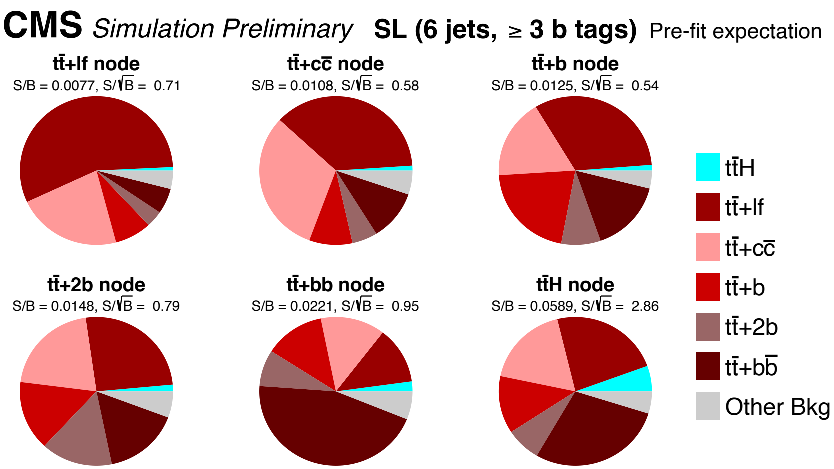

- **Categories based on number of jets + b-jets** used to constrain various background components
- **Single-lepton channel:** ANN used as multi-classifier to define background-enriched nodes + for signal extraction
- **Dilepton channel:** BDT ttH vs ttbar for signal extraction

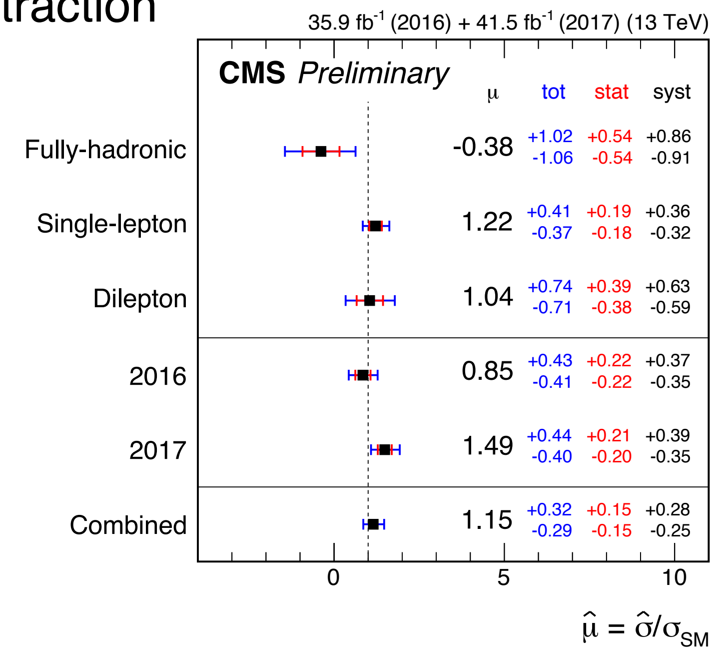

- **Fully hadronic channel:**
  - data-driven multijet background estimate
  - MEM ttH vs ttbb for signal extraction
- **Largest impact uncertainties:**
  - cross-sections of signal + tt+hf (50% prior)
  - b-tagging
  - data-driven multijet background
- **Sensitivity:** 3.9σ observed (3.5σ expected)

ttH H→bb

ATLAS-CONF-2020-058

- **Similar analysis strategy:** includes SL resolved, boosted and DL channels + STXS $p_T(H)$ measurement, BDTs used for reco jet assignment + signal extraction
- **tt+bb background** modelled with **4FS NLO** simulation with **extra b-jets from ME**
- **Dedicated samples used to assess dominant shape systematic uncertainties:**
  - ISR + FSR
  - PS + hadronization
  - NLO matching (uncorrelated between pT bins)
  - Relative fractions of tt+hf components

- **Free-floating tt+bb normalisation:**
  k(tt+bb)=1.26 ± 0.09
  tt+cc 100% normalisation priori uncertainty
- **pT(H) mismodelling** covered with **ad-hoc uncertainty** derived from inclusive signal region

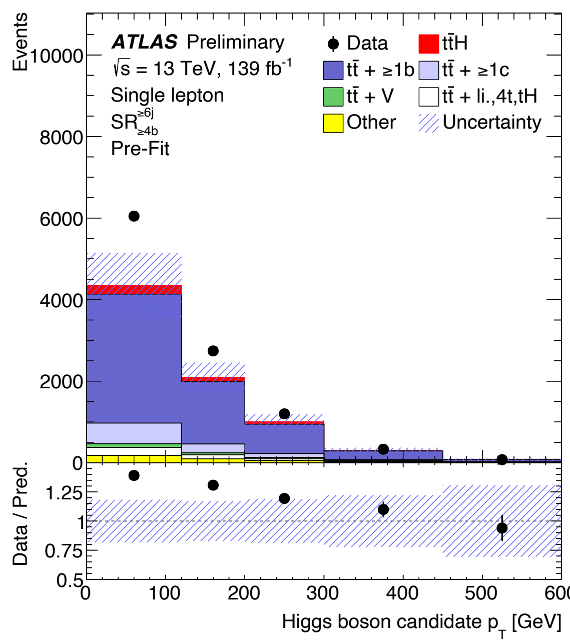

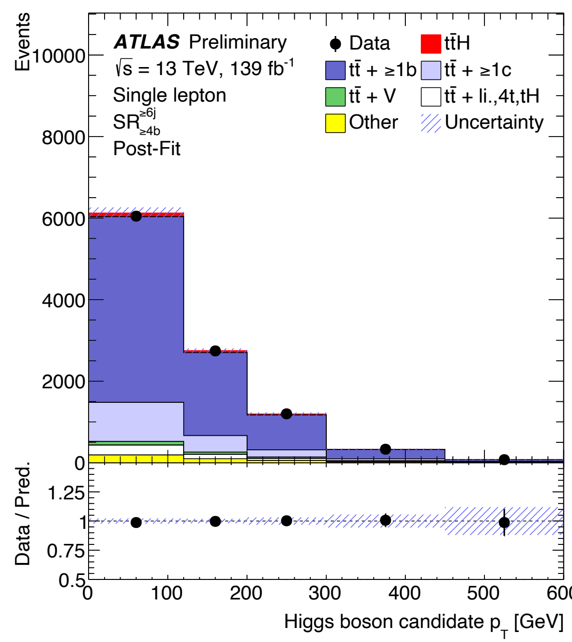

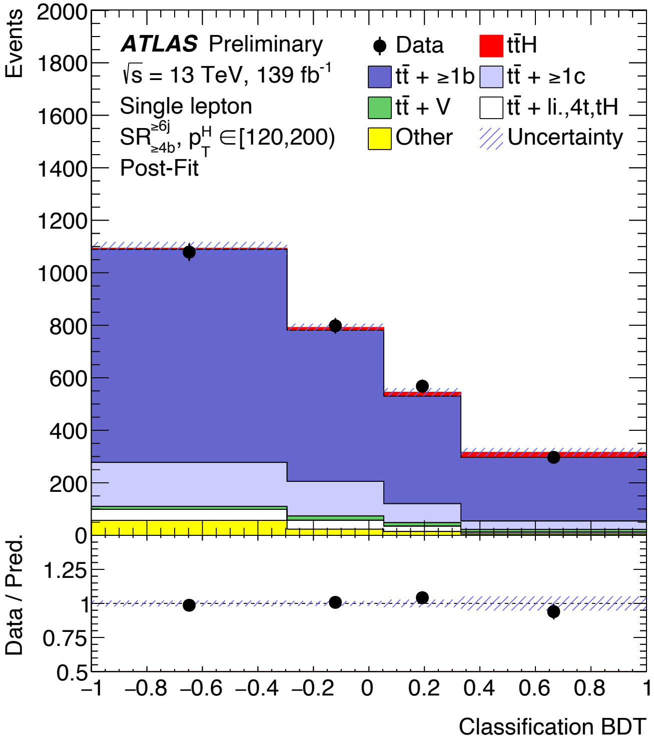

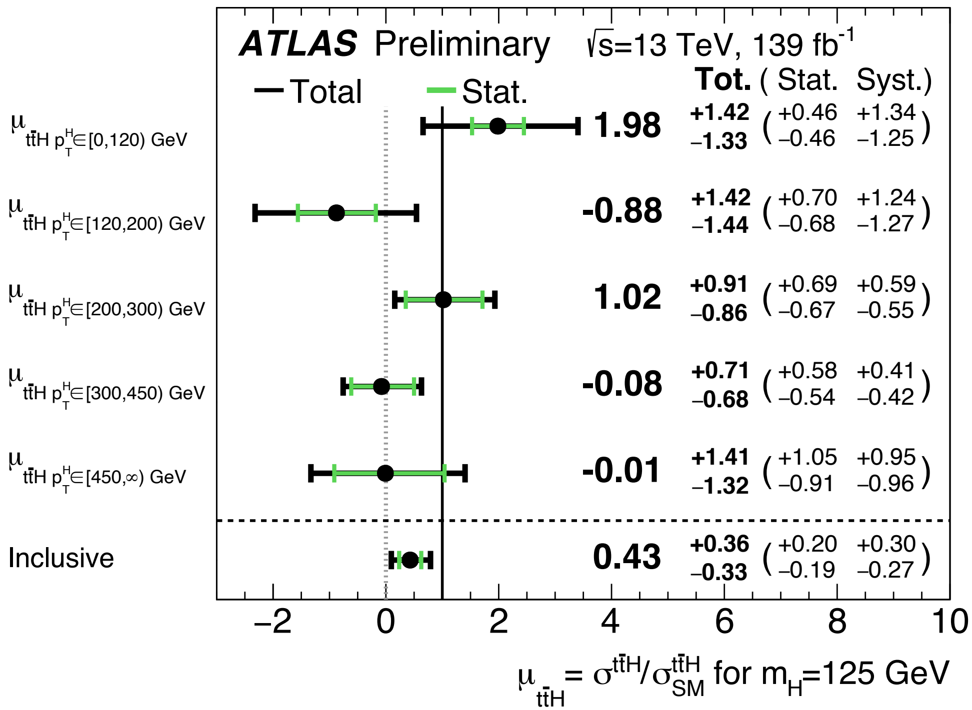

- Good post-fit agreement observed, with **uncertainty dominated by tt+hf modelling systematics**
- **Individual STXS signal strengths compatible with SM or μ=0 within 2σ,** sensitivity beyond pT=300 GeV thanks to boosted categories
- **Sensitivity:** 1.3σ observed (3.0σ expected)

- **Targets final-state with several leptons + τ_h:** 8 channels for ATLAS, 10 for CMS

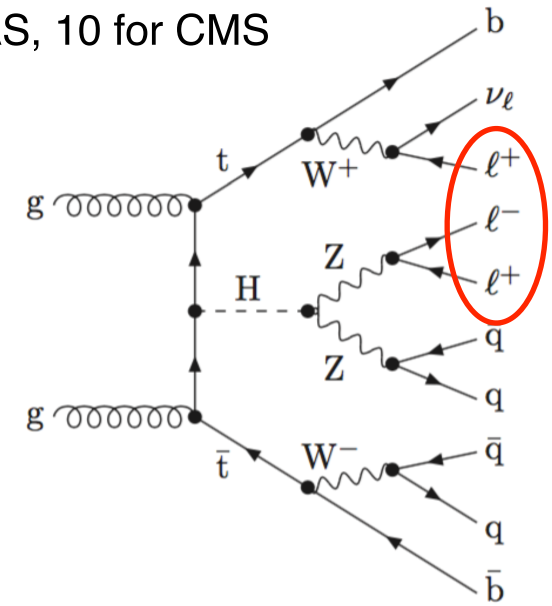

- **Main sources of background:**
  - **irreducible:** ttV, di-boson
  - **reducible:** non-prompt leptons, fake τ_h, charge mis-ID, conversions (ttbar + ttγ)

- **MVA selections used to separate prompt leptons** (from W/Z/τ decays) **from non-prompt leptons** (b decays, light hadrons)

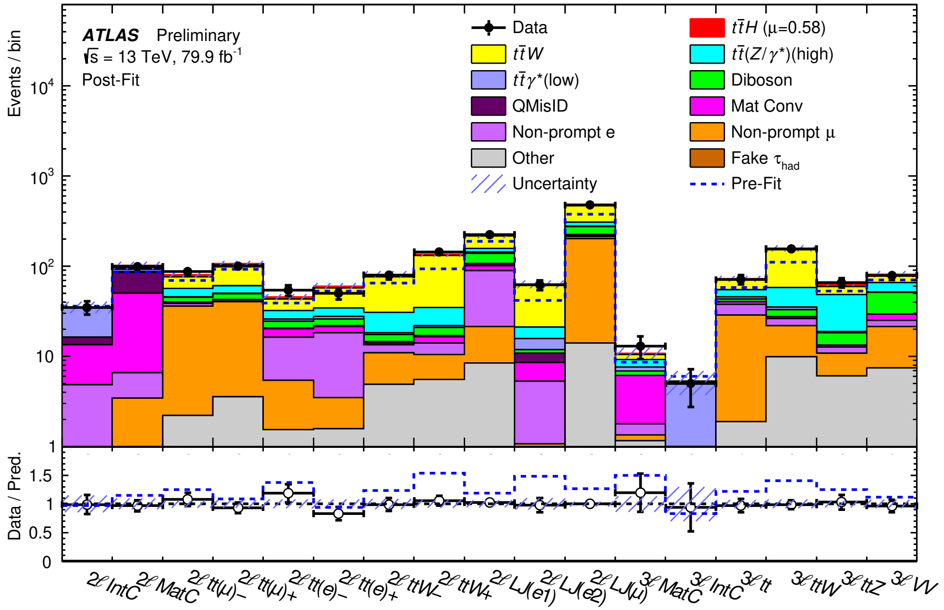

- **Subcategories based on lepton charge + flavour + b-jet multiplicity**

- **ATLAS analysis** relies on **simulation for background shape + control regions for normalisation**

- **BDTs used for signal extraction:** multi-dimensional binning w/ binary classifiers or multi-classifiers

ttH H→WW/ZZ/ττ

ATLAS-CONF-2019-045

- **Challenging modelling of ttW background:**
  - several uncorrelated free-floating normalisations factors
  - theoretical uncertainties
  - ad hoc extrapolation uncertainties for charge asymmetry + b-jet multiplicity

- **Observed excess in ttW** taking into account state-of-the-art QCD and EW corrections (σ(ttW)=727 fb), **confirmed w/ several cross-checks**

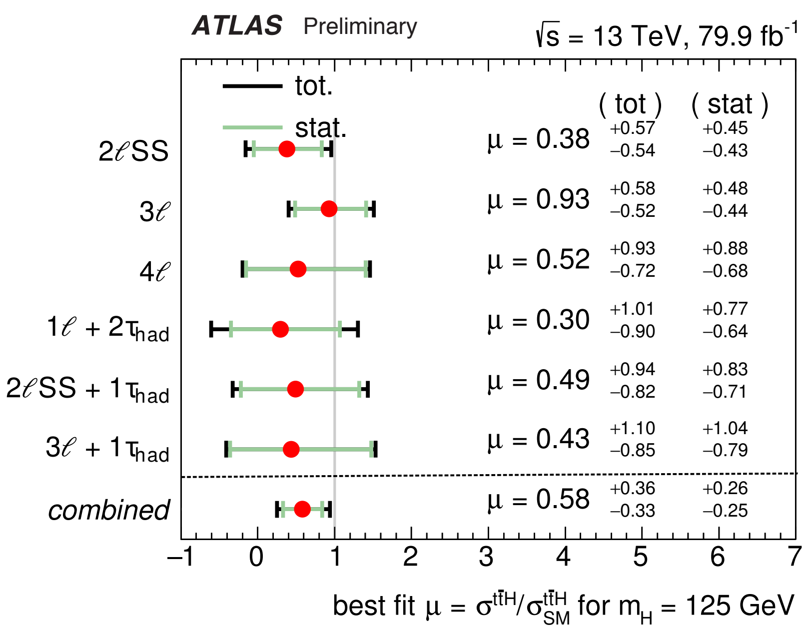

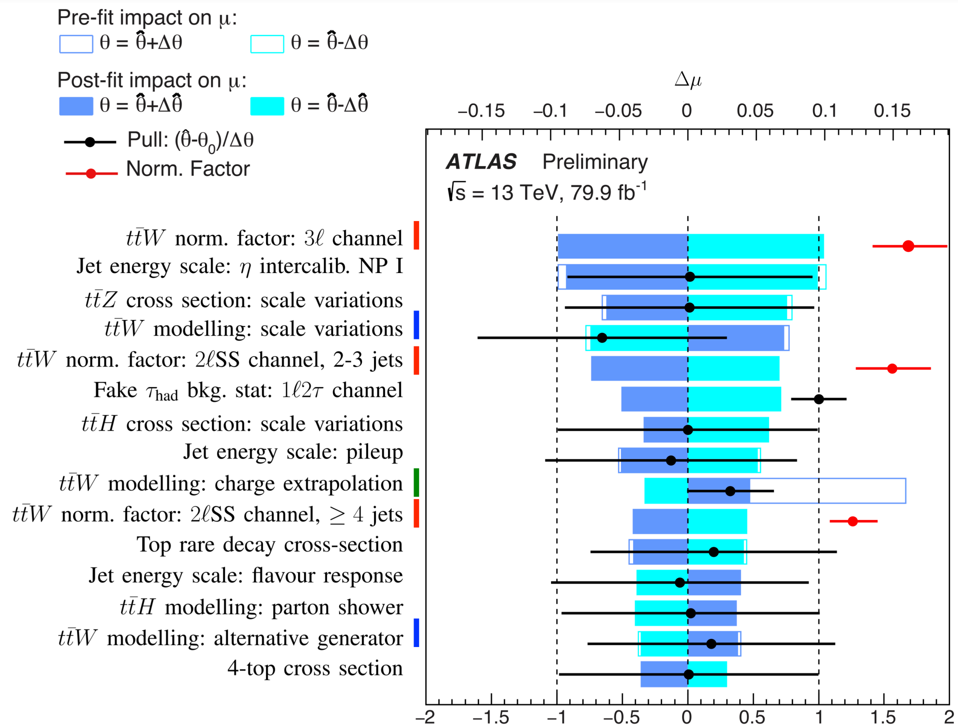

- **Systematic uncertainties getting larger than stat. uncertainty:** dominated by ttW modelling + jet energy scale

- **Sensitivity:** 1.8σ observed (3.1σ expected)

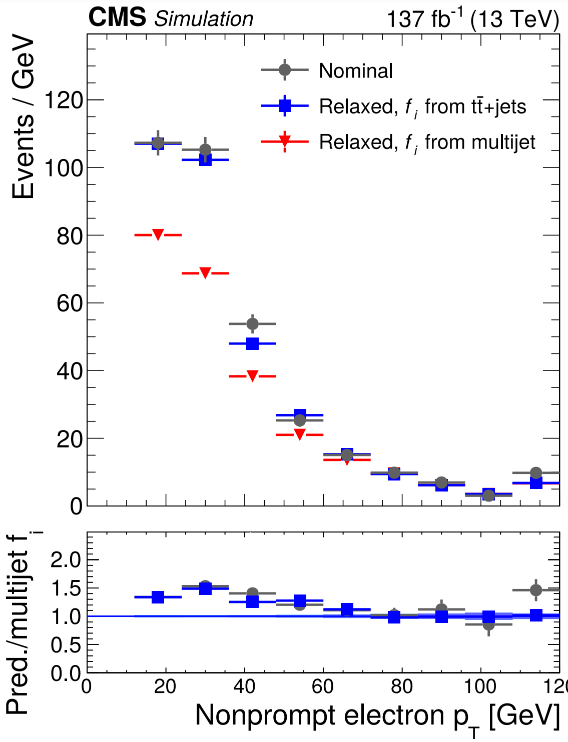

- **Misidentified lepton background data-driven estimation** with misID probability method: fake rate measured in data, w/ extrapolation correction + uncertainty

- **Irreducible backgrounds constrained with dedicated control regions:** ttZ + diboson from events with on-shell Z, ttW from ANN multi classifier node

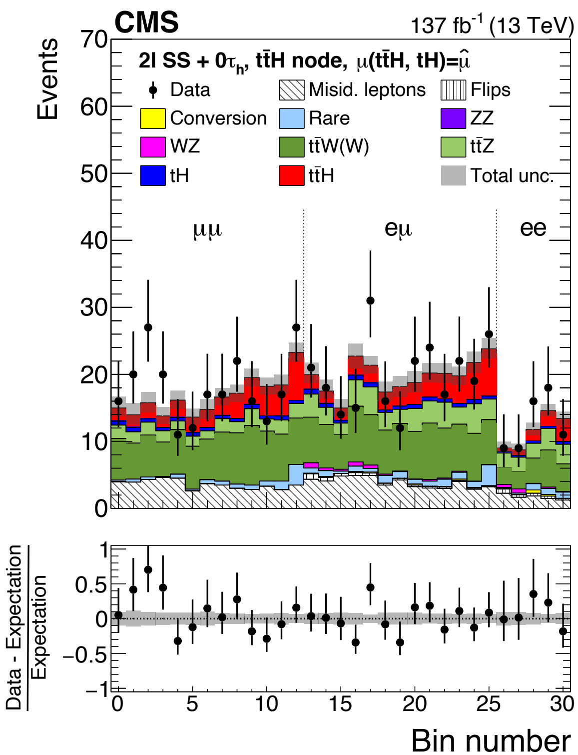

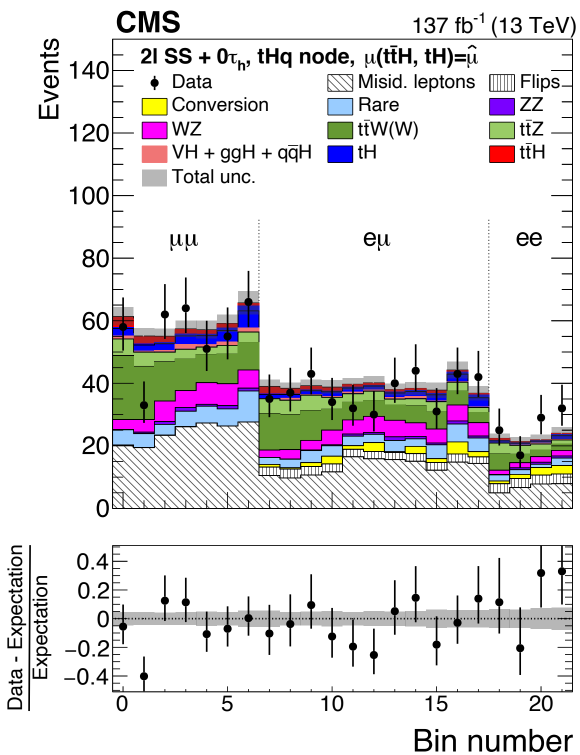

- **ANN multiclassifier used for signal extraction**

- **Separate ttH and tH nodes** in 2lSS, 2lSS+1τ_h, 3l categories: exploiting forward jet kinematic

ttH H→WW/ZZ/ττ

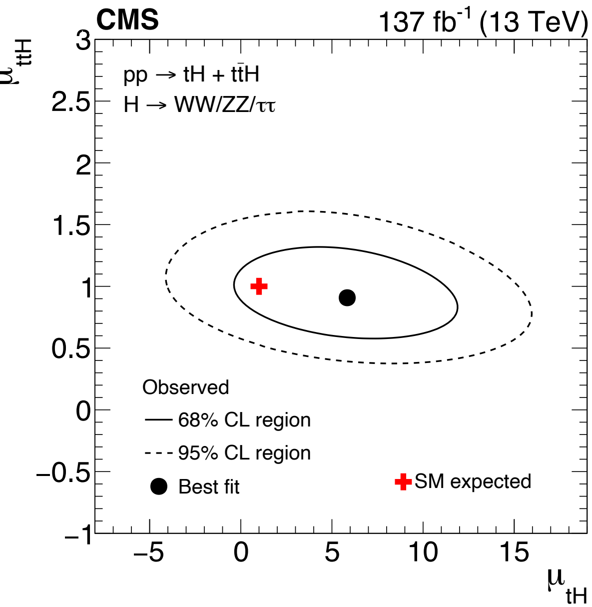

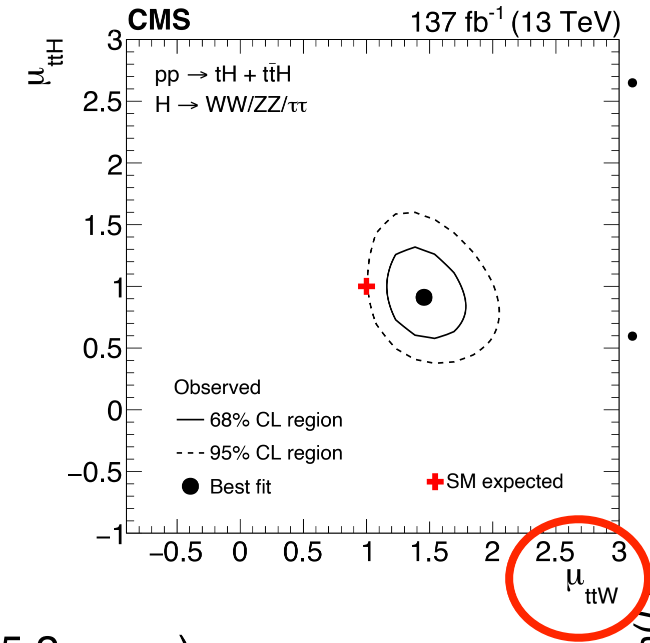

- Signal extraction with **uncorrelated signal strengths for ttH, tH, ttW and ttZ**
- **Similar ttW excess as in ATLAS analysis** (σ(ttW)=650 fb)
  μ(ttW) = 1.43 ± 0.21

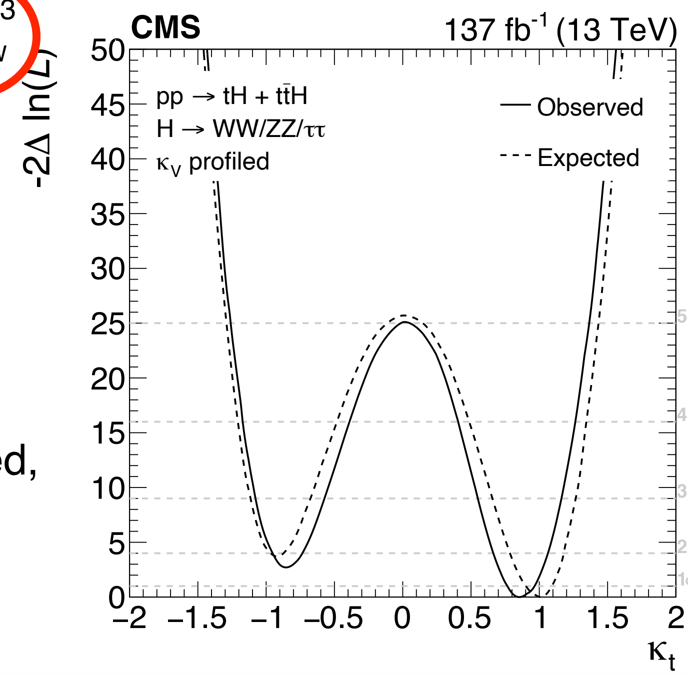

- **Sensitivity:** ttH 4.7σ obs. (5.2σ exp.)
  tH 1.4σ obs. (0.3σ exp.)
- **Signal strengths:** μ(ttH) = 0.92 ± 0.19 (stat.) $^{+0.17}_{-0.13}$ (syst.)
  μ(tH) = 5.7 ± 2.7 (stat.) ± 3.0 (syst.)
- **Constraint on Higgs-top coupling modifier κ_t** derived, taking into account impact on tH kinematics + ttH/tH rates:
  $-0.9 < \kappa_t < -0.7$ or $0.7 < \kappa_t < 1.1$ at 95% CL

ttH H→γγ

ATLAS-CONF-2020-026 + **CMS-HIG-19-015**

- **ttH + tH H->γγ studied as part of inclusive STXS measurements:** STXS bin assignment handled w/ 44-class multi-classifier BDT (ATLAS) or ttH vs tH DNN (CMS)
- **Categories** with increasing purity defined with **signal vs background BDT**
- **Fit of m($\gamma\gamma$) used for signal extraction**
- **Stat. limited measurements in each ttH bin** in agreement with SM
- **Upper limit on tH:**
  8 x SM ATLAS
  14 x SM CMS (8 exp.)

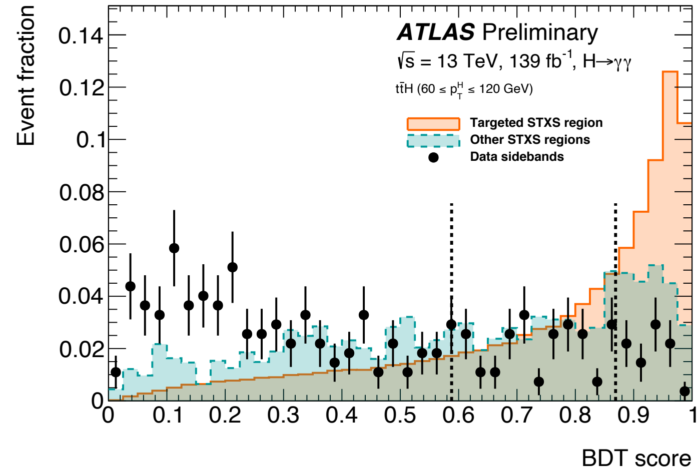

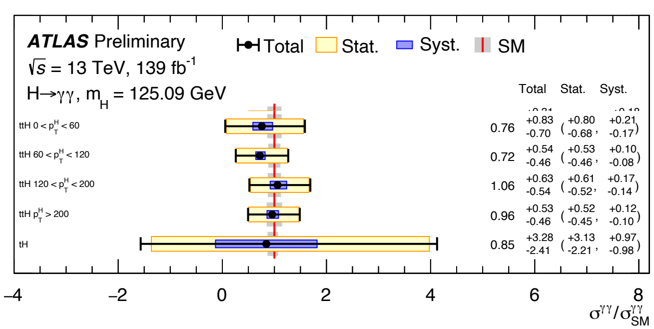

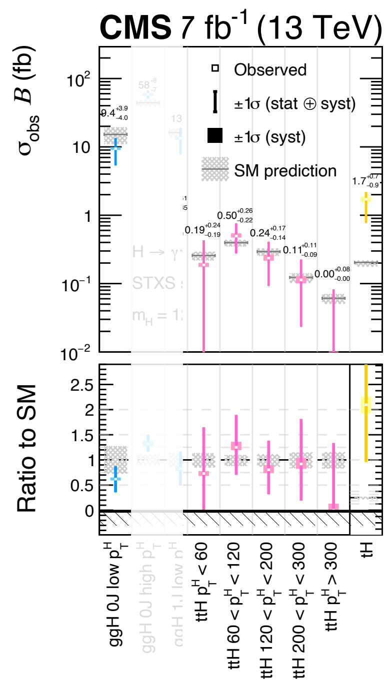

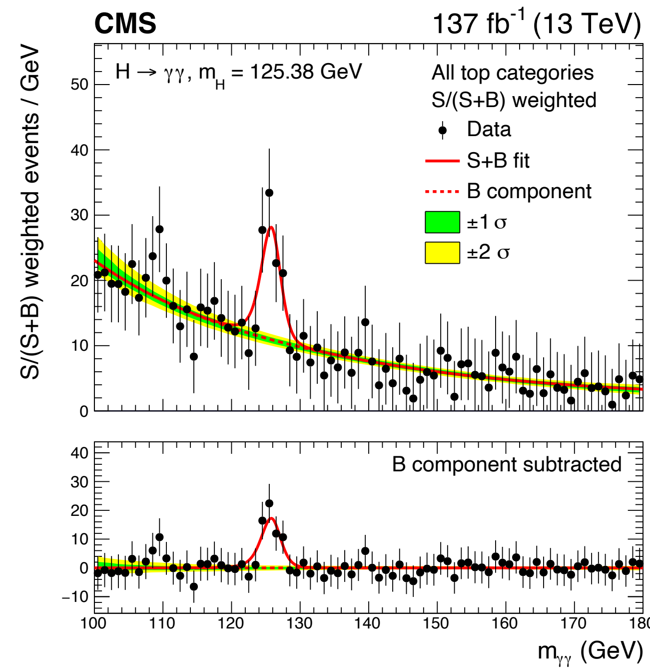

ttH H→γγ

ATLAS-HIGG-2019-01 + CMS-HIG-19-013

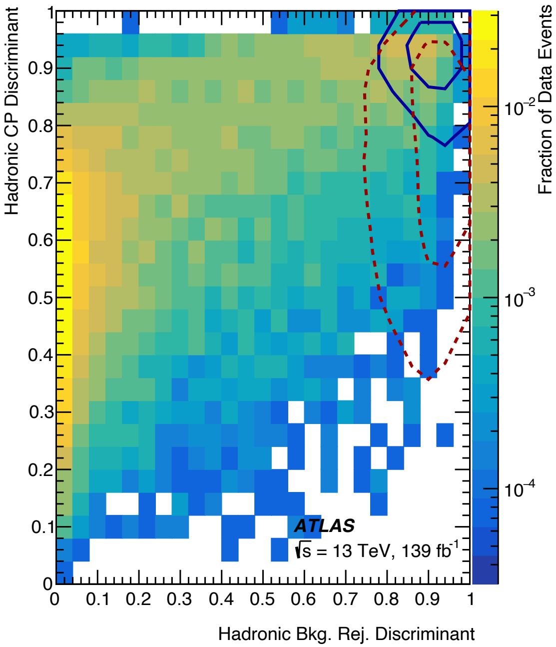

- **Dedicated ttH H->γγ analyses developed to constrain CP structure of top-Higgs coupling**

$$\mathcal{L} = -\frac{m_t}{v}\{\bar{\psi}_t\kappa_t\,[\cos(\alpha) + i\sin(\alpha)\gamma_5]\,\psi_t\}\,H \qquad f_{CP}^{Htt} = \frac{|\tilde{\kappa}_t|^2}{|\kappa_t|^2 + |\tilde{\kappa}_t|^2}\,\mathrm{sign}(\tilde{\kappa}_t/\kappa_t)$$

- **2D categories built based on signal vs background BDT** as in STXS **+ CP-even vs CP-odd signal, fit of m($\gamma\gamma$)**

- **ttH sensitivity under CP-even SM hypothesis:**
  - 5.2σ obs. (4.4σ exp.) ATLAS
  - 6.6σ obs. (4.7σ exp.) CMS

- **CP constraints**

  ATLAS:

  Pure CP-odd exclusion 3.9σ

  α=180° exclusion 2.5σ

  |α|<43° at 95% CL

  CMS:

  Pure CP-odd exclusion 3.2σ

  |α|<55° at 95% CL

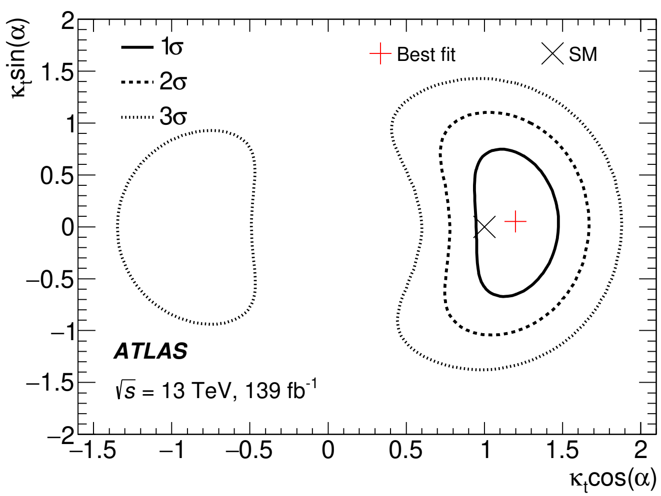

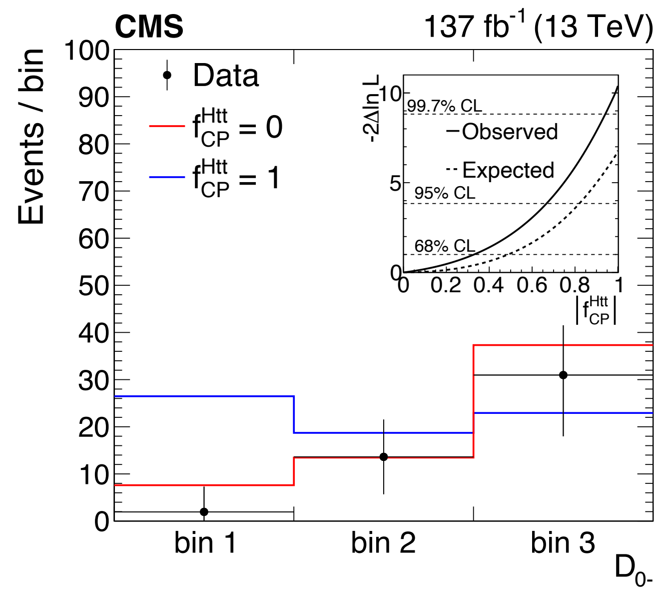

Conclusion

- Despite **very low cross-section and complex final state, observation of ttH process during Run 2** opened the door for more detailed studies

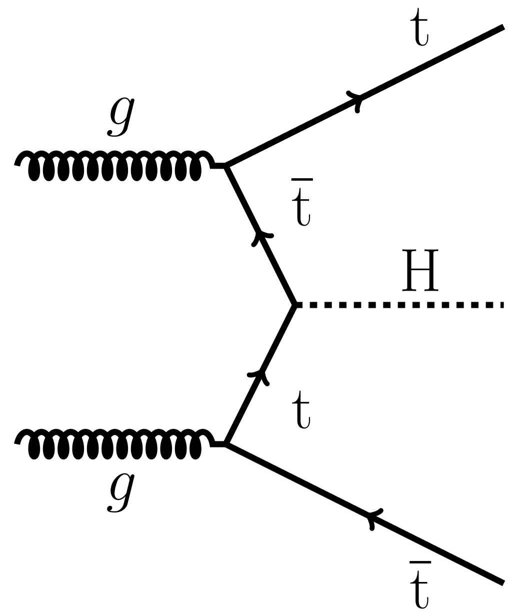

- Some final states getting more and more challenging due to **dominant background systematics: ttH H→bb and multilepton**
  => can benefit from **dedicated ttbb + ttW background measurements**

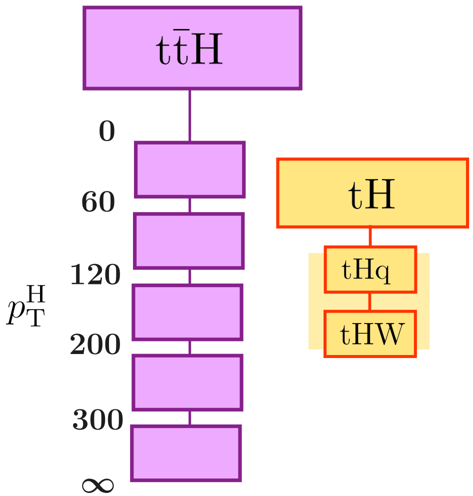

- **H→γγ channel still statistically limited** but already able to perform **detailed STXS pT measurements** together with ttH H→bb

- **Structure of top-Higgs coupling** can already be constrained with existing dataset: **κ_t=-1 or pure CP-odd coupling excluded**

- **Looking ahead for Run 3 and beyond for precision measurements in this production mode**

Back-up

- **Selections**

	FH channel	SL channel	DL channel
Number of leptons	0	1	2
p_{T} of leptons (e/μ) [GeV]	—	$> 30/29$	$> 25/25$ GeV
p_{T} of additional leptons [GeV]	< 15	< 15	< 15
$\|\eta\|$ of leptons	< 2.4	< 2.4	< 2.4
Number of jets	≥ 6	≥ 4	≥ 2
p_{T} of jets [GeV]	> 40	> 30	$> 30, 30, 20$
$\|\eta\|$ of jets	< 2.4	< 2.4	< 2.4
Number of b-tagged jets	≥ 2	≥ 2	≥ 1
$p_{\mathrm{T}}^{\mathrm{miss}}$	—	> 20 GeV	> 40 GeV

- **Data-driven multijet background:**
  based on quark-gluon likelihood ratio + b-tagging

	$N_{\text{b tag}} = 2$, $N_{\text{b tag loose}} \geq 3$	$N_{\text{b tag}} \geq 3$
QGLR > 0.5	CR (to extract distribution)	SR (final analysis)
QGLR < 0.5	Validation CR (to validate distribution)	VR (comparison with data)

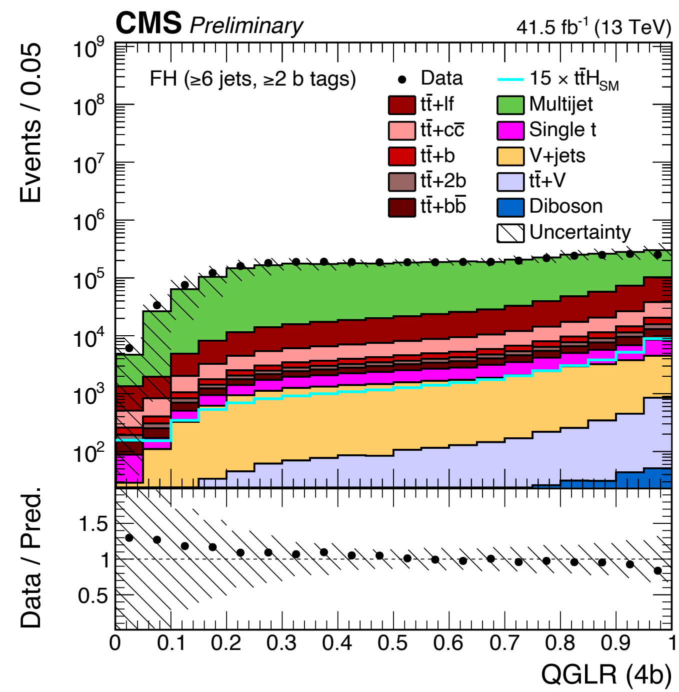

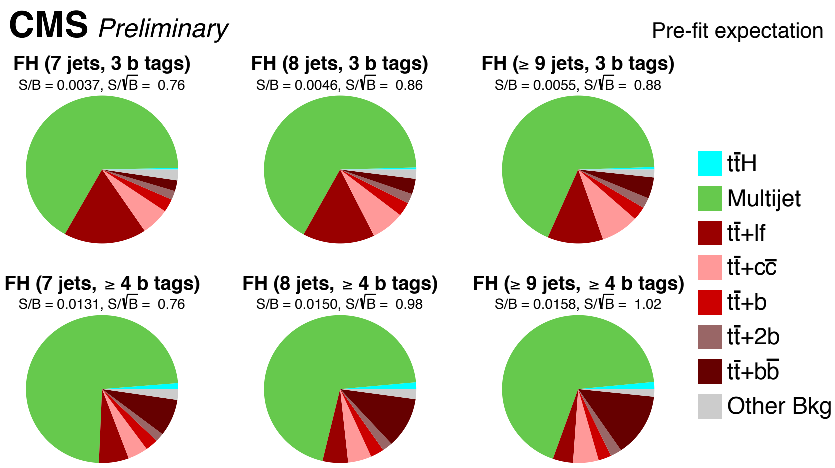

CMS Preliminary
Pre-fit expectation
FH (7 jets, 3 b tags)
S/B = 0.0037, S/√B = 0.76
FH (8 jets, 3 b tags)
S/B = 0.0046, S/√B = 0.86
FH (≥ 9 jets, 3 b tags)
S/B = 0.0055, S/√B = 0.88
FH (7 jets, ≥ 4 b tags)
S/B = 0.0131, S/√B = 0.76
FH (8 jets, ≥ 4 b tags)
S/B = 0.0150, S/√B = 0.98
FH (≥ 9 jets, ≥ 4 b tags)
S/B = 0.0158, S/√B = 1.02
tt̄H
Multijet
tt̄+lf
tt̄+cc̄
tt̄+b
tt̄+2b
tt̄+bb̄
Other Bkg

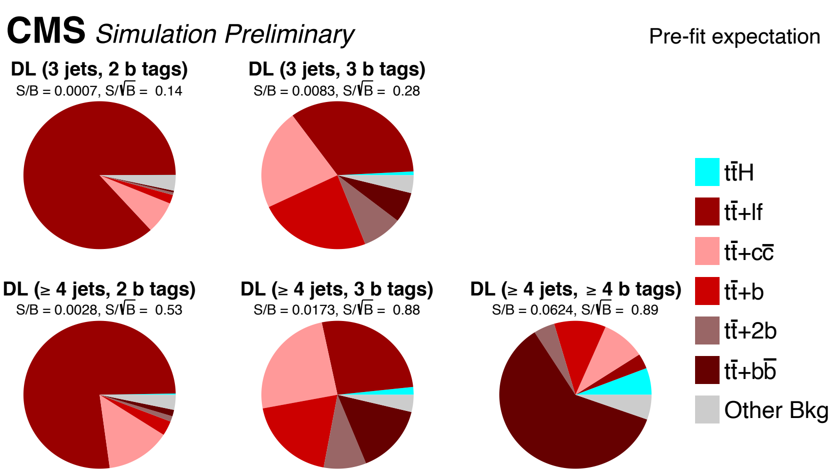

CMS Simulation Preliminary
Pre-fit expectation
DL (3 jets, 2 b tags)
S/B = 0.0007, S/√B = 0.14
DL (3 jets, 3 b tags)
S/B = 0.0083, S/√B = 0.28
DL (≥ 4 jets, 2 b tags)
S/B = 0.0028, S/√B = 0.53
DL (≥ 4 jets, 3 b tags)
S/B = 0.0173, S/√B = 0.88
DL (≥ 4 jets, ≥ 4 b tags)
S/B = 0.0624, S/√B = 0.89
tt̄H
tt̄+lf
tt̄+cc̄
tt̄+b
tt̄+2b
tt̄+bb̄
Other Bkg

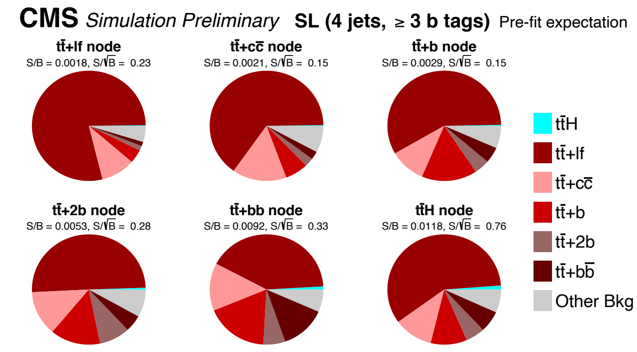

CMS Simulation Preliminary SL (4 jets, ≥ 3 b tags) Pre-fit expectation
tt̄+lf node
S/B = 0.0018, S/√B = 0.23
tt̄+cc̄ node
S/B = 0.0021, S/√B = 0.15
tt̄+b node
S/B = 0.0029, S/√B = 0.15
tt̄+2b node
S/B = 0.0053, S/√B = 0.28
tt̄+bb node
S/B = 0.0092, S/√B = 0.33
tt̄H node
S/B = 0.0118, S/√B = 0.76
tt̄H
tt̄+lf
tt̄+cc̄
tt̄+b
tt̄+2b
tt̄+bb̄
Other Bkg

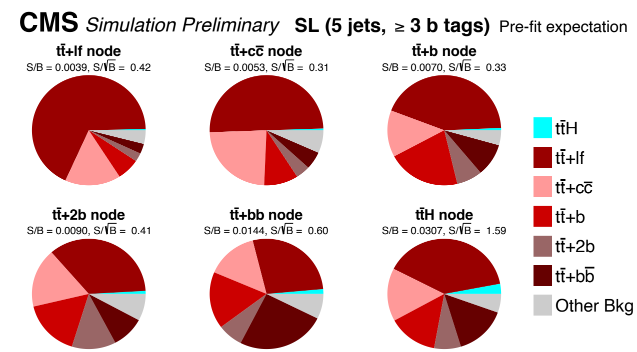

CMS Simulation Preliminary SL (5 jets, ≥ 3 b tags) Pre-fit expectation
tt̄+lf node
S/B = 0.0039, S/√B = 0.42
tt̄+cc̄ node
S/B = 0.0053, S/√B = 0.31
tt̄+b node
S/B = 0.0070, S/√B = 0.33
tt̄+2b node
S/B = 0.0090, S/√B = 0.41
tt̄+bb node
S/B = 0.0144, S/√B = 0.60
tt̄H node
S/B = 0.0307, S/√B = 1.59
tt̄H
tt̄+lf
tt̄+cc̄
tt̄+b
tt̄+2b
tt̄+bb̄
Other Bkg

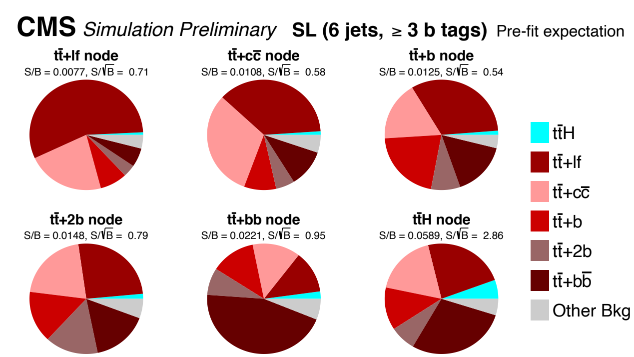

CMS Simulation Preliminary SL (6 jets, ≥ 3 b tags) Pre-fit expectation
tt̄+lf node
S/B = 0.0077, S/√B = 0.71
tt̄+cc̄ node
S/B = 0.0108, S/√B = 0.58
tt̄+b node
S/B = 0.0125, S/√B = 0.54
tt̄+2b node
S/B = 0.0148, S/√B = 0.79
tt̄+bb node
S/B = 0.0221, S/√B = 0.95
tt̄H node
S/B = 0.0589, S/√B = 2.86
tt̄H
tt̄+lf
tt̄+cc̄
tt̄+b
tt̄+2b
tt̄+bb̄
Other Bkg

- **Representative input variables to ANN used in single-lepton channel**

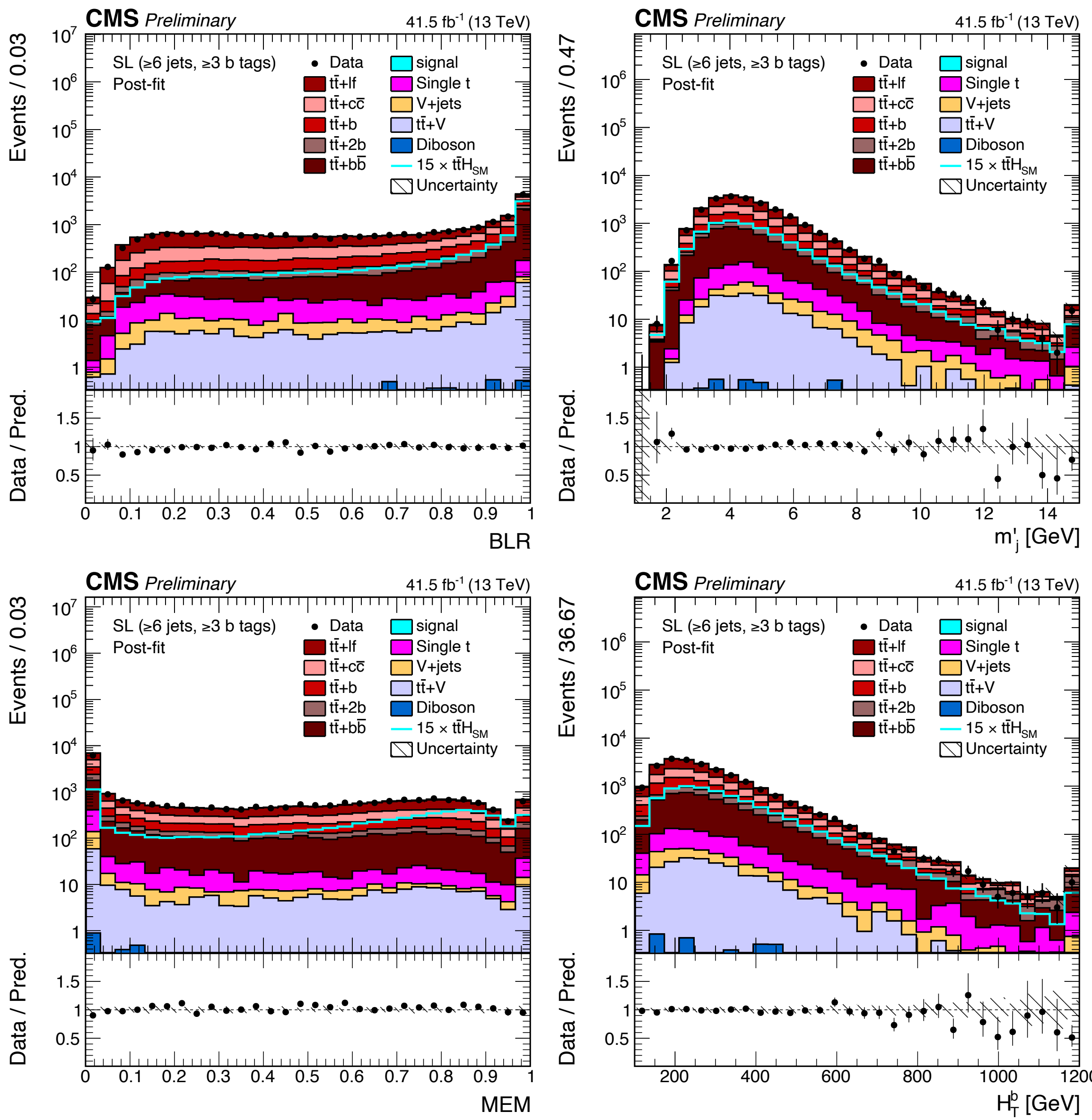

- **Representative input variables to BDT used in dilepton channel**

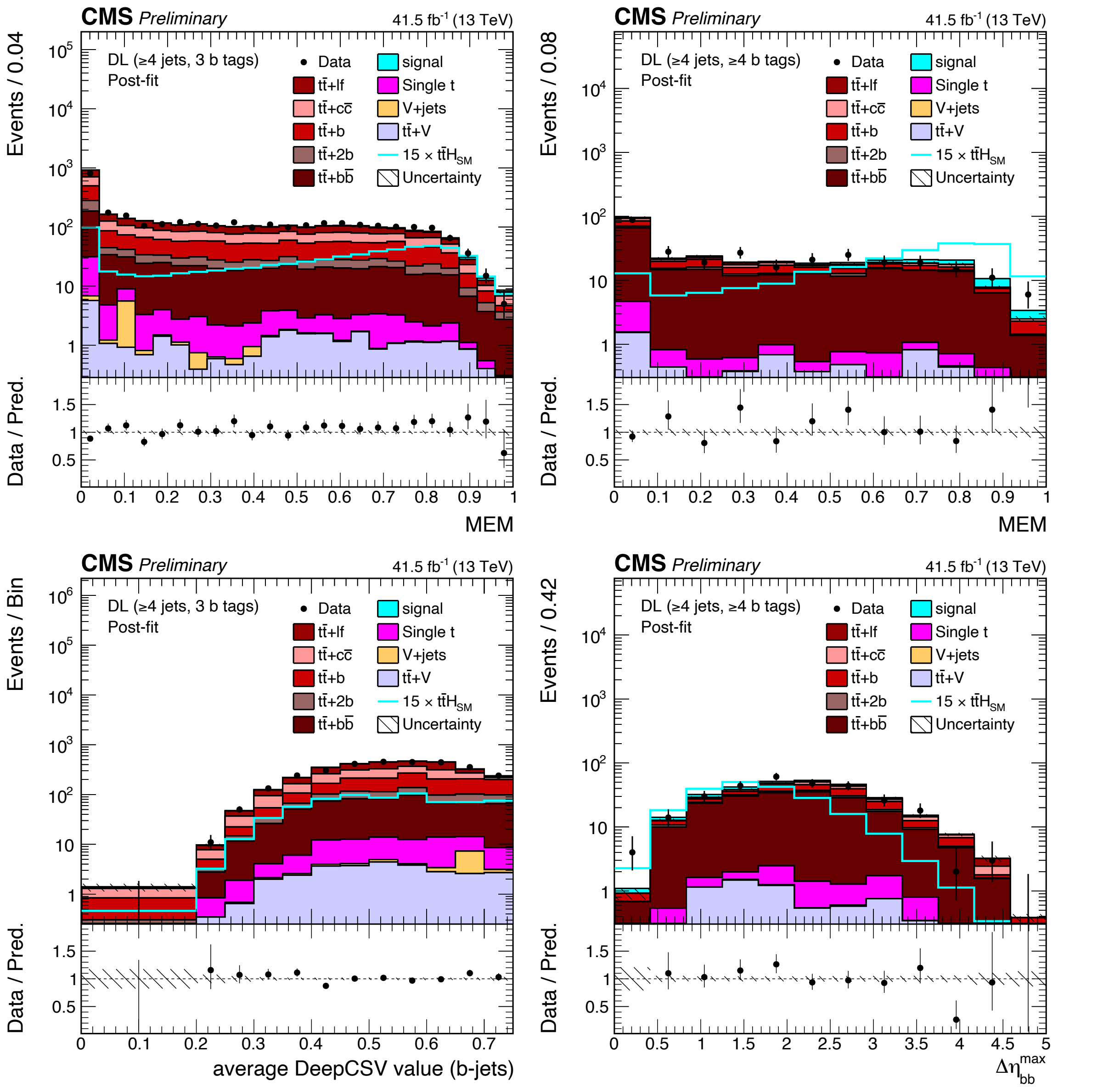

- **Single-lepton ANN nodes**

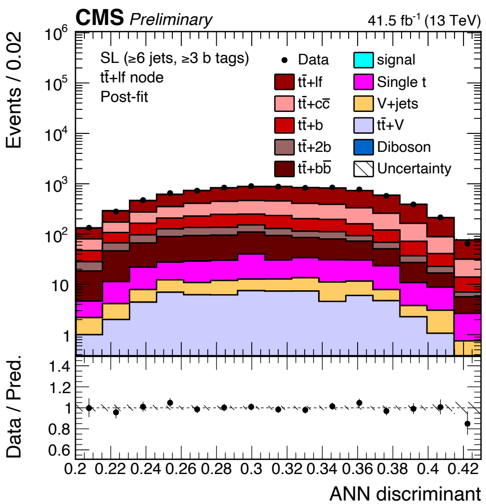

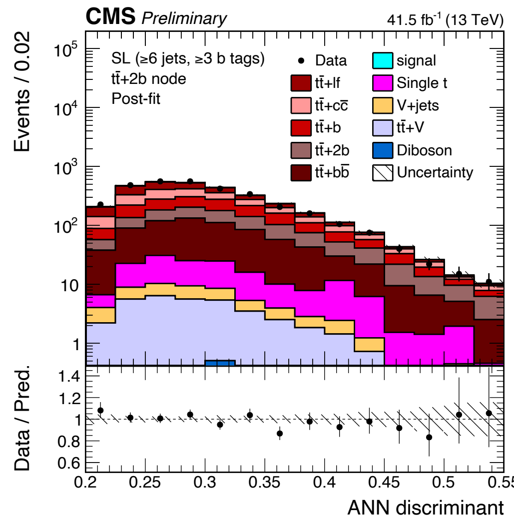

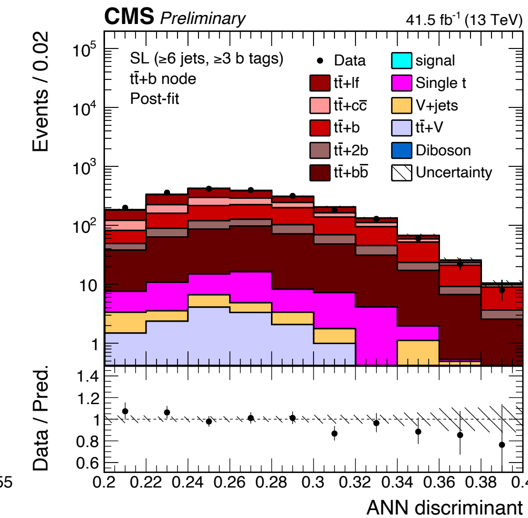

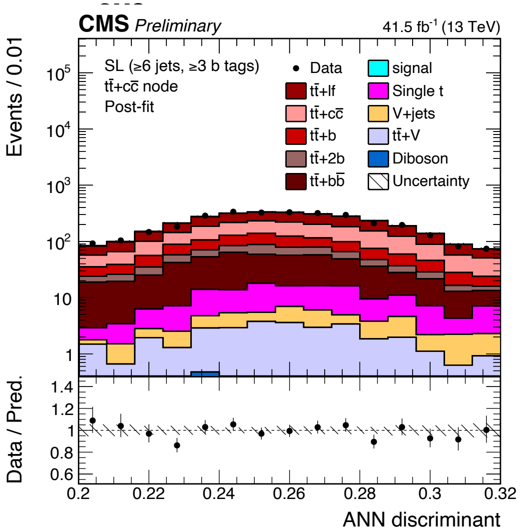

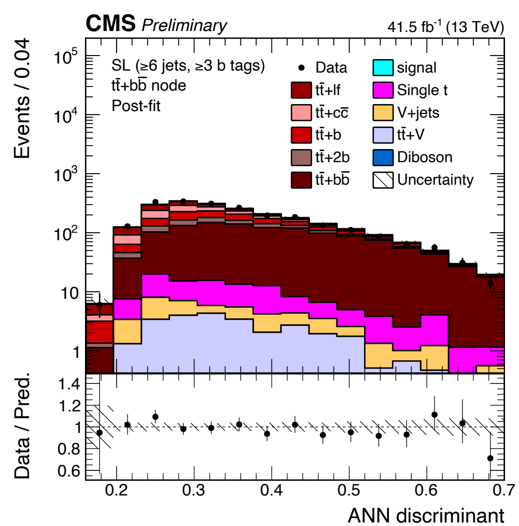

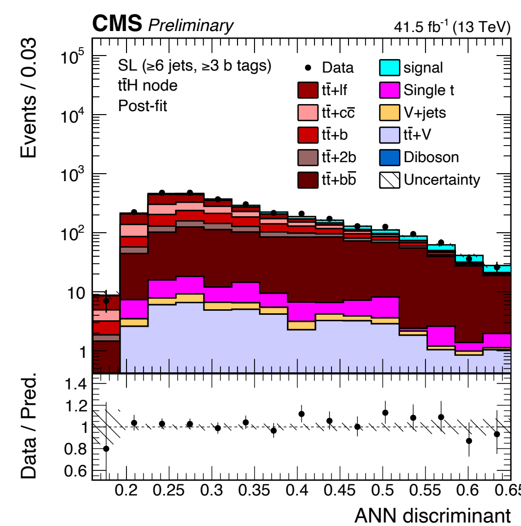

- **Single-lepton + dilepton input variables 1/2**

Variable	Definition	SL (4 jets, ≥ 3 b-tags)	SL (5 jets, ≥ 3 b-tags)	SL (≥ 6 jets, ≥ 3 b-tags)	DL (3 jets, 2 b-tags)	DL (3 jets, 3 b-tags)	DL (≥ 4 jets, 2 b-tags)	DL (≥ 4 jets, 3 b-tags)	DL (≥ 4 jets, ≥ 4 b-tags)
MEM	maxtrix element method discriminant	+	+	+	−	−	−	+	+
BLR	likelihood ratio discriminating between events with 4 b quark jets and 2 b quark jets	+	−	+	−	−	−	−	−
$\mathrm{BLR}^{\mathrm{trans}}$	$\ln[\mathrm{BLR}/(1-\mathrm{BLR})]$	+	−	+	−	−	−	−	−
$p_{\mathrm{T}}(\text{jet } 1)$	p_{T} of the 1. jet, ranked in jet p_{T}	−	+	−	−	−	−	−	−
$p_{\mathrm{T}}(\text{jet } 3)$	p_{T} of the 3. jet, ranked in jet p_{T}	−	+	−	−	−	−	−	−
$H_{\mathrm{T}}^{\mathrm{b}}$	scalar sum of p_{T} of b-tagged jets	+	+	+	+	−	−	−	+
$\sum_{\mathrm{j,lep}} p_{\mathrm{T}}$	scalar sum of p_{T} of leptons and jets	−	−	−	+	+	−	+	−
$N_{\mathrm{b}}^{\mathrm{tight}}$	number of b-tagged jets at a working point with 0.1% probability of tagging gluon and light-flavour jets	+	+	−	−	−	−	−	−
$d(\text{jet } 4)$	b-tagging discriminant value of 4. jet, ranked in jet p_{T}	+	−	−	−	−	−	−	−
d_2	2. highest b-tagging discriminant value of all jets	+	+	+	−	−	−	−	−
$d_{\mathrm{j}}^{\mathrm{avg}}$	average b-tagging discriminant value of all jets	+	+	+	+	−	+	+	−
$d_{\mathrm{b}}^{\mathrm{avg}}$	average b-tagging discriminant value of all b-tagged jets	+	+	+	−	+	−	+	+
$d_{\mathrm{b}}^{\mathrm{min}}$	minimal b-tagging discriminant value of all b-tagged jets	+	+	−	−	−	−	−	−
$\frac{1}{N_{\mathrm{b}}}\sum_{b}^{N_{\mathrm{b}}}\left(d-d_{\mathrm{b}}^{\mathrm{avg}}\right)^2$	squared difference between the b-tagged discriminant value of a b-tagged jet and the average b-tagging discriminant values of all b-tagged jets, averaged over all b-tagged jets	+	−	+	−	−	−	−	−
m_{j}'	sum of the masses of all jets divided by the number of dijet pairs	−	−	+	−	−	−	−	−
$m_{\mathrm{b,b}}^{\text{closest to 125}}$	mass of pair of b-tagged jets closest to 125 GeV	−	+	−	−	+	−	−	−
$m_{\mathrm{lep,b}}^{\min\Delta R}$	mass of pair of lepton and b-tagged jet closest in ΔR	−	−	+	−	−	−	−	−
$m_{\mathrm{j,j}}^{\min\Delta R}$	mass of pair of jets closest in ΔR	−	−	−	+	+	−	−	−
$m_{\mathrm{b,b}}^{\min\Delta R}$	mass of pair of b-tagged jets closest in ΔR	−	−	−	+	−	+	+	+

- **Single-lepton + dilepton input variables 2/2**

Variable	Definition	SL (4 jets, ≥ 3 b-tags)	SL (5 jets, ≥ 3 b-tags)	SL (≥ 6 jets, ≥ 3 b-tags)	DL (3 jets, 2 b-tags)	DL (3 jets, 3 b-tags)	DL (≥ 4 jets, 2 b-tags)	DL (≥ 4 jets, 3 b-tags)	DL (≥ 4 jets, ≥ 4 b-tags)
$m_{\mathrm{j,b}}^{\min\Delta R}$	mass of pair of jet and b-tagged jet closest in ΔR	−	−	−	−	−	+	−	+
$m_{\mathrm{b,b}}^{\mathrm{avg}}$	average mass of all pairs of b-tagged jets	+	−	−	−	−	−	−	−
$m_{\mathrm{b,b}}^{\max m}$	mass of pair of b-tagged jets with largest mass	−	−	−	−	+	−	+	−
$m_{\mathrm{j,j,j}}^{\max p_T}$	mass of tri-jet system with highest p_T	−	−	−	+	−	−	−	+
$p_{T;\mathrm{b,b}}^{\min\Delta R}$	sum p_{T} of pair of closest b-tagged jets	−	−	−	+	−	+	+	+
$p_{T;\mathrm{j,j}}^{\min\Delta R}$	sum p_{T} of pair of closest jets	−	−	−	−	+	+	−	−
$\Delta R_{\mathrm{j,j}}^{\max}$	largest ΔR between any two jets	−	+	−	−	−	−	−	−
$\Delta R_{\mathrm{b,b}}^{\mathrm{avg}}$	average ΔR between b-tagged jets	−	+	+	−	−	−	+	+
$\Delta R_{\mathrm{j,j}}^{\mathrm{avg}}$	average ΔR between two jets	−	−	−	+	+	+	−	−
$\Delta R_{\mathrm{j,b}}^{\mathrm{avg}}$	average ΔR between a jet and a b-tagged jets	−	−	−	−	−	+	−	−
$\Delta R_{\mathrm{j,j}}^{\min}$	minimal ΔR between any two jets	−	−	−	+	+	−	−	−
$\Delta R_{\mathrm{b,b}}^{\min}$	minimal ΔR between any two b-tagged jets	−	−	−	−	−	−	+	+
$\Delta R_{\mathrm{lep,b}}^{\min}$	minimal ΔR between lepton and b-tagged jet	−	+	−	−	−	−	−	−
$\Delta\eta_{\mathrm{j,j}}^{\max}$	largest $\Delta\eta$ between any two jets	−	−	−	+	+	+	−	+
$\Delta\eta_{\mathrm{b,b}}^{\max}$	largest $\Delta\eta$ between any two b-tagged jets	−	−	−	−	−	−	+	+
S^{j}	$\frac{3}{2}(\lambda_2+\lambda_3)$, with λ_i the eigenvalues of the momentum tensor computed with jets	+	+	−	−	−	−	−	−
S^{b}	$\frac{3}{2}(\lambda_2+\lambda_3)$, with λ_i the eigenvalues of the momentum tensor computed with b-tagged jets	−	+	−	−	−	−	−	−
S_T^{j}	$\frac{2\lambda_2}{\lambda_2+\lambda_1}$, with λ_i the eigenvalues of the momentum tensor computed with jets	+	−	−	−	−	−	−	−
$C^{\mathrm{j,lep}}$	scalar sum of the jet and lepton p_{T} divided by the sum of the energies of all jets and leptons	−	−	−	+	+	+	−	−
C^{b}	scalar sum of the b-tagged jet p_{T} divided by the sum of the energies of all b-tagged jets	−	−	−	+	−	+	−	−
H_0	0th Fox–Wolfram moment computed with all jets	−	−	−	+	−	−	+	−
R_1	ratio H_1/H_0 of 0th and first Fox–Wolfram moment computed with all jets	−	−	−	−	+	−	−	−

Variable	Definition	SL (4 jets, ≥ 3 b-tags)	SL (5 jets, ≥ 3 b-tags)	SL (≥ 6 jets, ≥ 3 b-tags)	DL (3 jets, 2 b-tags)	DL (3 jets, 3 b-tags)	DL (≥ 4 jets, 2 b-tags)	DL (≥ 4 jets, 3 b-tags)	DL (≥ 4 jets, ≥ 4 b-tags)
R_1^{b}	ratio H_1/H_0 of 0th and first Fox–Wolfram moment computed with all b-tagged jets	−	−	−	−	−	+	−	−
$\tau_{\mathrm{j,j}}^{\max m}$	twist angle between pair of jets with maximum mass	−	−	−	−	+	−	−	−
$\tau_{\mathrm{b,b}}^{\max m}$	twist angle between pair of b-tagged jets maximum mass	−	−	−	−	−	−	+	−
$N_{\mathrm{Higgs}}^{\mathrm{j,j}}$	multiplicity of dijet pairs with invariant mass between 100 GeV and 140 GeV	−	−	−	−	−	+	−	+

- **Final variables used for signal extraction**

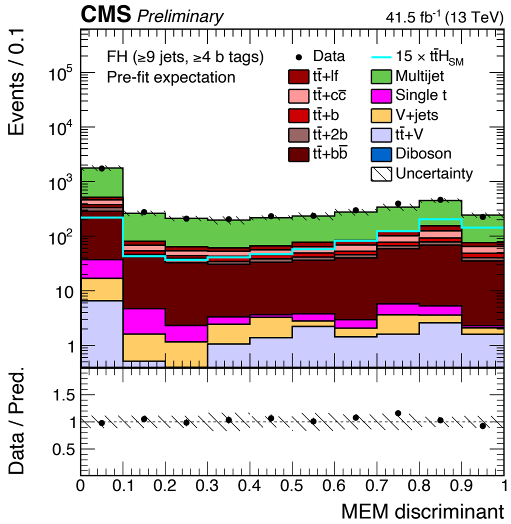

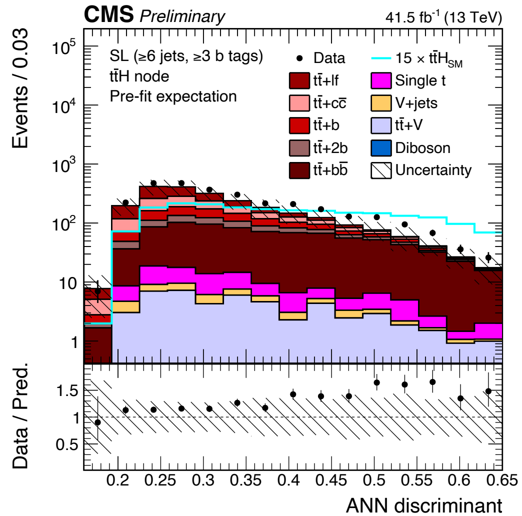

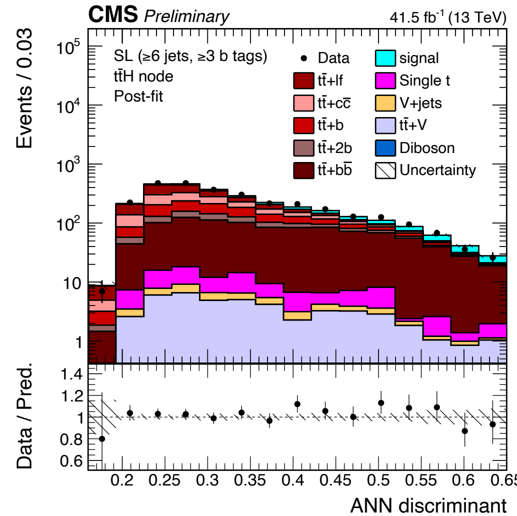

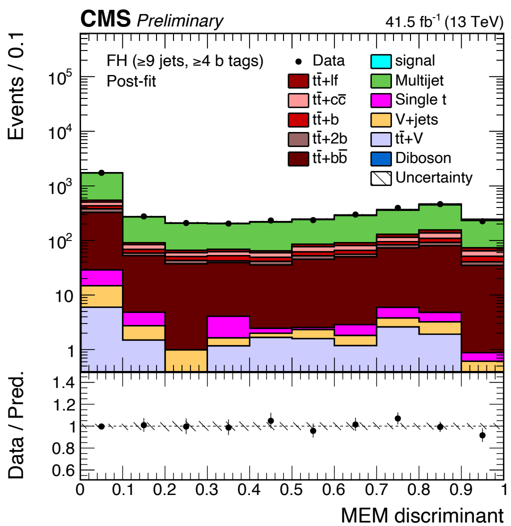

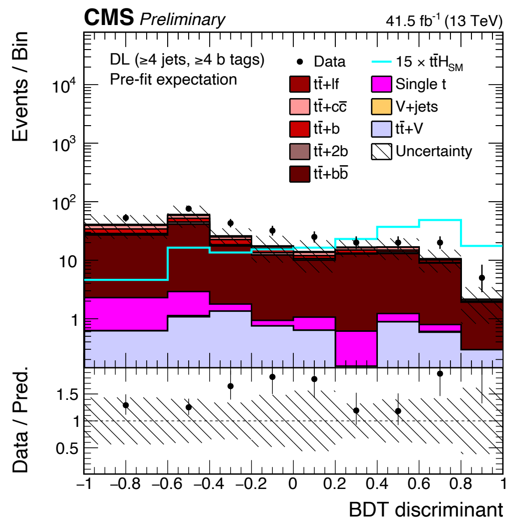

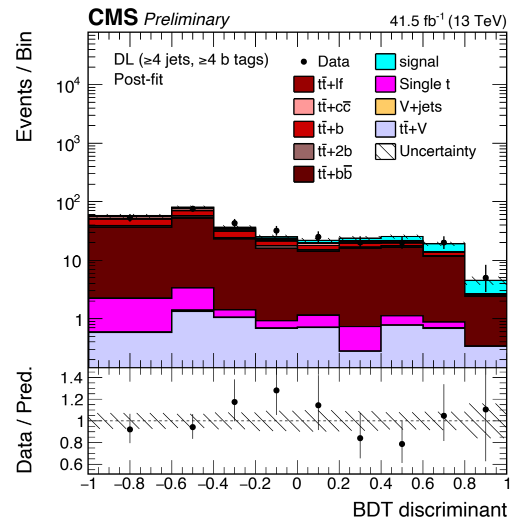

- **Systematics 1/2**

Source	Type	Remarks
Integrated luminosity	rate	Signal and all backgrounds
Lepton identification/isolation	shape	Signal and all backgrounds
Trigger efficiency	shape	Signal and all backgrounds
Trigger prefiring correction	rate	Signal and all backgrounds
Pileup	shape	Signal and all backgrounds
Jet energy scale	shape	Signal and all backgrounds
Jet energy resolution	shape	Signal and all backgrounds
b tag hf fraction	shape	Signal and all backgrounds
b tag hf stats (linear)	shape	Signal and all backgrounds
b tag hf stats (quadratic)	shape	Signal and all backgrounds
b tag lf fraction	shape	Signal and all backgrounds
b tag lf stats (linear)	shape	Signal and all backgrounds
b tag lf stats (quadratic)	shape	Signal and all backgrounds
b tag charm (linear)	shape	Signal and all backgrounds
b tag charm (quadratic)	shape	Signal and all backgrounds
QGL reweighting	shape	Signal and all backgrounds
TF_{loose} correction	shape	QCD multijet estimate
H_T reweighting	shape	QCD multijet estimate
Multijet normalisation	rate	QCD multijet estimate
Renorm./fact. scales ($t\bar{t}H$)	rate	Scale uncertainty of NLO $t\bar{t}H$ prediction
Renorm./fact. scales ($t\bar{t}$)	rate	Scale uncertainty of NNLO $t\bar{t}$ prediction
$t\bar{t}$+hf cross sections	rate	Additional 50% rate uncertainty of $t\bar{t}$+hf predictions
Renorm./fact. scales (t)	rate	Scale uncertainty of NLO single t prediction
Renorm./fact. scales (V)	rate	Scale uncertainty of NNLO W and Z prediction
Renorm./fact. scales (VV)	rate	Scale uncertainty of NLO diboson prediction

- **Systematics 2/2**

PDF (gg)	rate	PDF uncertainty for gg initiated processes except $t\bar{t}H$
PDF (gg $t\bar{t}H$)	rate	PDF uncertainty for $t\bar{t}H$
PDF ($q\bar{q}$)	rate	PDF uncertainty of $q\bar{q}$ initiated processes ($t\bar{t}$+W,W,Z)
PDF (qg)	rate	PDF uncertainty of qg initiated processes (single t)
PDF shape variations ($t\bar{t}H$, $t\bar{t}$)	shape	Based on the NNPDF replicas, same for $t\bar{t}H$ and additional jet flavours
μ_R scale ($t\bar{t}$)	shape	Renormalisation scale uncertainty of the $t\bar{t}$ ME generator (POWHEG), same for additional jet flavours
μ_F scale ($t\bar{t}$)	shape	Factorisation scale uncertainty of the $t\bar{t}$ ME generator (POWHEG), same for additional jet flavours
PS scale: ISR ($t\bar{t}$)	shape	Initial state radiation uncertainty of the PS (for $t\bar{t}$ events), same for additional jet flavours
PS scale: FSR ($t\bar{t}$)	shape	Final state radiation uncertainty of the PS (for $t\bar{t}$ events), same for additional jet flavours
ME-PS matching ($t\bar{t}$)	rate	NLO ME to PS matching, *hdamp* [?] (for $t\bar{t}$ events), independent for additional jet flavours
Underlying event ($t\bar{t}$)	rate	Underlying event (for $t\bar{t}$ events), independent for additional jet flavours
Bin-by-bin event count	shape	Statistical uncertainty of the signal and background prediction due to the limited sample size

- **Systematics**

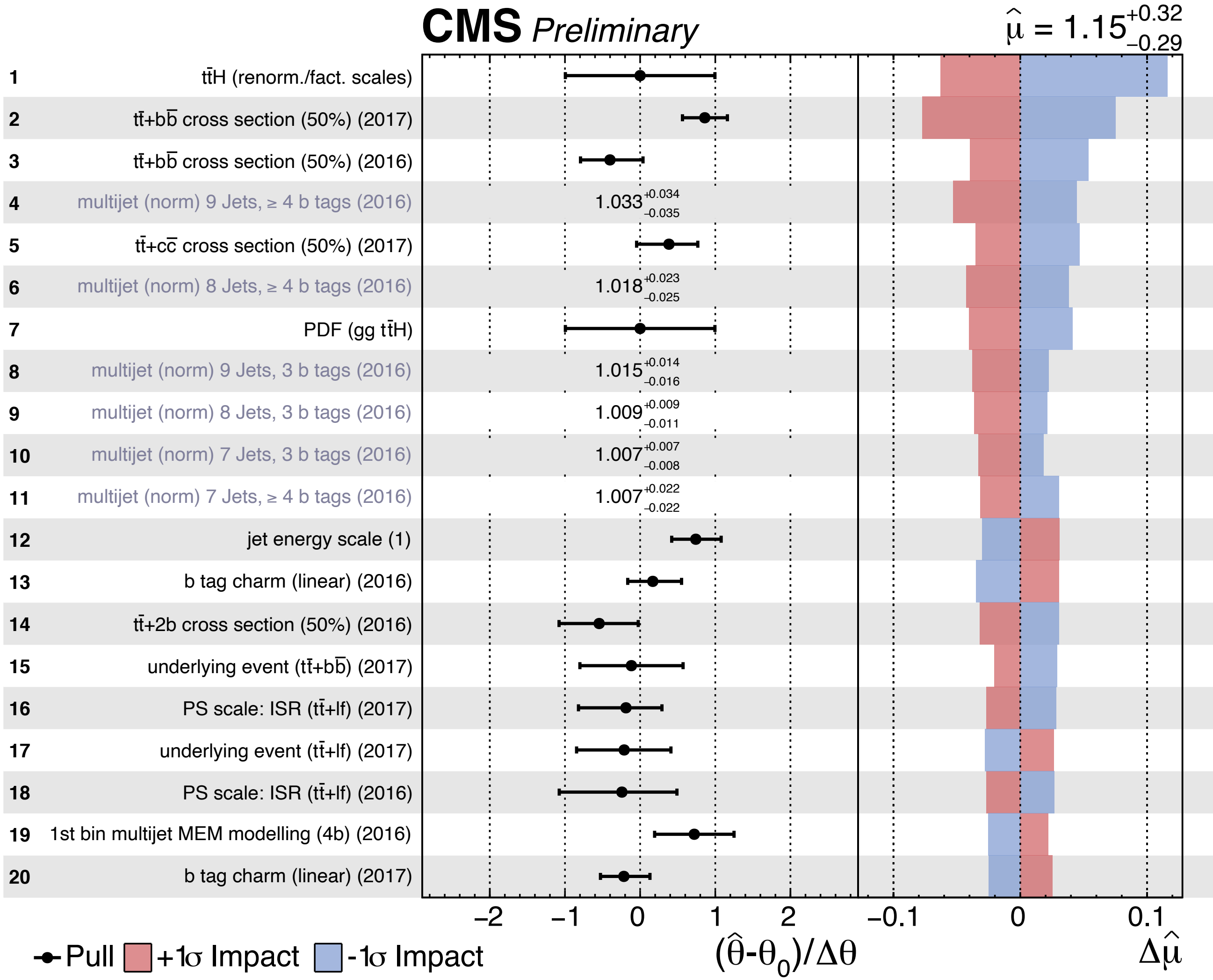

ttH H→bb

CMS-PAS-HIG-18-030

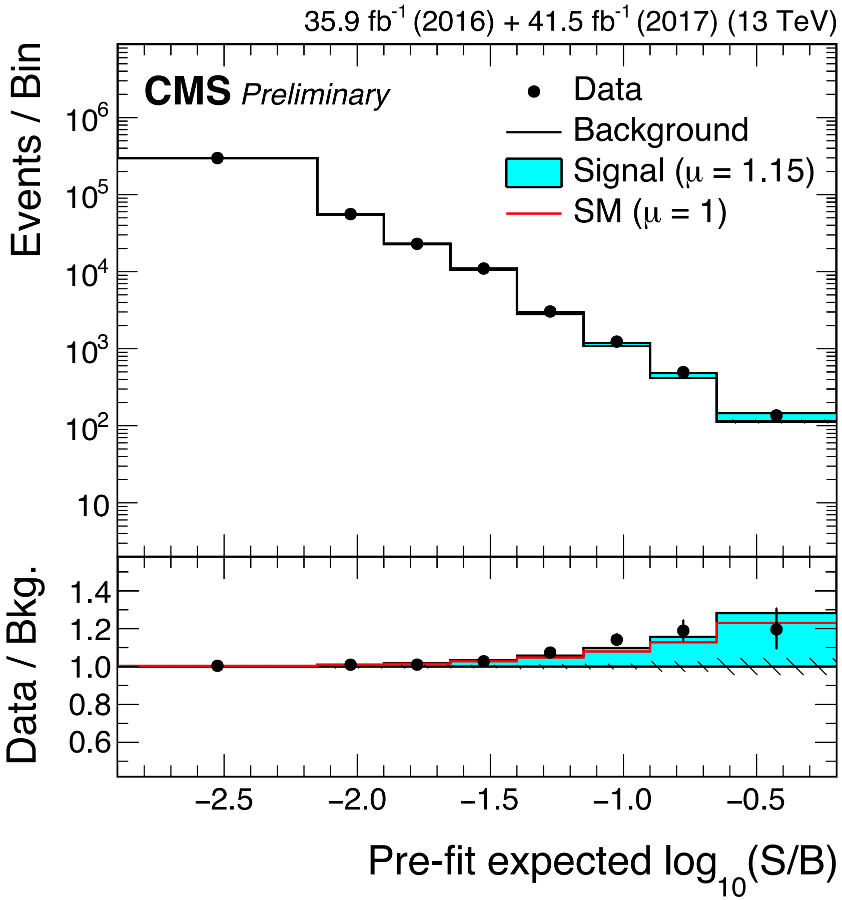

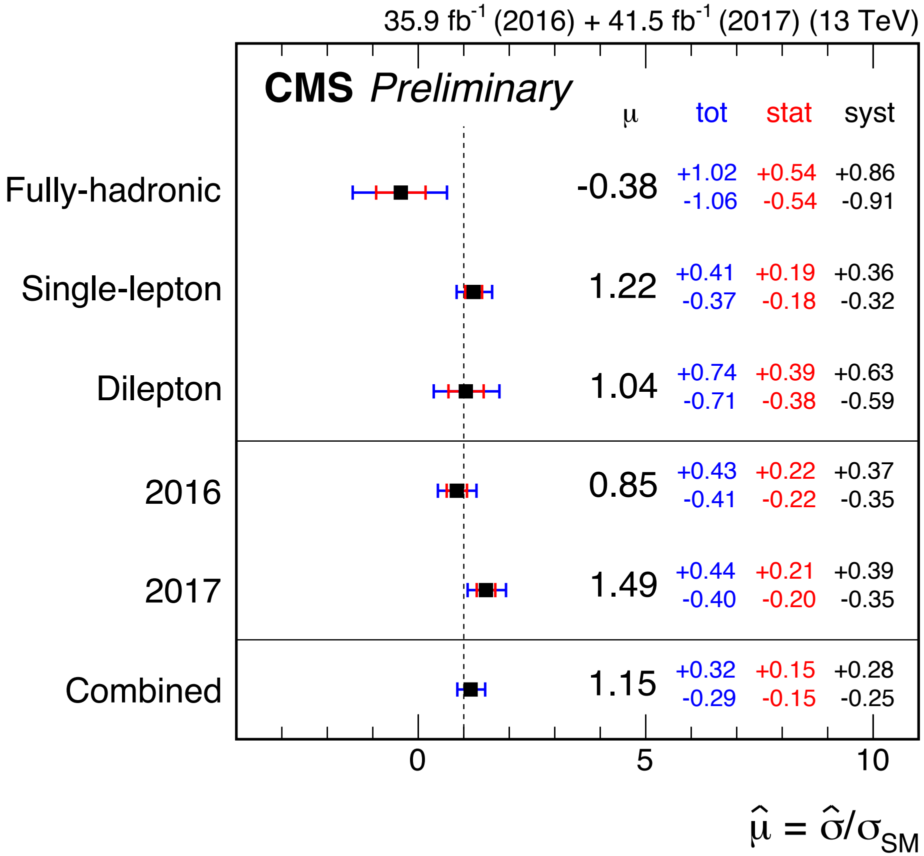

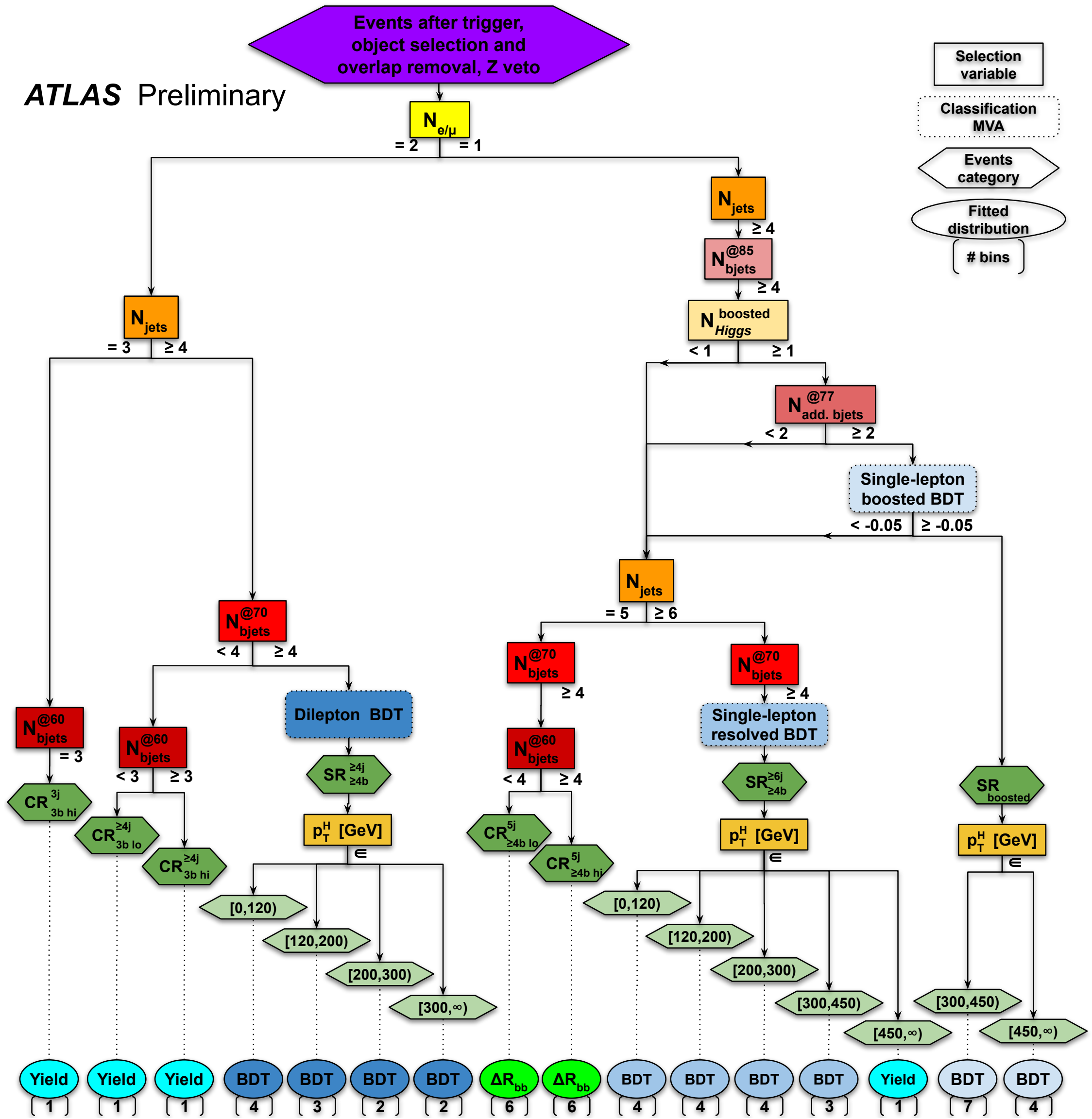

ATLAS Preliminary
Events after trigger, object selection and overlap removal, Z veto
Selection variable
Classification MVA
Events category
Fitted distribution
bins
Single-lepton boosted BDT
Dilepton BDT
Single-lepton resolved BDT
[0,120)
[120,200)
[200,300)
[300,∞)
[300,450)
[450,∞)
Yield
BDT

ttH H→bb

ATLAS-CONF-2020-058

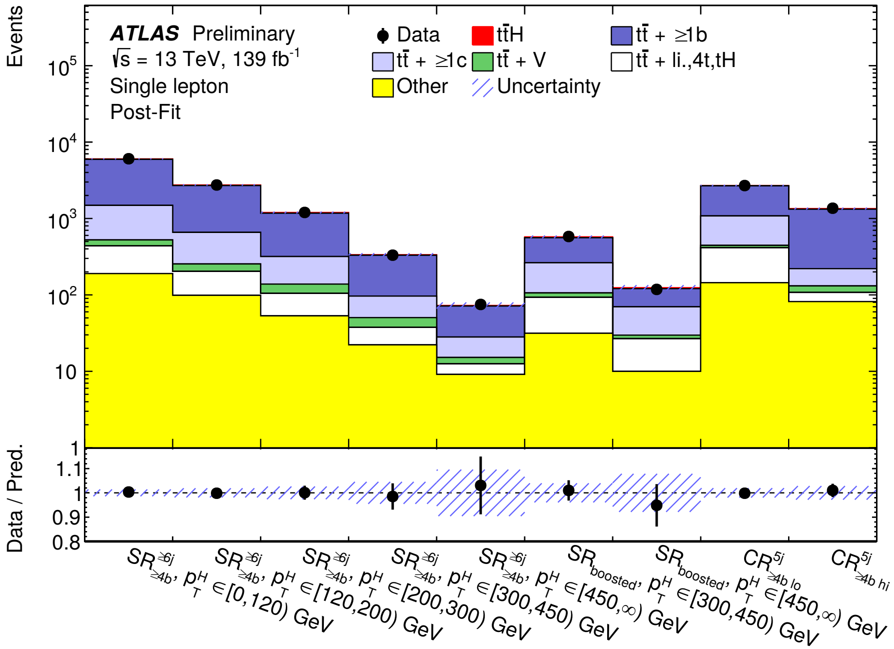

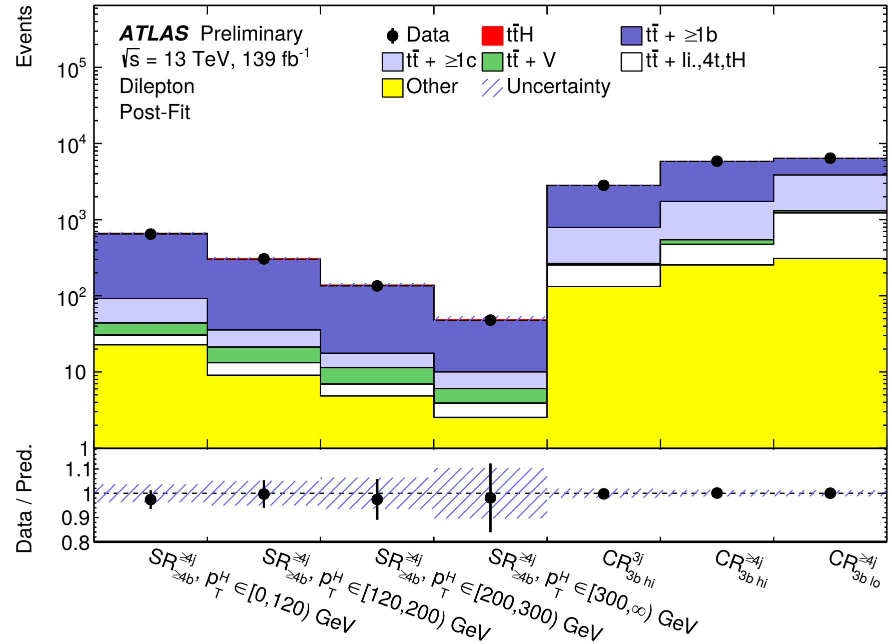

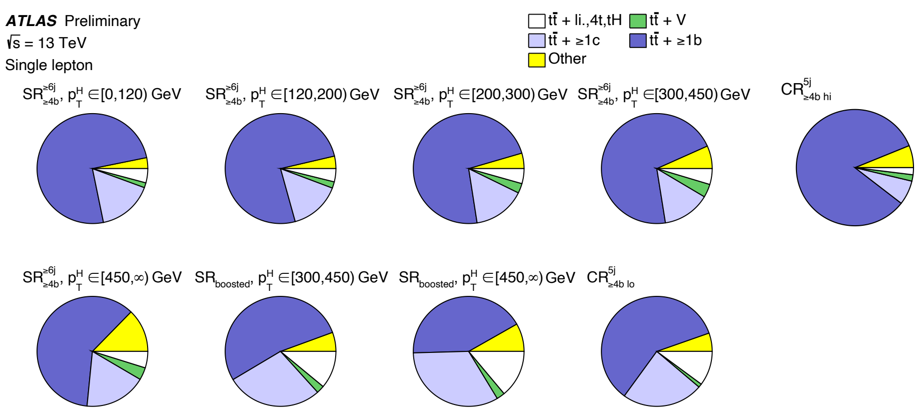

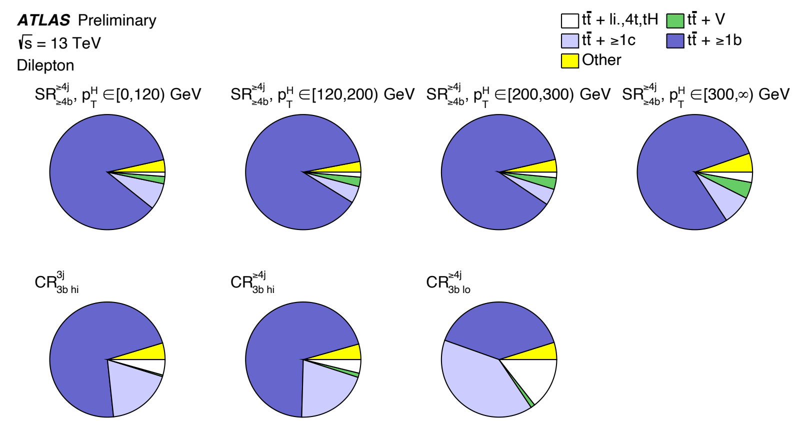

- **Dilepton BDT distributions**

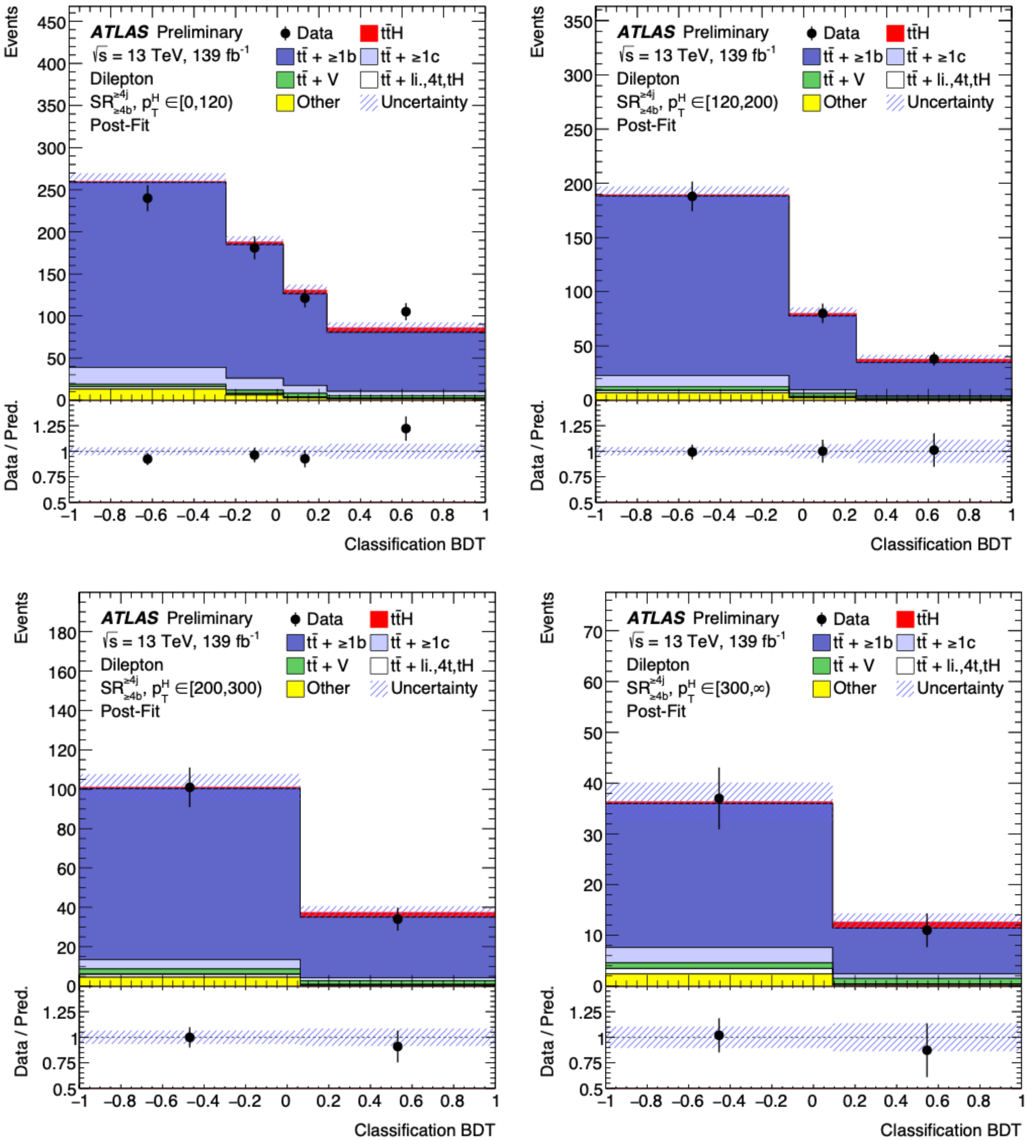

- **Single-lepton BDT distributions**

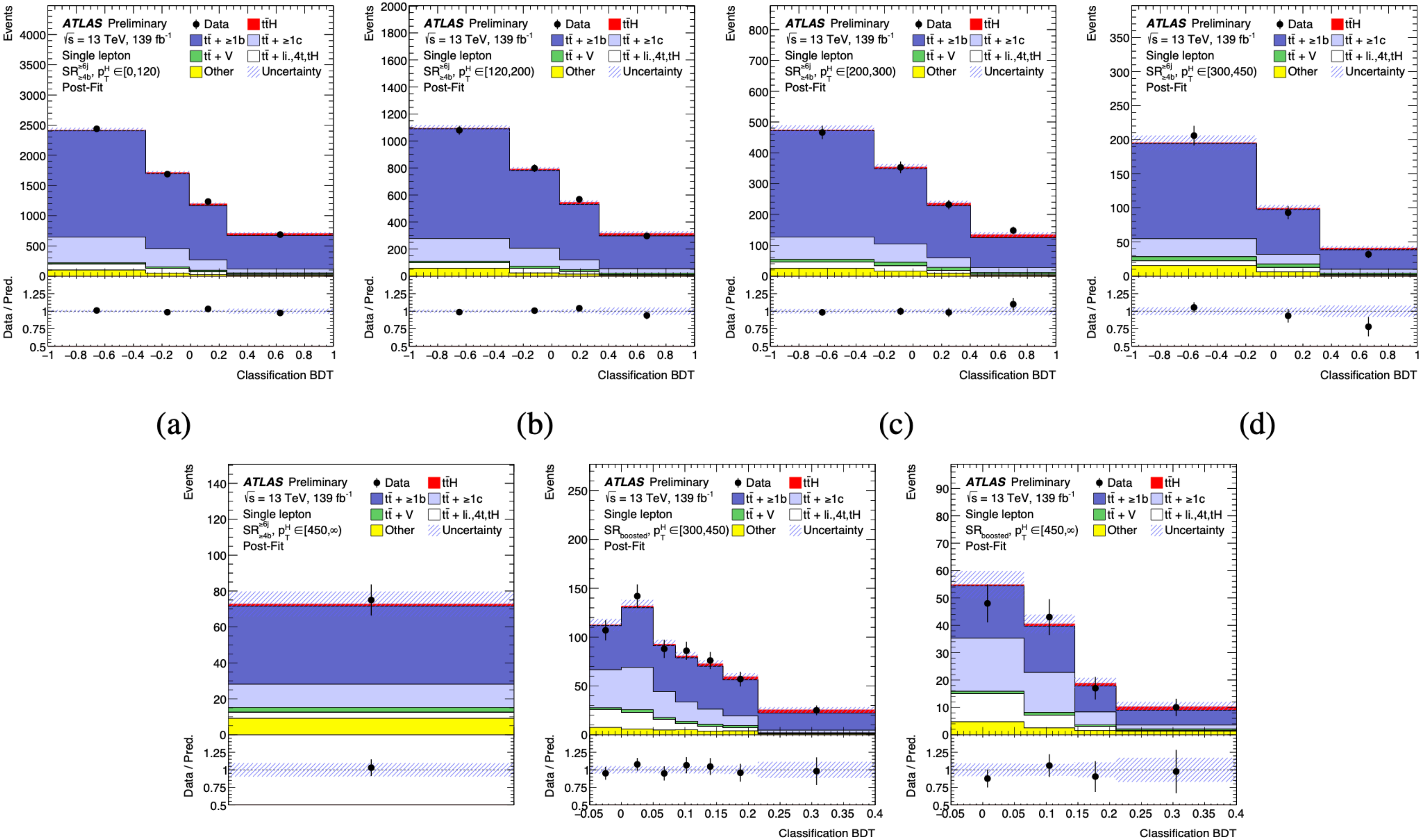

ttH H→bb

ATLAS-CONF-2020-058

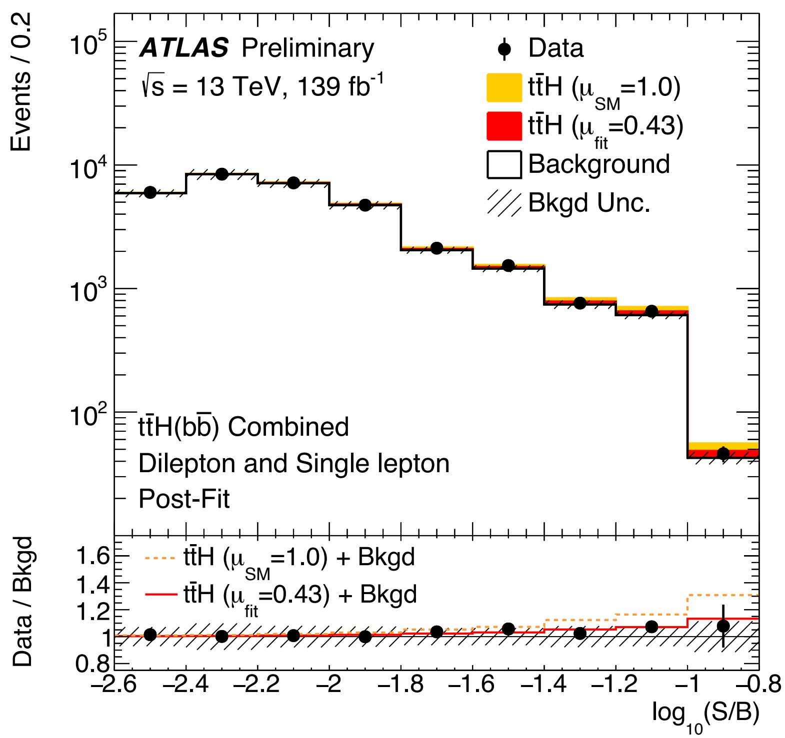

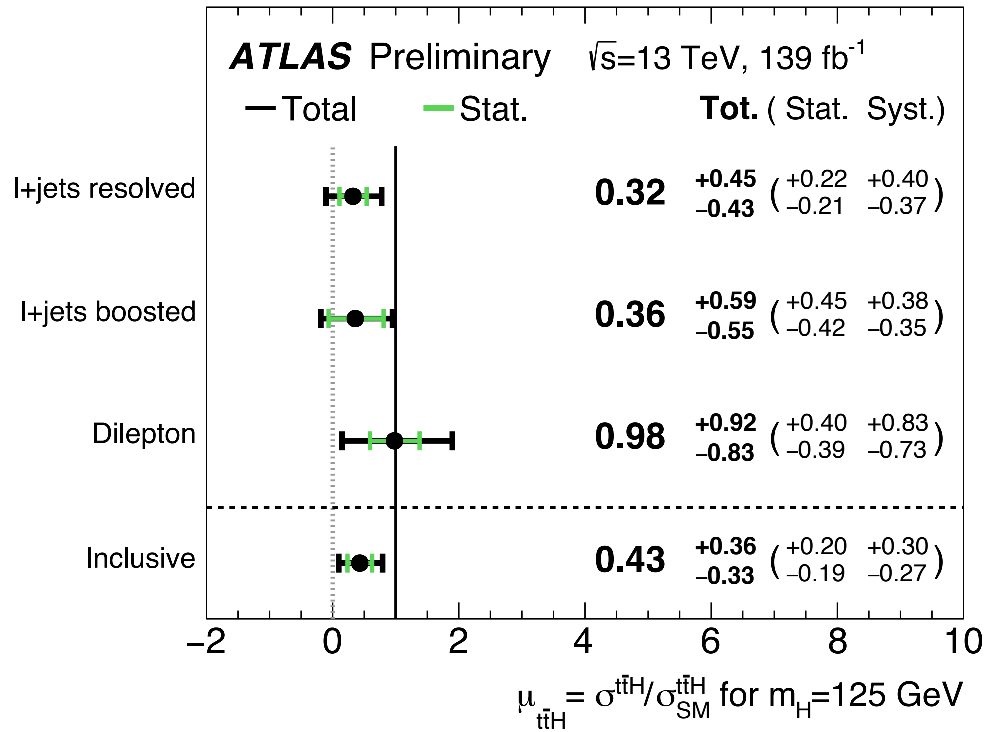

- **ttbar samples + systematics**

$t\bar{t}$ and single-top				
$t\bar{t}$	PowhegBox v2	NNPDF3.0NLO	Pythia8.230	NNLO+NNLL [45,46,47,48,49,50,51]
	PowhegBox v2	NNPDF3.0NLO	Herwig7.04	NNLO+NNLL [45,46,47,48,49,50,51]
	MadGraph5_aMC@NLO v2.6.0	NNPDF3.0NLO	Pythia8.230	NNLO+NNLL [45,46,47,48,49,50,51]
$t\bar{t}+b\bar{b}$	PowhegBoxRes	NNPDF3.0NLOnf4	Pythia8.230	–
	Sherpa v2.2.1	NNPDF3.0NNLOnf4	Sherpa	–
tW	PowhegBox v2 [DR]	NNPDF3.0NLO	Pythia8.230	NLO+NNLL [52,53]
	PowhegBox v2 [DS]	NNPDF3.0NLO	Pythia8.230	NLO+NNLL [52,53]
	PowhegBox v2 [DR]	NNPDF3.0NLO	Herwig7.04	NLO+NNLL [52,53]
	MadGraph5_aMC@NLO v2.6.2 [DR]	CT10NLO	Pythia8.230	NLO+NNLL [52,53]
t-channel	PowhegBox v2	NNPDF3.0NLOnf4	Pythia8.230	NLO [54,55]
	PowhegBox v2	NNPDF3.0NLOnf4	Herwig7.04	NLO [54,55]
	MadGraph5_aMC@NLO v2.6.2	NNPDF3.0NLOnf4	Pythia8.230	NLO [54,55]
s-channel	PowhegBox v2	NNPDF3.0NLO	Pythia8.230	NLO [54,55]
	PowhegBox v2	NNPDF3.0NLO	Herwig7.04	NLO [54,55]
	MadGraph5_aMC@NLO v2.6.2	NNPDF3.0NLO	Pythia8.230	NLO [54,55]

Uncertainty source	Description		Components
$t\bar{t}$ cross-section	$\pm 6\%$		$t\bar{t}+$ light
$t\bar{t}+\geq 1b$ normalisation	Free-floating		$t\bar{t}+\geq 1b$
$t\bar{t}+\geq 1c$ normalisation	$\pm 100\%$		$t\bar{t}+\geq 1c$
NLO matching	MadGraph5_aMC@NLO+Pythia8 vs. PowhegBox+Pythia8		All
PS & hadronisation	PowhegBox+Herwig7 vs. PowhegBox+Pythia8		All
ISR	Varying α_S^{ISR} (PS), μ_{R}&μ_{F} (ME)	in PowhegBoxRes+Pythia8	$t\bar{t}+\geq 1b$
		in PowhegBox+Pythia8	$t\bar{t}+\geq 1c$, $t\bar{t}+$ light
FSR	Varying α_S^{FSR} (PS)	in PowhegBoxRes+Pythia8	$t\bar{t}+\geq 1b$
		in PowhegBox+Pythia8	$t\bar{t}+\geq 1c$, $t\bar{t}+$ light
$t\bar{t}+\geq 1b$ fractions	PowhegBox+Herwig7 vs. PowhegBox+Pythia8		$t\bar{t}+1b/1B$, $t\bar{t}+\geq 2b$
p_{T}^{bb} shape	Shape mismodelling measured from data		$t\bar{t}+\geq 1b$

ttH H→bb

ATLAS-CONF-2020-058

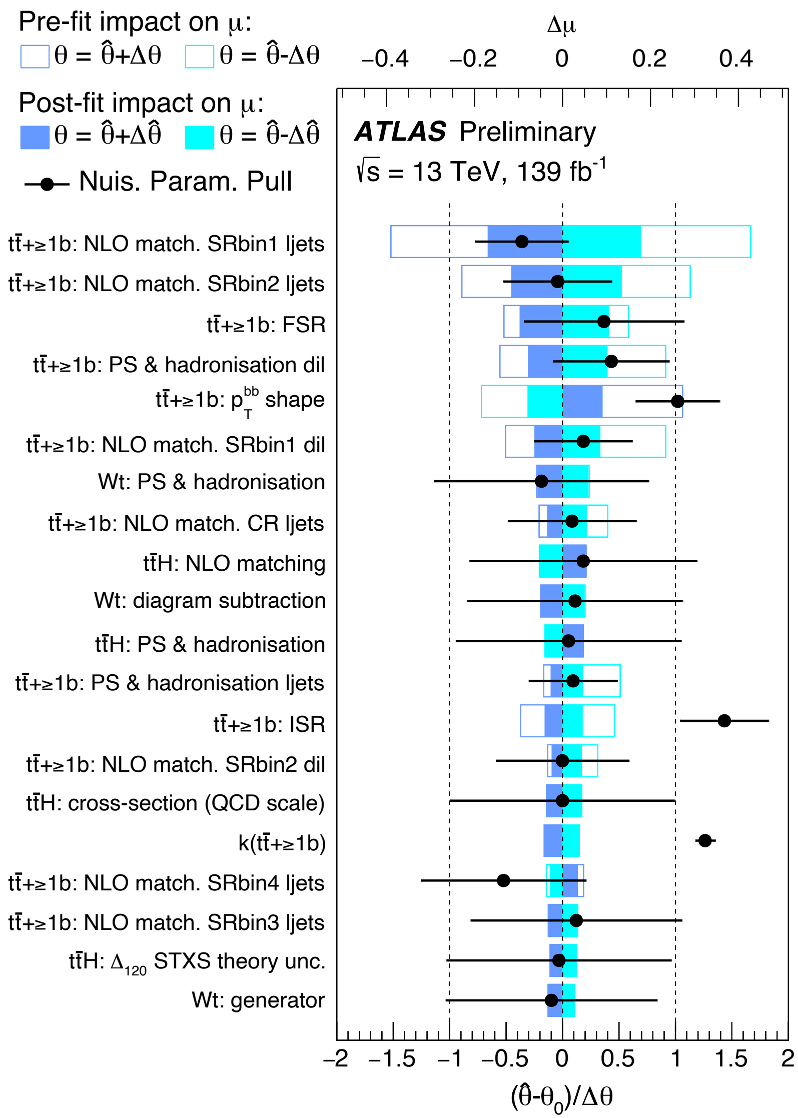

- **Selections**

Channel	Selection criteria
Common	$N_{\text{jets}} \geq 2$ and $N_{b\text{-jets}} \geq 1$
2ℓSS	Two same-charge (SS) very tight (T*) leptons, $p_{\text{T}} > 20$ GeV No τ_{had} candidates $m(\ell^+\ell^-) > 12$ GeV for all SF pairs **13 categories**: enriched with $t\bar{t}H$, $t\bar{t}W$, $t\bar{t}$, mat. conv, int. conv., split by lepton flavour, charge, jet and b-jet multiplicity
3ℓ	Three loose (L) leptons with $p_{\text{T}} > 10$ GeV; sum of light-lepton charges $= \pm 1$ Two SS very tight (T*) leptons, $p_{\text{T}} > 15$ GeV One OS (w.r.t the SS pair) loose-isolated (L*) lepton, $p_{\text{T}} > 10$ GeV No τ_{had} candidates $m(\ell^+\ell^-) > 12$ GeV and $\lvert m(\ell^+\ell^-) - 91.2\text{ GeV}\rvert > 10$ GeV for all SFOS pairs $\lvert m(3\ell) - 91.2\text{ GeV}\rvert > 10$ GeV **7 categories**: enriched with $t\bar{t}H$, $t\bar{t}W$, $t\bar{t}Z$, VV, $t\bar{t}$, mat. conv, int. conv
4ℓ	Four loose-isolated (L*) leptons; sum of light lepton charges $= 0$ $m(\ell^+\ell^-) > 12$ GeV and $\lvert m(\ell^+\ell^-) - 91.2\text{ GeV}\rvert > 10$ GeV for all SFOS pairs $m(4\ell) < 115$ GeV or $m(4\ell) > 130$ GeV **2 categories**: Zenr (Z-enriched;1 or 2 SFOS pairs) or Zdep (Z-depleted; 0 SFOS pairs)
$1\ell 2\tau_{\text{had}}$	One tight (T) lepton, $p_{\text{T}} > 27$ GeV Two OS τ_{had} candidates At least one tight τ_{had} candidate $N_{\text{jets}} \geq 3$
2ℓSS$1\tau_{\text{had}}$	2ℓSS selection, except: One medium τ_{had} candidate $N_{\text{jets}} \geq 4$
$3\ell 1\tau_{\text{had}}$	3ℓ selection, except: One medium τ_{had} candidate, of opposite charge to the total charge of the light leptons Two SS tight (T) leptons

- **b-jet multiplicity + lepton charge asymmetry**

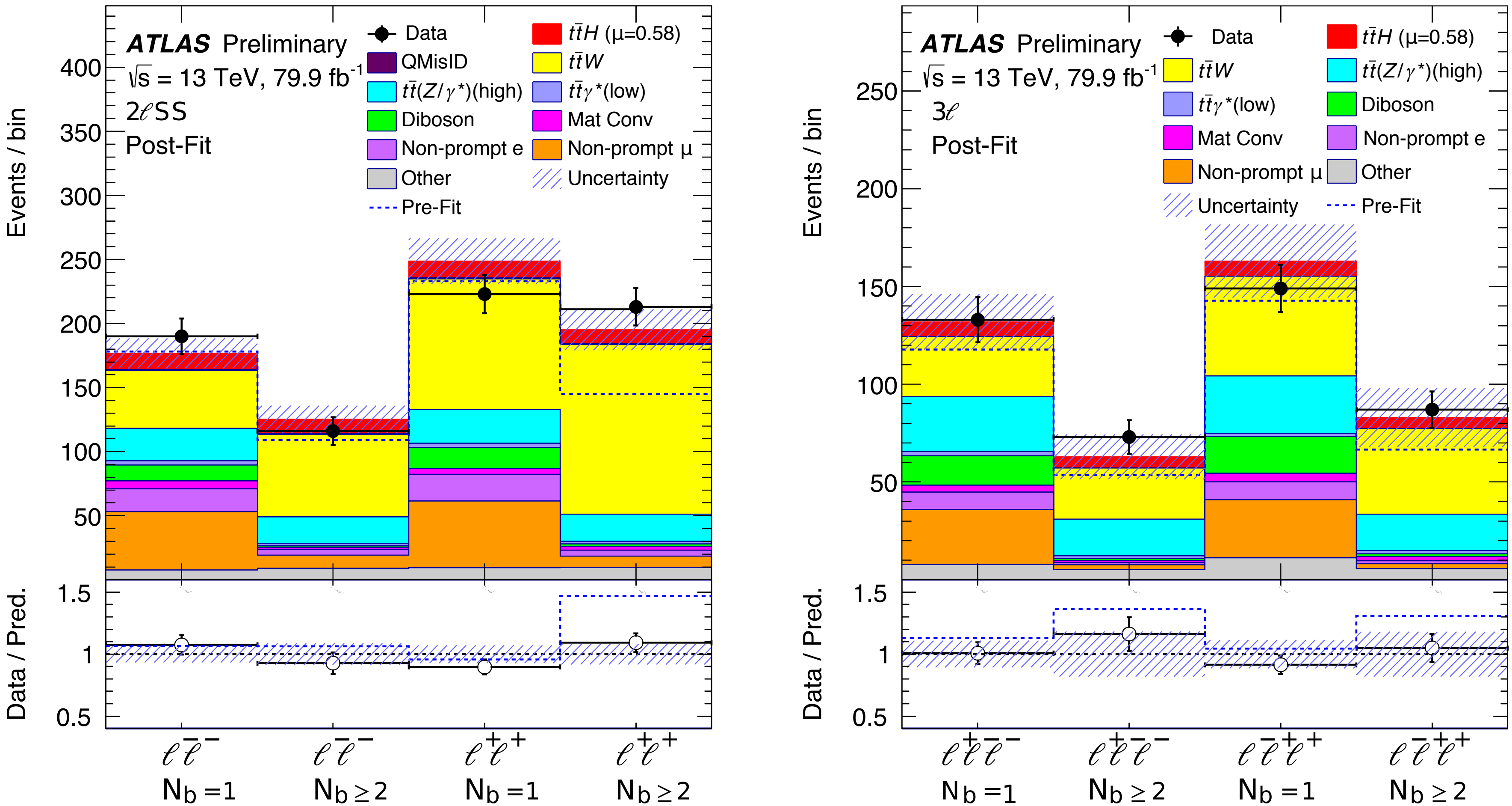

- **Signal regions**

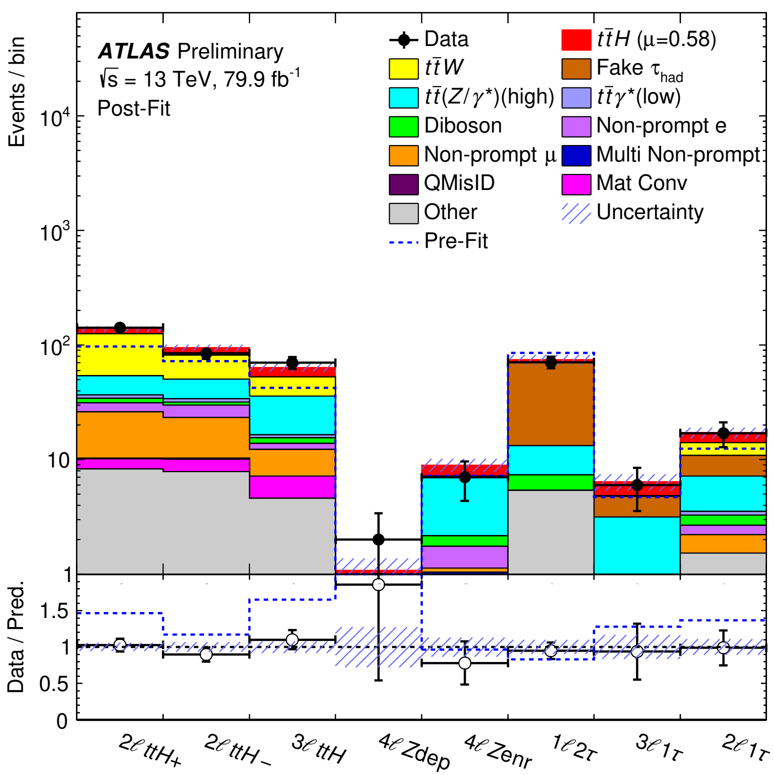

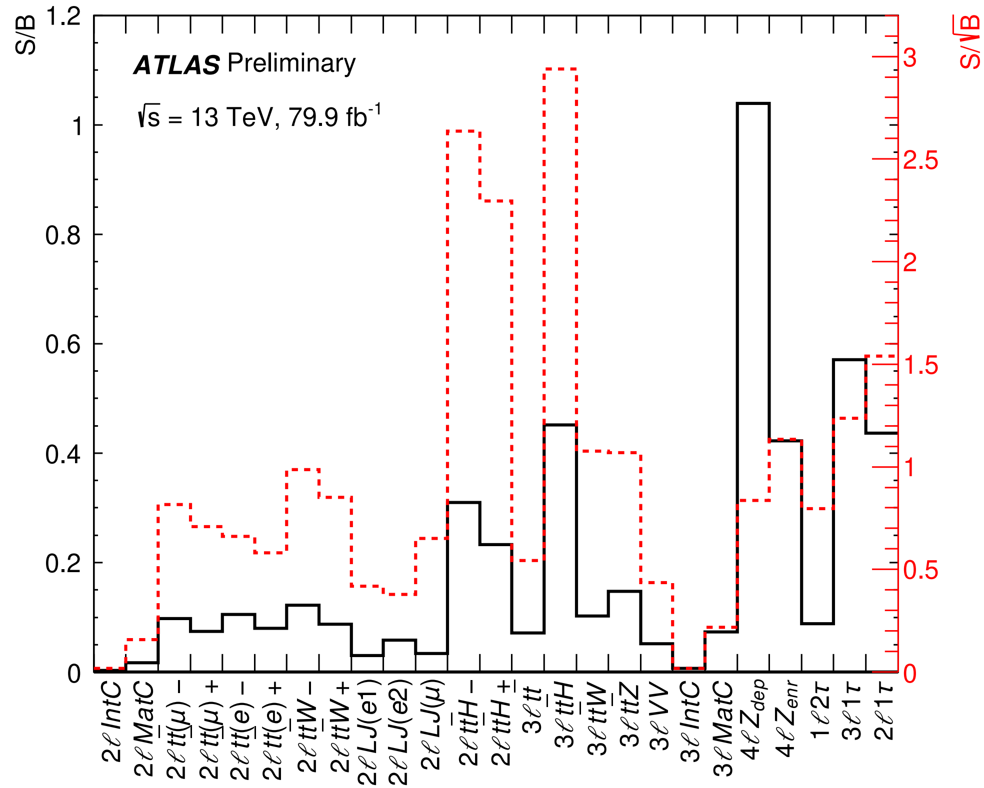

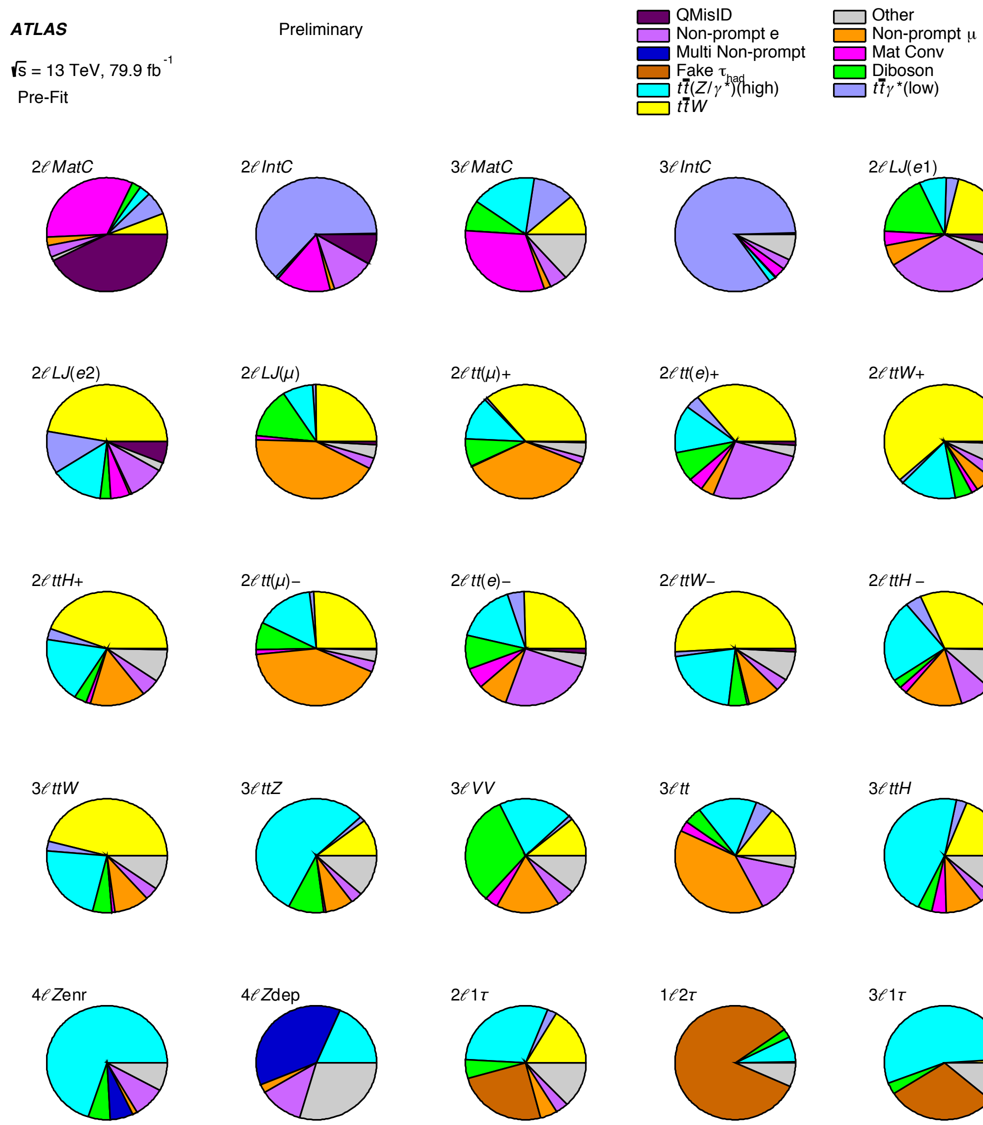
ATLAS Preliminary
√s = 13 TeV, 79.9 fb⁻¹
Pre-Fit
QMisID
Non-prompt e
Multi Non-prompt
Fake τhad
tt̄(Z/γ*)(high)
tt̄W
Other
Non-prompt μ
Mat Conv
Diboson
tt̄γ*(low)
2ℓ MatC
2ℓ IntC
3ℓ MatC
3ℓ IntC
2ℓ LJ(e1)
2ℓ LJ(e2)
2ℓ LJ(μ)
2ℓ tt(μ)+
2ℓ tt(e)+
2ℓ ttW+
2ℓ ttH+
2ℓ tt(μ)−
2ℓ tt(e)−
2ℓ ttW−
2ℓ ttH −
3ℓ ttW
3ℓ ttZ
3ℓ VV
3ℓ tt
3ℓ ttH
4ℓ Zenr
4ℓ Zdep
2ℓ1τ
1ℓ2τ
3ℓ1τ

ttH H→WW/ZZ/ττ

ATLAS-CONF-2019-045

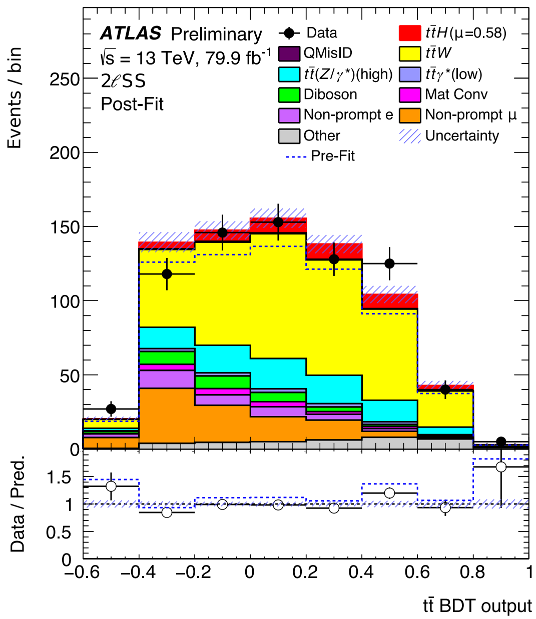

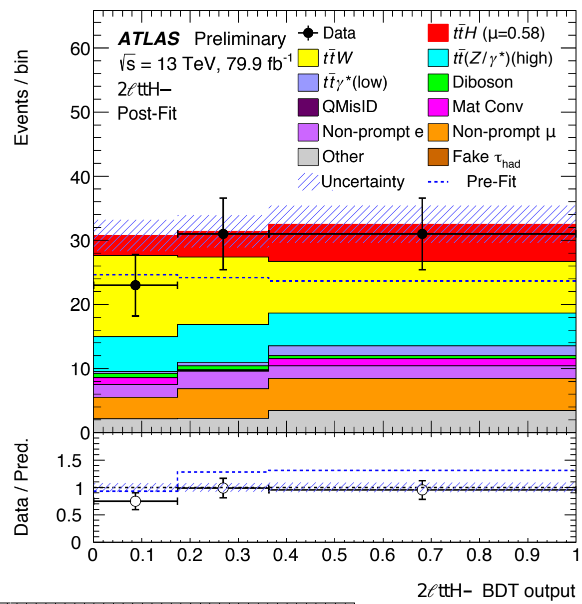

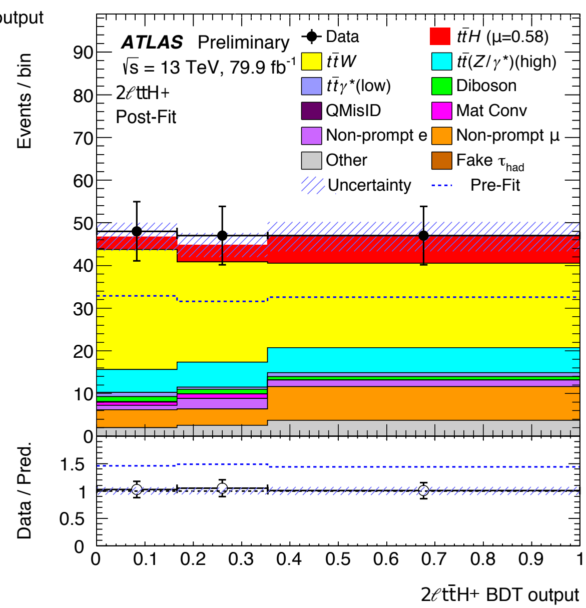

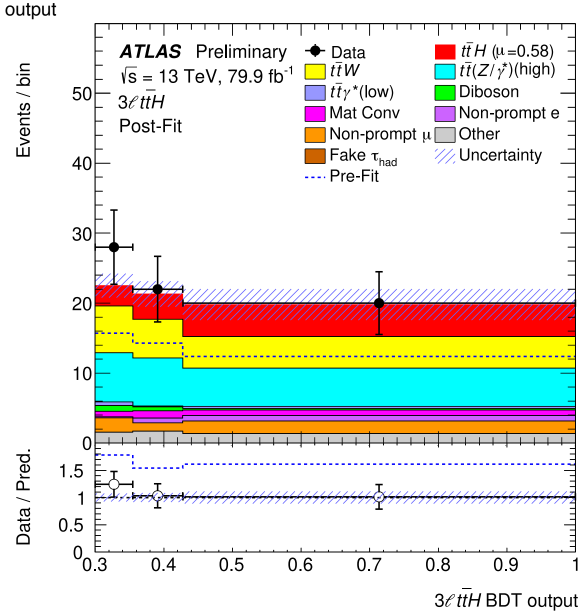

- **BDT outputs**

- **Systematics**

Uncertainty source	$\Delta\hat{\mu}$	
Jet energy scale and resolution	+0.13	−0.13
$t\bar{t}(Z/\gamma^*)$ (high mass) modelling	+0.09	−0.09
$t\bar{t}W$ modelling (radiation, generator, PDF)	+0.08	−0.08
Fake τ_{had} background estimate	+0.07	−0.07
$t\bar{t}W$ modelling (extrapolation)	+0.05	−0.05
$t\bar{t}H$ cross section	+0.05	−0.05
Simulation sample size	+0.05	−0.05
$t\bar{t}H$ modelling	+0.04	−0.04
Other background modelling	+0.04	−0.04
Jet flavour tagging and τ_{had} identification	+0.04	−0.04
Other experimental uncertainties	+0.03	−0.03
Luminosity	+0.03	−0.03
Diboson modelling	+0.01	−0.01
$t\bar{t}\gamma^*$ (low mass) modelling	+0.01	−0.01
Charge misassignment	+0.01	−0.01
Template fit (non-prompt leptons)	+0.01	−0.01
Total systematic uncertainty	+0.25	−0.22
Intrinsic statistical uncertainty	+0.23	−0.22
$t\bar{t}W$ normalisation factors	+0.10	−0.10
Non-prompt leptons normalisation factors (HF, material conversions)	+0.05	−0.05
Total statistical uncertainty	+0.26	−0.25
Total uncertainty	+0.36	−0.33

- **Selections 1/3**

Selection step	$2\ell SS + 0\tau_h$	$2\ell SS + 1\tau_h$
Targeted $t\bar{t}H$ decay	$t \to b\ell\nu$, $t \to bqq'$ with $H \to WW \to \ell\nu qq'$	$t \to b\ell\nu$, $t \to bqq'$ with $H \to \tau\tau \to \ell\nu\nu\tau_h\nu$
Targeted tH decays	$t \to b\ell\nu$, $H \to WW \to \ell\nu qq$	$t \to b\ell\nu$, $H \to \tau\tau \to \ell\tau_h + \nu$'s
Trigger	Single- and double-lepton triggers	
Lepton p_T	$p_T > 25\ /\ 15\,GeV$	$p_T > 25\ /\ 15\,GeV$ (e) or $10\,GeV$ (μ)
Lepton η	$\lvert\eta\rvert < 2.5$ (e) or 2.4 (μ)	
τ_h p_T	—	$p_T > 20\,GeV$
τ_h η	—	$\lvert\eta\rvert < 2.3$
τ_h identification	—	very loose
Charge requirements	2 SSleptons and charge quality requirements	2 SSleptons and charge quality requirements $\sum_{\ell,\tau_h} q = \pm 1$
Multiplicity of central jets	$\geq$3 jets	$\geq$3 jets
b tagging requirements	$\geq$1 tight b-tagged jet or $\geq$2 loose b-tagged jets	
Missing transverse momentum	$L_D > 30\,GeV$†	
Dilepton invariant mass	$\lvert m_{\ell\ell} - m_Z\rvert > 10\,GeV$‡ and $m_{\ell\ell} > 12\,GeV$	

Selection step	$3\ell + 0\tau_h$	$3\ell + 1\tau_h$
Targeted $t\bar{t}H$ decays	$t \to b\ell\nu$, $t \to b\ell\nu$ with $H \to WW \to \ell\nu qq'$; $t \to b\ell\nu$, $t \to bqq'$ with $H \to WW \to \ell\nu\ell\nu$; $t \to b\ell\nu$, $t \to bqq'$ with $H \to ZZ \to \ell\ell qq'$ or $\ell\ell\nu\nu$	$t \to b\ell\nu$, $t \to b\ell\nu$ with $H \to \tau\tau \to \ell\nu\nu\tau_h\nu$
Targeted tH decays	$t \to b\ell\nu$, $H \to WW \to \ell\nu\ell\nu$	—
Trigger	Single-, double- and triple-lepton triggers	
Lepton p_T	$p_T > 25\ /\ 15\ /\ 10\,GeV$	
Lepton η	$\lvert\eta\rvert < 2.5$ (e) or 2.4 (μ)	
τ_h p_T	—	$p_T > 20\,GeV$
τ_h η	—	$\lvert\eta\rvert < 2.3$
τ_h identification	—	very loose
Charge requirements	$\sum_{\ell} q = \pm 1$	$\sum_{\ell,\tau_h} q = 0$
Multiplicity of central jets	$\geq$2 jets	
b tagging requirements	$\geq$1 tight b-tagged jet or $\geq$2 loose b-tagged jets	
Missing transverse momentum	$L_D > 0\ /\ 30\ /\ 45\,GeV$‡	
Dilepton invariant mass	$m_{\ell\ell} > 12\,GeV$ and $\lvert m_{\ell\ell} - m_Z\rvert > 10\,GeV$§	
Four-lepton invariant mass	$m_{4\ell} > 140\,GeV$¶	—

† A complete description of this requirement can be found in the main text.
‡ Applied to all SFOS lepton pairs and to pairs of electrons of SS charge.
§ Applied to all SFOS lepton pairs.
¶ If the event contains two SFOS pairs of leptons that pass the loose lepton selection criteria.

- **Selections 2/3**

Selection step	$0\ell + 2\tau_h$	$1\ell + 1\tau_h$
Targeted $t\bar{t}H$ decays	$t \to bqq'$, $t \to bqq'$ with $H \to \tau\tau \to \tau_h\nu\tau_h\nu$	$t \to bqq'$, $t \to bqq'$ with $H \to \tau\tau \to \ell\nu\nu\tau_h\nu$
Trigger	Double-τ_h trigger	Single-lepton and lepton+τ_h triggers
Lepton p_T	—	$p_T > 30$ (e) or 25 GeV (μ)
Lepton η	—	$\|\eta\| < 2.1$
τ_h p_T	$p_T > 40$ GeV	$p_T > 30$ GeV
τ_h η	$\|\eta\| < 2.1$	
τ_h identification	loose	medium
Charge requirements	$\sum_{\tau_h} q = 0$	$\sum_{\ell,\tau_h} q = 0$
Multiplicity of central jets	$\geq$4 jets	
b tagging requirements	$\geq$1 tight b-tagged jet or $\geq$2 loose b-tagged jets	
Dilepton invariant mass	$m_{\ell\ell} > 12$ GeV	

Selection step	$1\ell + 2\tau_h$	$2\ell + 2\tau_h$
Targeted $t\bar{t}H$ decays	$t \to b\ell\nu$, $t \to bqq'$ with $H \to \tau^+\tau^- \to \tau_h\nu\tau_h\nu$	$t \to b\ell\nu$, $t \to b\ell\nu$ with $H \to \tau^+\tau^- \to \tau_h\nu\tau_h\nu$
Trigger	Single-lepton and lepton+τ_h triggers	Single- and double-lepton triggers
Lepton p_T	$p_T > 30$ (e) or 25 GeV (μ)	$p_T > 25$ / 10 (15) GeV (e)
Lepton η	$\|\eta\| < 2.1$	$\|\eta\| < 2.5$ (e) or 2.4 (μ)
τ_h p_T	$p_T > 30$ / 20 GeV	$p_T > 20$ GeV
τ_h η	$\|\eta\| < 2.1$	$\|\eta\| < 2.3$
τ_h identification	medium	medium
Charge requirements	$\sum_{\ell,\tau_h} q = \pm 1$	$\sum_{\ell,\tau_h} q = 0$
Multiplicity of central jets	$\geq$3 jets	$\geq$2 jets
b tagging requirements	$\geq$1 tight b-tagged jet or $\geq$2 loose b-tagged jets	
Missing transverse momentum	—	$L_D > 0$ / 30 / 45 GeV†
Dilepton invariant mass	$m_{\ell\ell} > 12$ GeV	

† A complete description of this requirement can be found in the main text.

- **Selections 3/3**

Selection step	$2\ell\text{OS} + 1\tau_h$	$4\ell + 0\tau_h$
Targeted $t\bar{t}H$ decays	$t \to b\ell\nu$, $t \to bqq'$ with $H \to \tau^+\tau^- \to \ell\nu\nu\tau_h\nu$	$t \to b\ell\nu$, $t \to b\ell\nu$ with $H \to WW \to \ell\nu\ell\nu$ $t \to b\ell\nu$, $t \to b\ell\nu$ with $H \to ZZ \to \ell\ell qq'$ or $\ell\ell\nu\nu$
Trigger	Single- and double-lepton triggers	Single-, double- and triple-lepton triggers
Lepton p_T	$p_T > 25\ /\ 15\,\text{GeV}$ (e) or $10\,\text{GeV}$ (μ)	$p_T > 25\ /\ 15\ /\ 15\ /\ 10\,\text{GeV}$
Lepton η	$\lvert\eta\rvert < 2.5$ (e) or 2.4 (μ)	
τ_h p_T	$p_T > 20\,\text{GeV}$	—
τ_h η	$\lvert\eta\rvert < 2.3$	—
τ_h identification	tight	—
Charge requirements	$\sum_{\ell} q = 0$ and $\sum_{\ell,\tau_h} q = \pm 1$	$\sum_{\ell} q = 0$
Multiplicity of central jets	$\geq$3 jets	$\geq$2 jets
b tagging requirements	$\geq$1 tight b-tagged jet or $\geq$2 loose b-tagged jets	
Missing transverse momentum	$L_D > 30\,\text{GeV}^{\dagger}$	$L_D > 0\ /\ 30\ /\ 45\,\text{GeV}^{\ddagger}$
Dilepton invariant mass	$m_{\ell\ell} > 12\,\text{GeV}$	$\lvert m_{\ell\ell} - m_Z\rvert > 10\,\text{GeV}^{\S}$ and $m_{\ell\ell} > 12\,\text{GeV}$
Four-lepton invariant mass	—	$m_{4\ell} > 140\,\text{GeV}^{\P}$

† Only applied to events containing two electrons.
‡ A complete description of this requirement can be found in the main text.
§ Applied to all SFOS lepton pairs.
¶ If the event contains two SFOS pairs of leptons passing the loose lepton selection criteria.

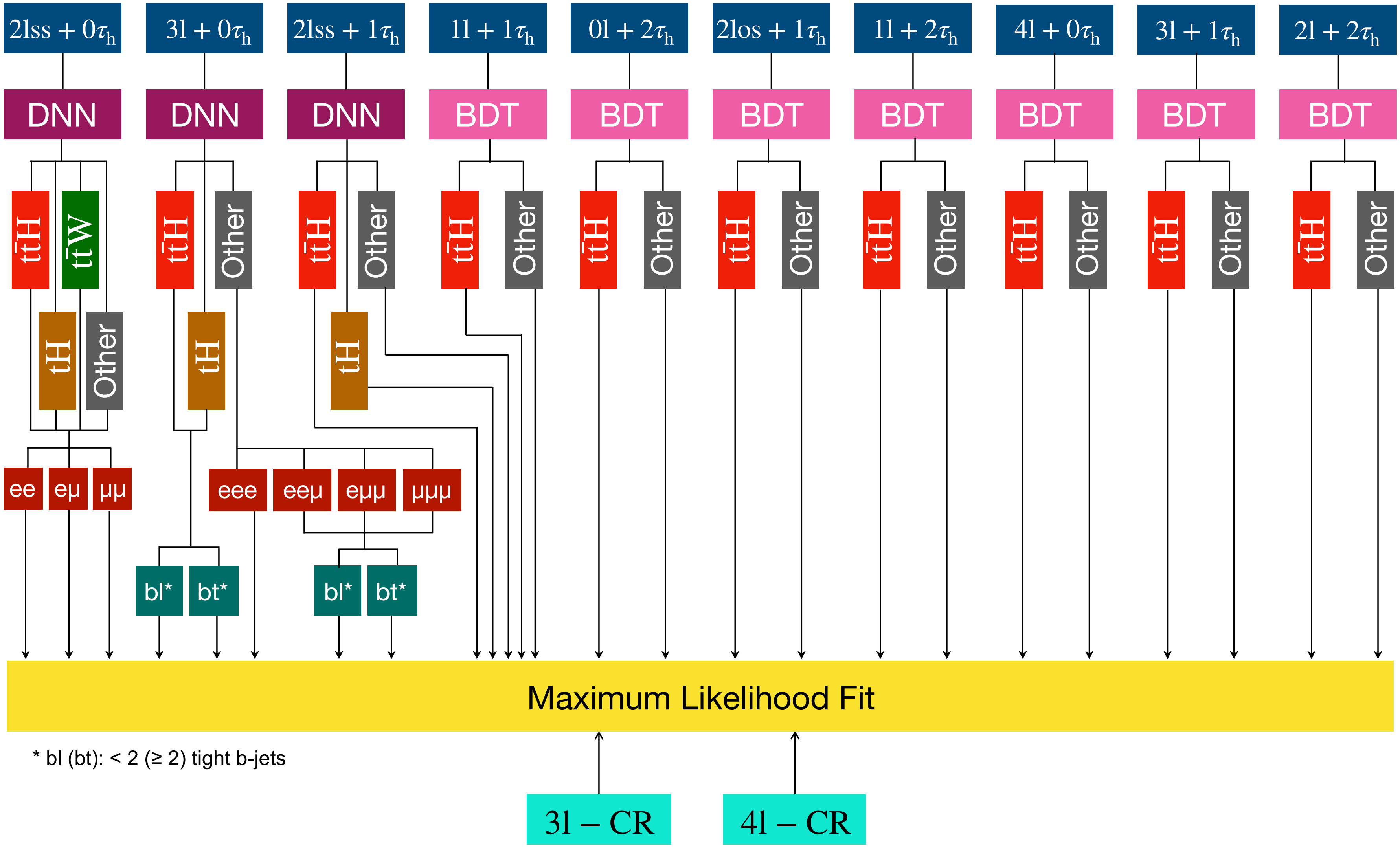

* bl (bt): < 2 (≥ 2) tight b-jets

- **Lepton fake rate measurement from multijet data**

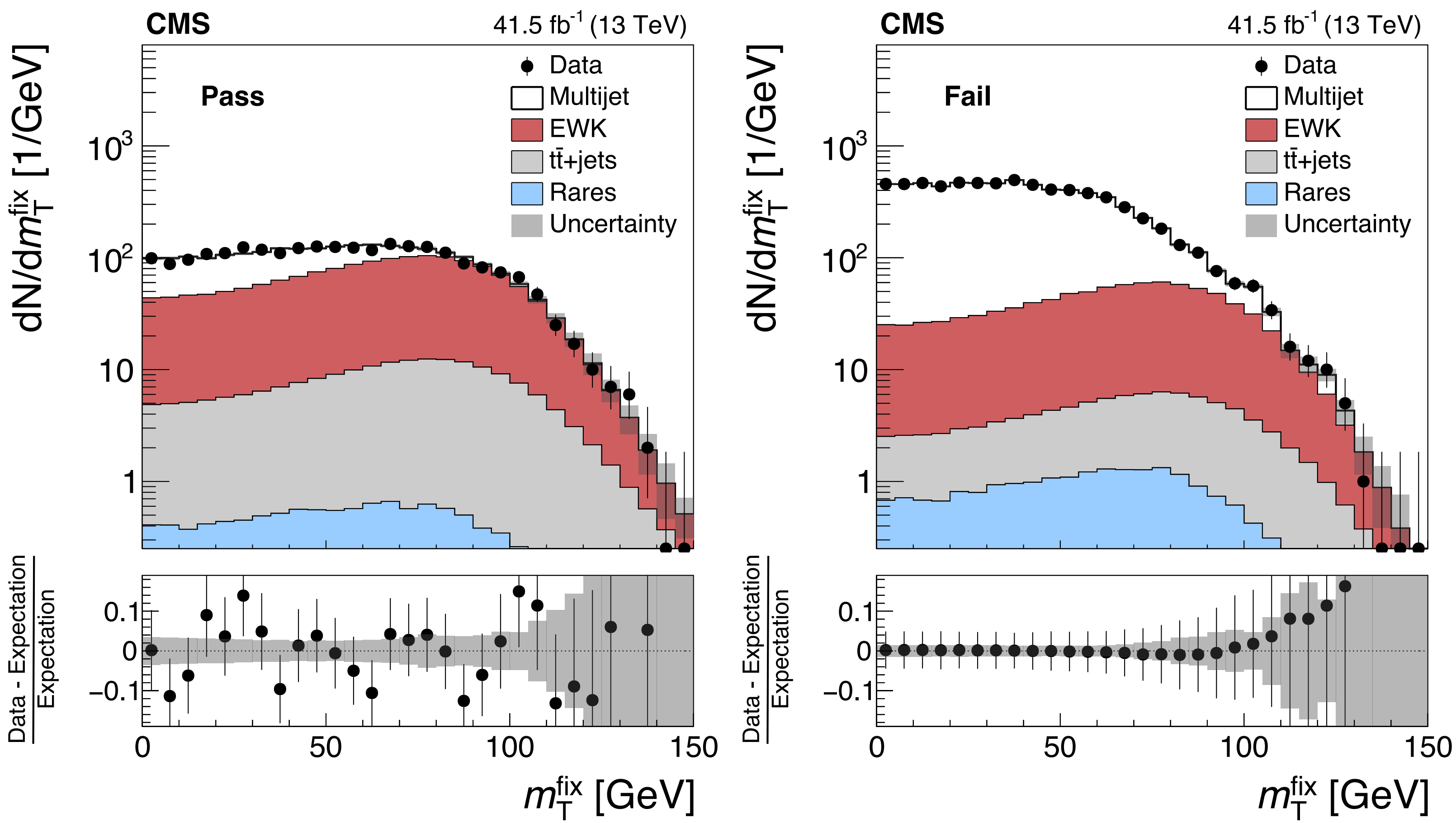

- **Lepton fake rate measurement from multijet data**

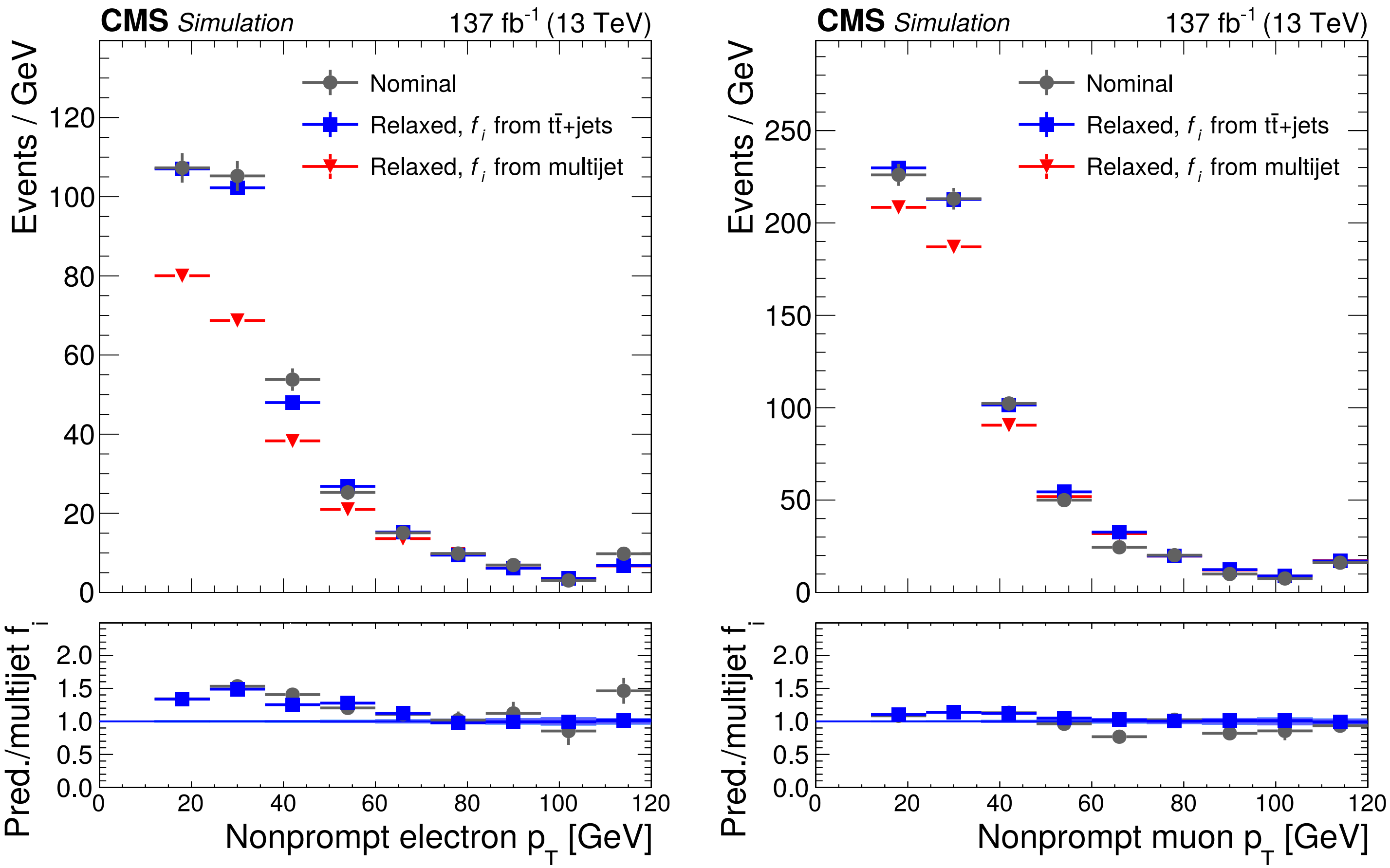

- **Charge flip measurement**

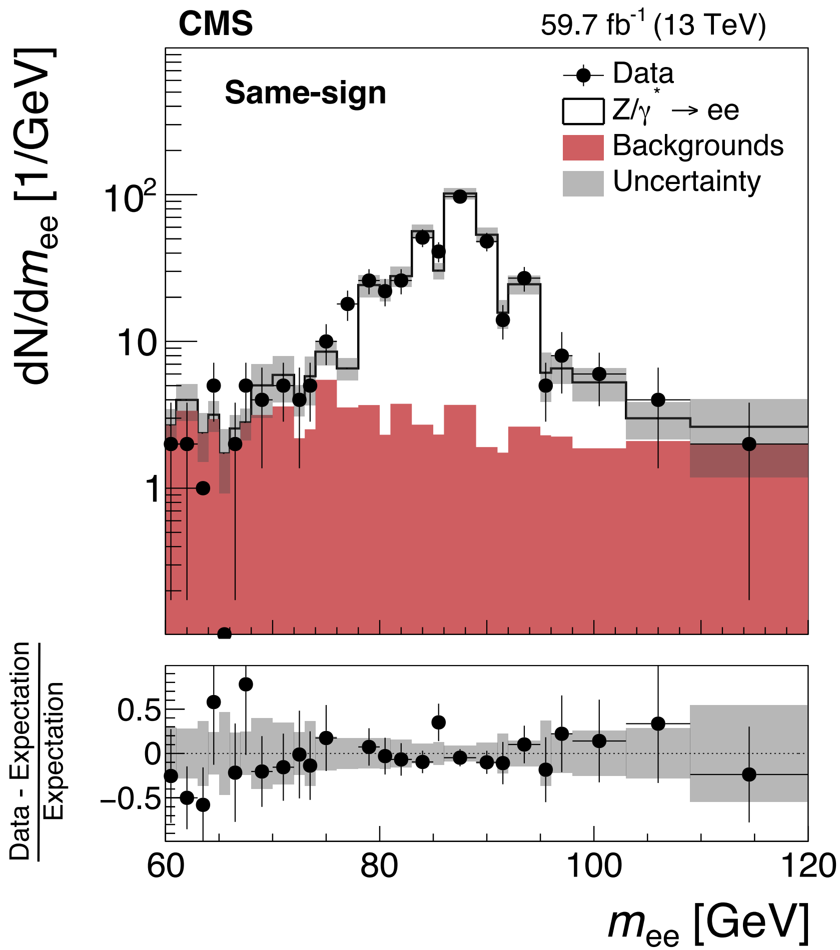

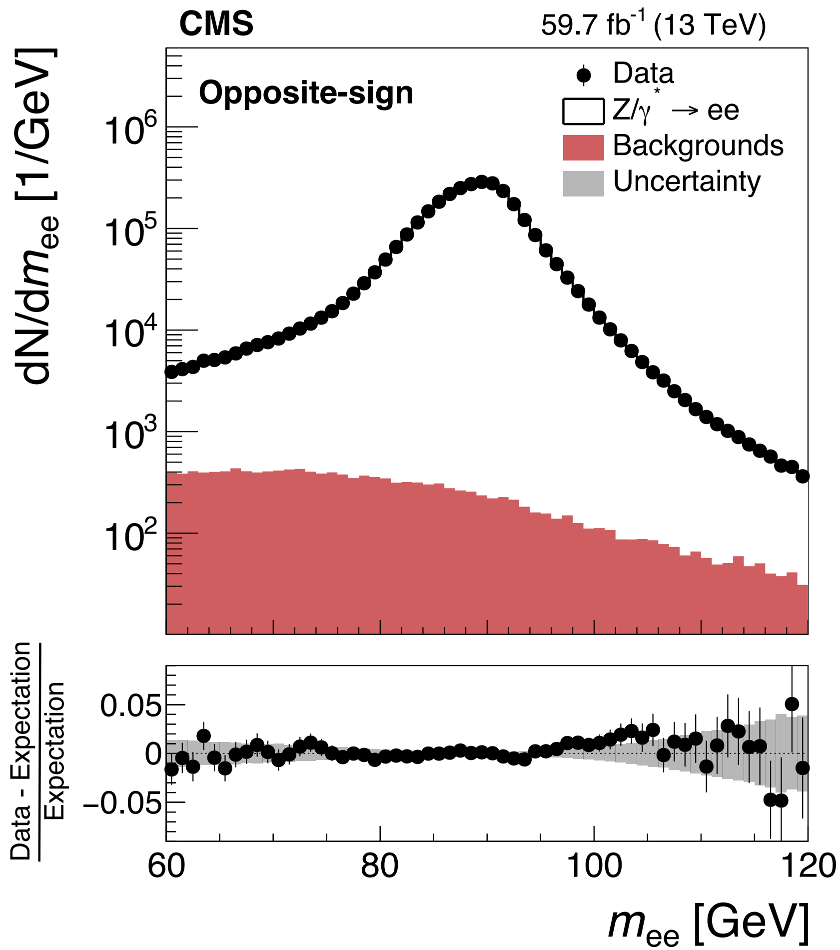

ttH H→WW/ZZ/ττ

CMS-HIG-19-008

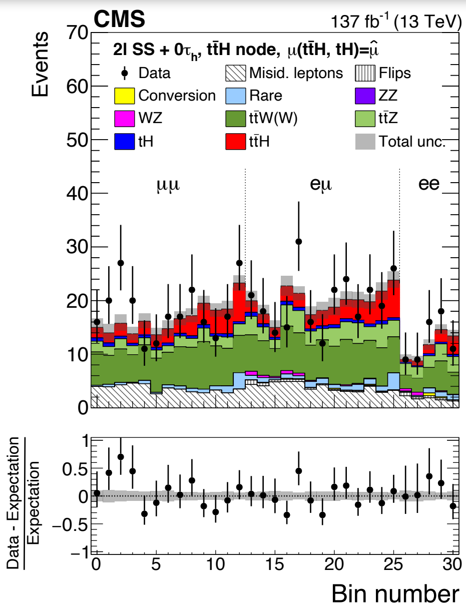

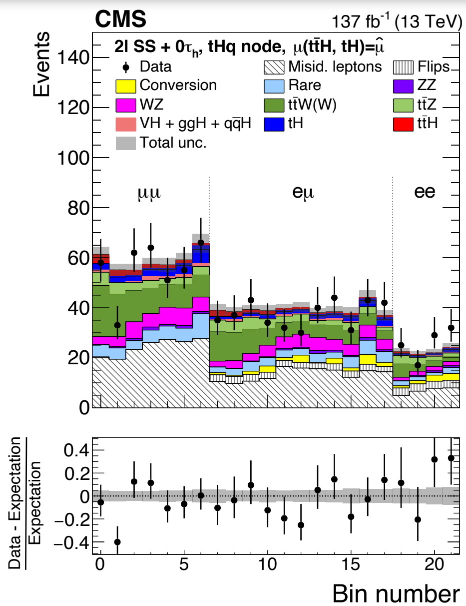

- **2lSS ANN output nodes**

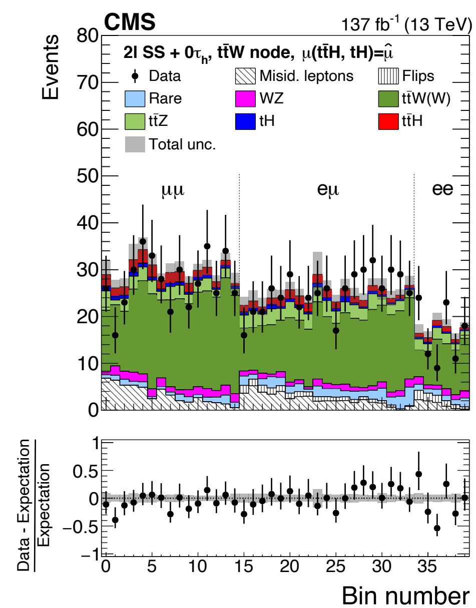

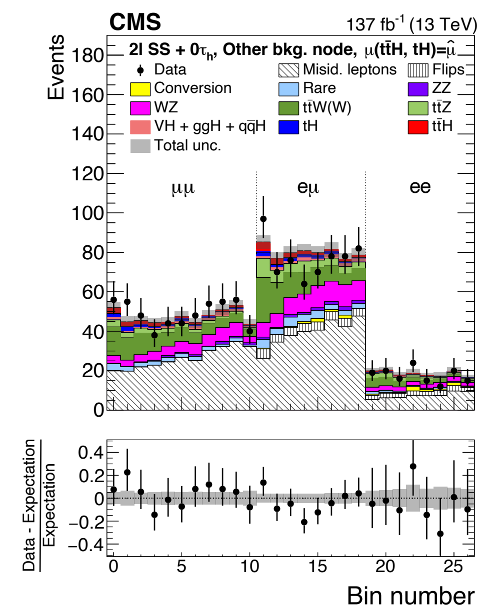

ttH H→WW/ZZ/$\tau\tau$

CMS-HIG-19-008

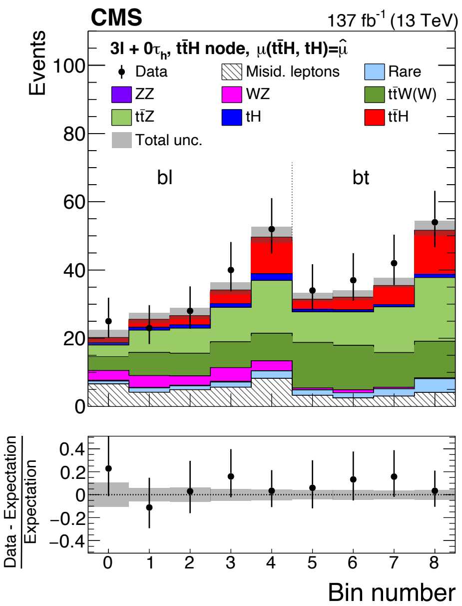

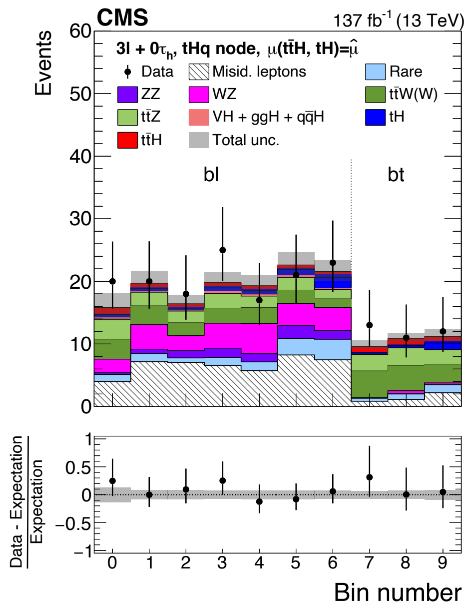

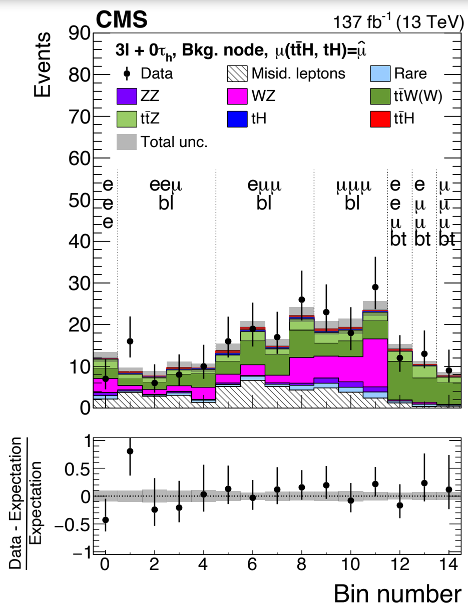

- **3l ANN output nodes**

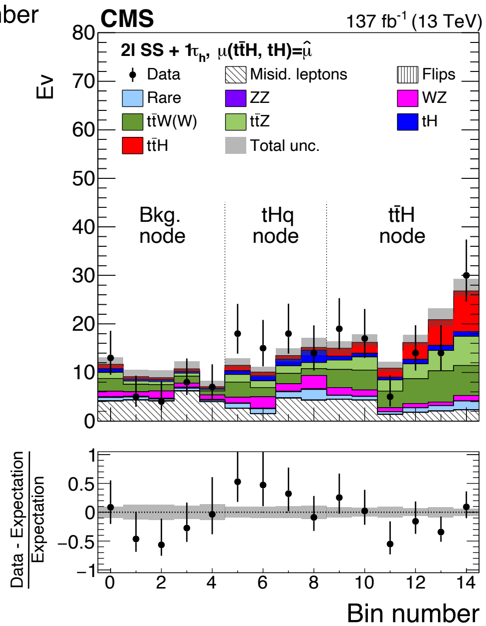

- **2lSS+1τ ANN output nodes**

ttH H→WW/ZZ/ττ

CMS-HIG-19-008

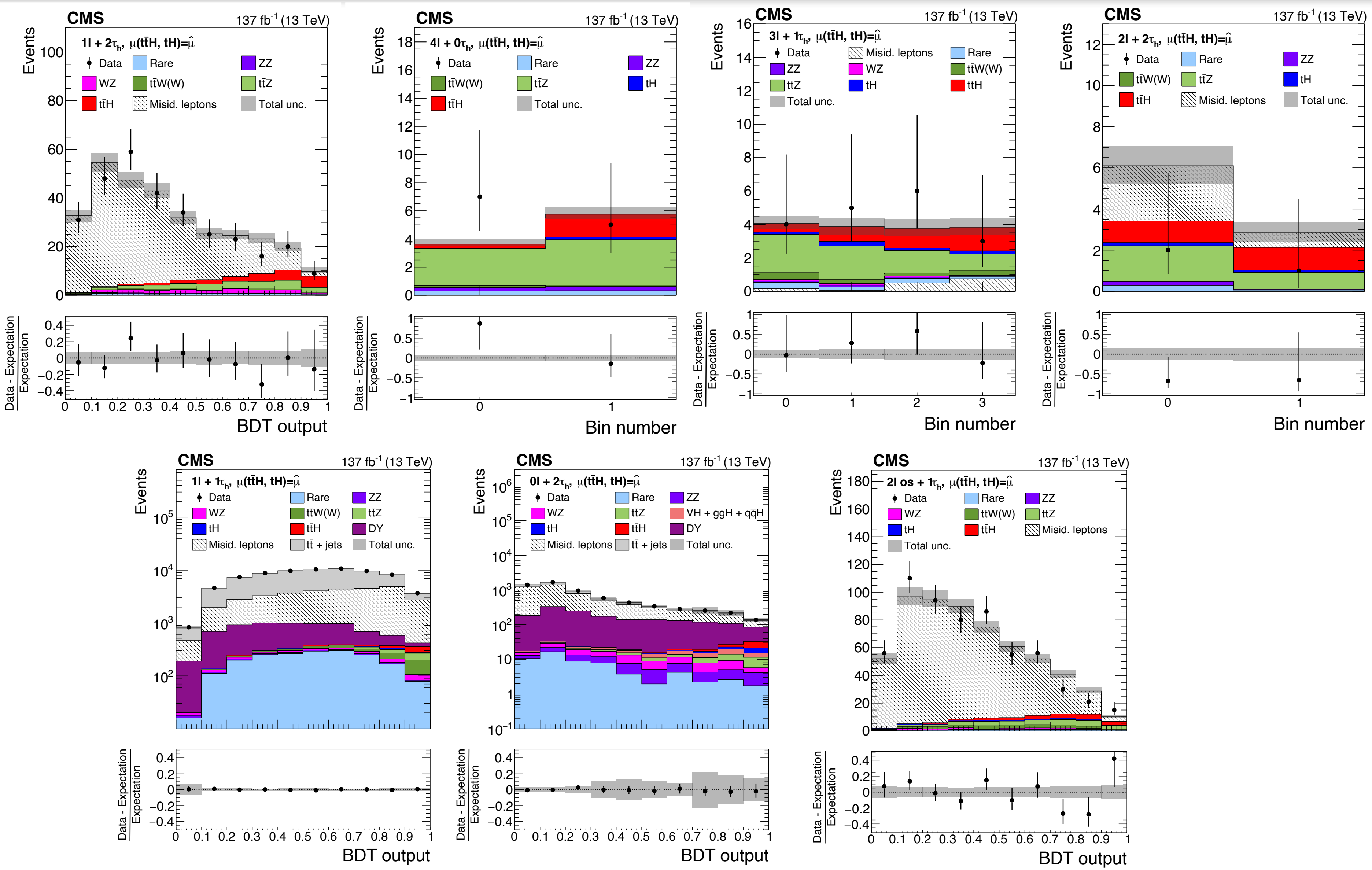

- **Control regions**

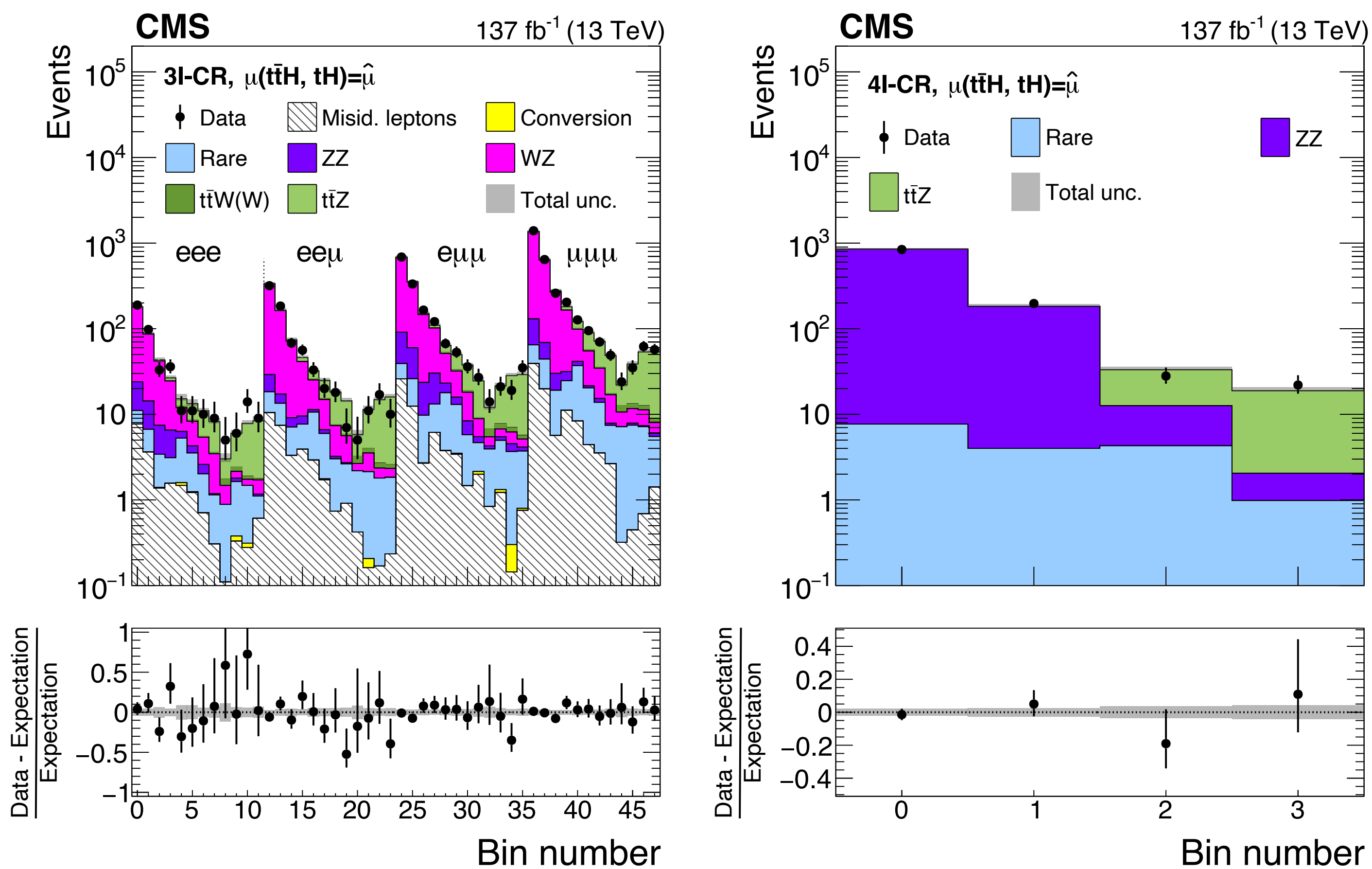

- **Systematics**

Source	$\Delta\mu_{t\bar{t}H}/\mu_{t\bar{t}H}$ [%]	$\Delta\mu_{tH}/\mu_{tH}$ [%]	$\Delta\mu_{t\bar{t}W}/\mu_{t\bar{t}W}$ [%]	$\Delta\mu_{t\bar{t}Z}/\mu_{t\bar{t}Z}$ [%]
Trigger efficiency	2.3	8.1	1.2	1.9
e, μreconstruction and identification efficiency	2.9	7.1	1.7	3.2
τ_h identification efficiency	4.6	9.1	1.7	1.3
b tagging efficiency and mistag rate	3.6	13.6	1.3	2.9
Misidentified leptons and flips	6.0	36.8	2.6	1.4
Jet energy scale and resolution	3.4	8.3	1.1	1.2
MC sample and sideband statistical uncertainty	7.1	27.2	2.4	2.3
Theory-related sources	4.6	18.2	2.0	4.2
Normalization of MC-estimated processes	13.3	12.3	13.9	11.3
Integrated luminosity	2.2	4.6	1.8	3.1
Statistical uncertainty	20.9	48.0	5.9	5.8

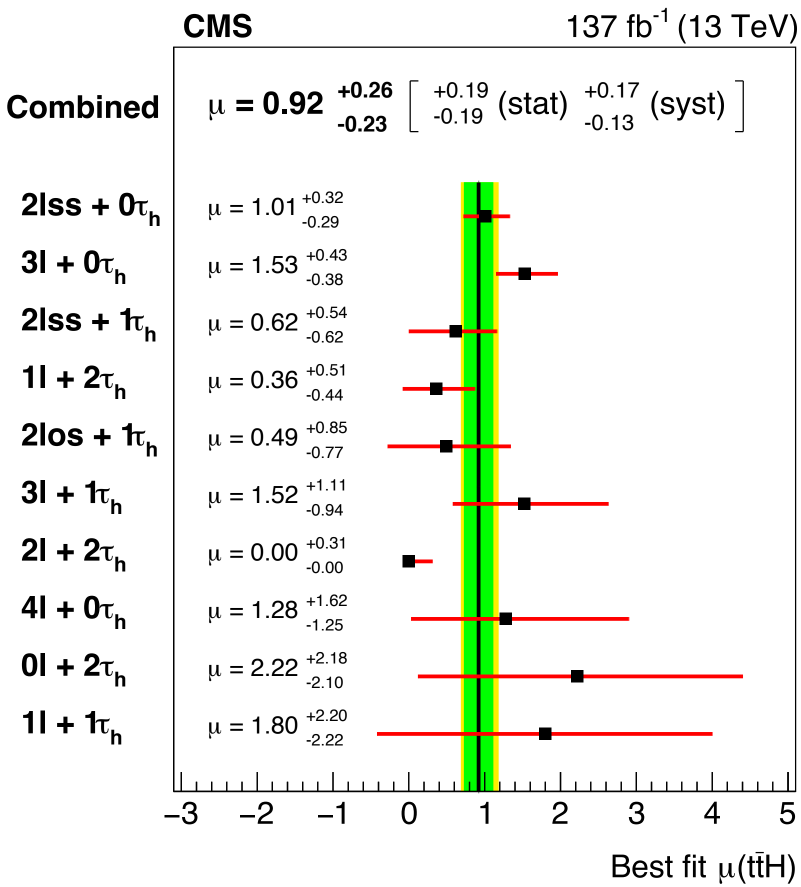

CMS
137 fb^{-1} (13 TeV)
Combined
μ = 0.92 $^{+0.26}_{-0.23}$ [$^{+0.19}_{-0.19}$ (stat) $^{+0.17}_{-0.13}$ (syst)]
2lss + 0τ_h
μ = 1.01 $^{+0.32}_{-0.29}$
3l + 0τ_h
μ = 1.53 $^{+0.43}_{-0.38}$
2lss + 1τ_h
μ = 0.62 $^{+0.54}_{-0.62}$
1l + 2τ_h
μ = 0.36 $^{+0.51}_{-0.44}$
2los + 1τ_h
μ = 0.49 $^{+0.85}_{-0.77}$
3l + 1τ_h
μ = 1.52 $^{+1.11}_{-0.94}$
2l + 2τ_h
μ = 0.00 $^{+0.31}_{-0.00}$
4l + 0τ_h
μ = 1.28 $^{+1.62}_{-1.25}$
0l + 2τ_h
μ = 2.22 $^{+2.18}_{-2.10}$
1l + 1τ_h
μ = 1.80 $^{+2.20}_{-2.22}$
−3 −2 −1 0 1 2 3 4 5
Best fit $\mu(t\bar{t}H)$

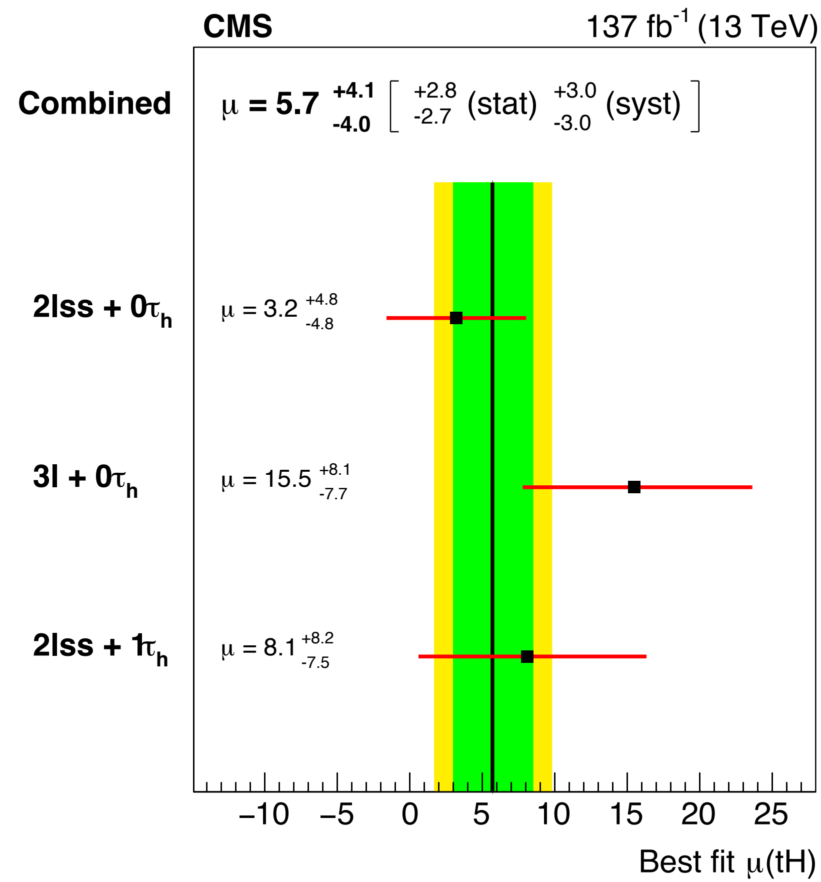

CMS
137 fb^{-1} (13 TeV)
Combined
μ = 5.7 $^{+4.1}_{-4.0}$ [$^{+2.8}_{-2.7}$ (stat) $^{+3.0}_{-3.0}$ (syst)]
2lss + 0τ_h
μ = 3.2 $^{+4.8}_{-4.8}$
3l + 0τ_h
μ = 15.5 $^{+8.1}_{-7.7}$
2lss + 1τ_h
μ = 8.1 $^{+8.2}_{-7.5}$
−10 −5 0 5 10 15 20 25
Best fit $\mu(tH)$

CMS-HIG-19-008

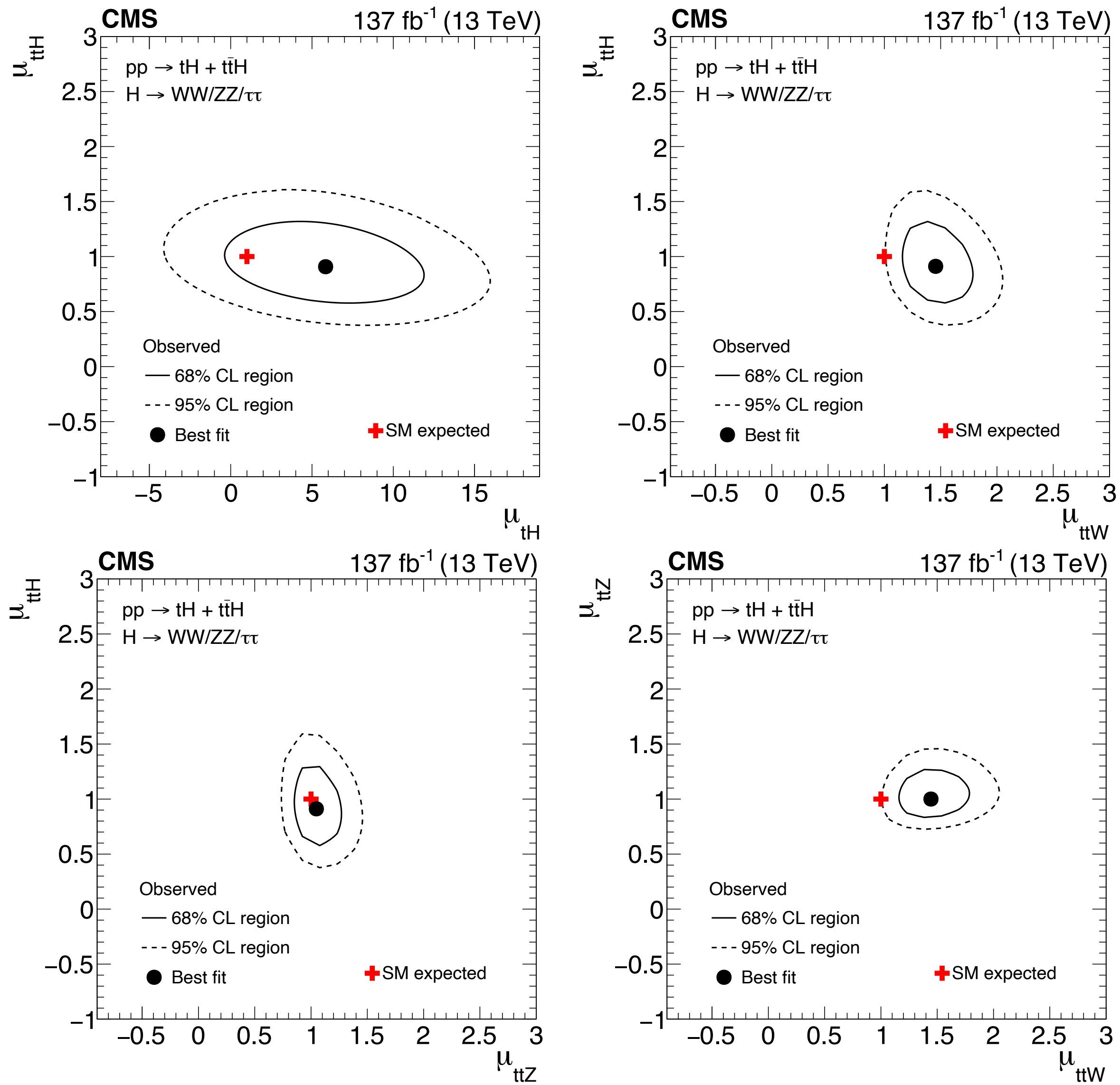

ttH H→WW/ZZ/ττ

ATLAS-CONF-2019-045 / CMS-HIG-19-008

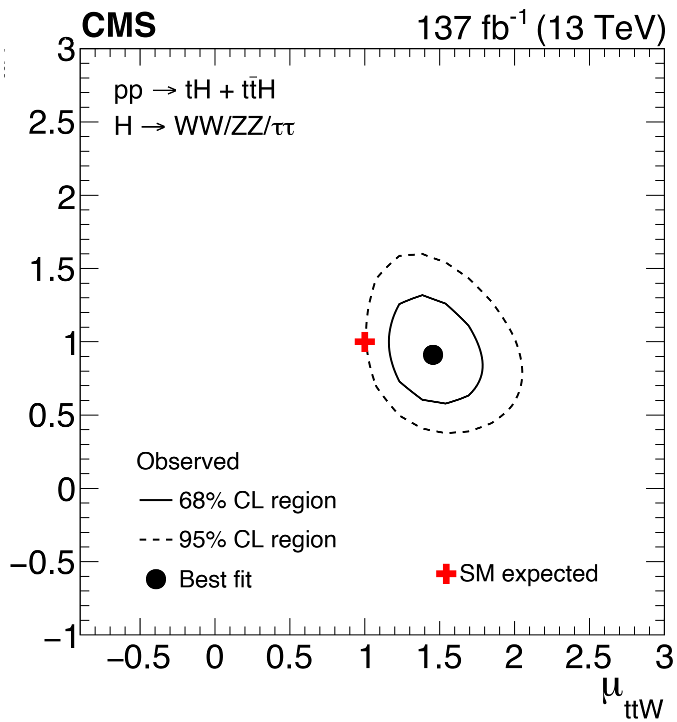

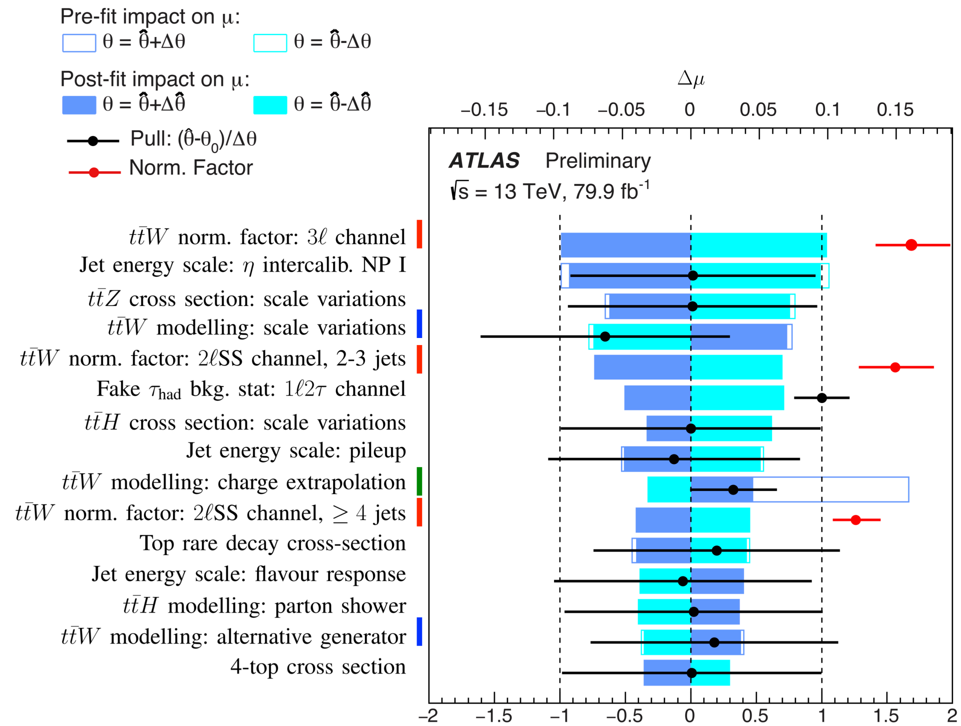

μ(ttW) = 1.43 ± 0.21

Inclusive μ(ttW) = 1.39 ± 0.17

- **Different ttW cross-sections used for ATLAS + CMS:** ATLAS used state-of-the art corrections from ttW+1-jet diagrams, scale factor 1.09 for nominal cross-section (601 ± 76 fb) https://arxiv.org/abs/1711.02116

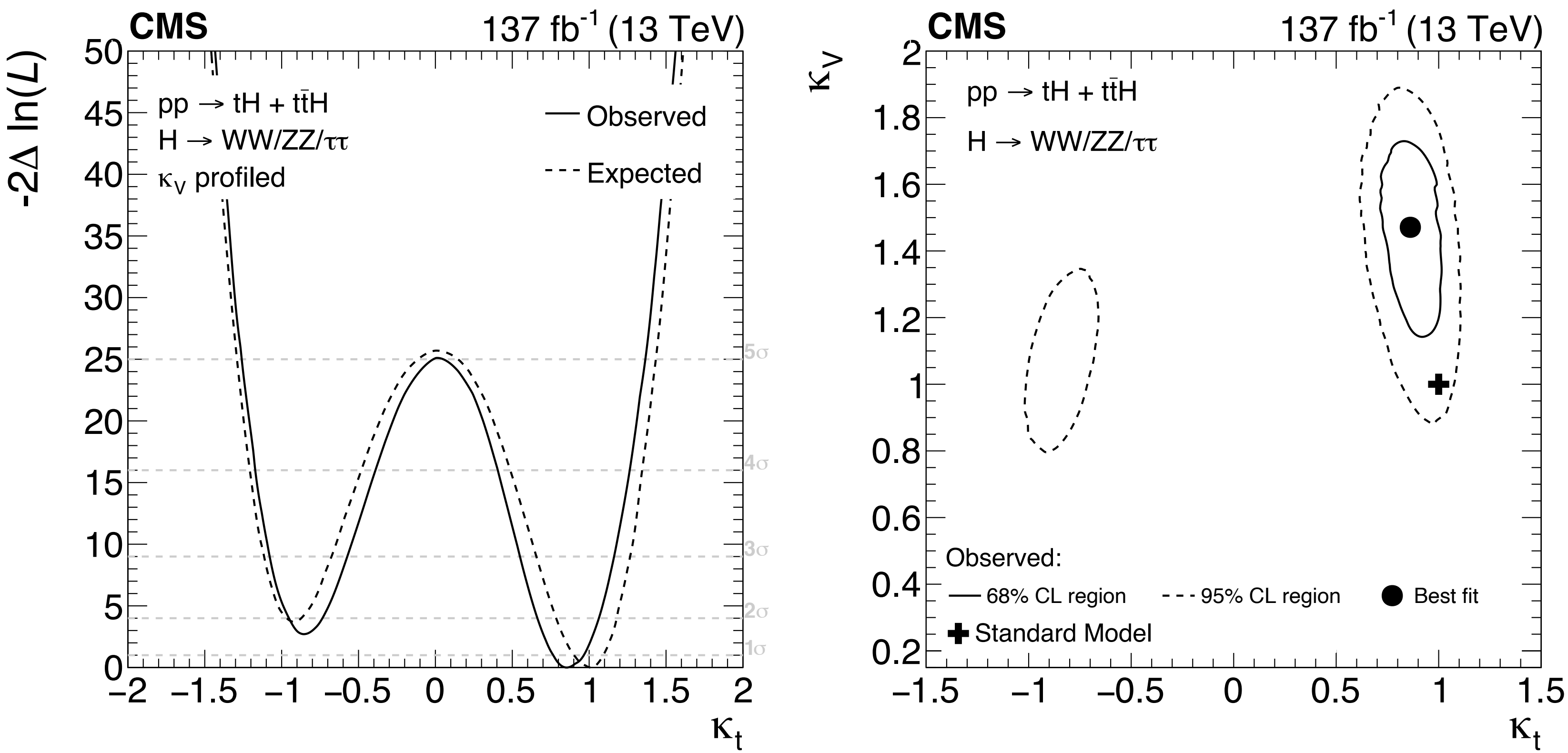
CMS
137 fb-1 (13 TeV)
-2Δ ln(L)
pp → tH + tt̄H
H → WW/ZZ/ττ
κV profiled
Observed
Expected
5σ
4σ
3σ
2σ
1σ
κt
κV
Observed:
68% CL region
95% CL region
Best fit
Standard Model

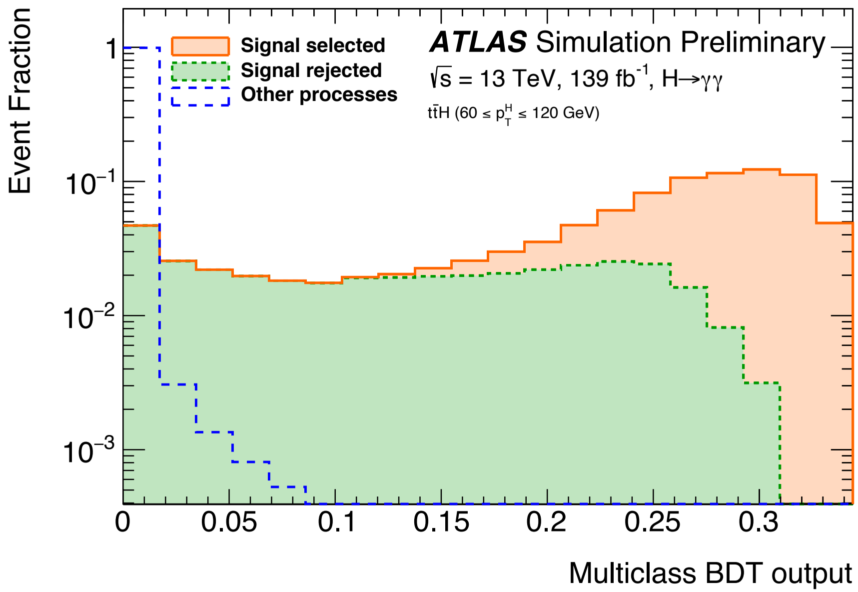

- **ttH STXS BDT multi-classifier**

- **ttH vs background BDT**

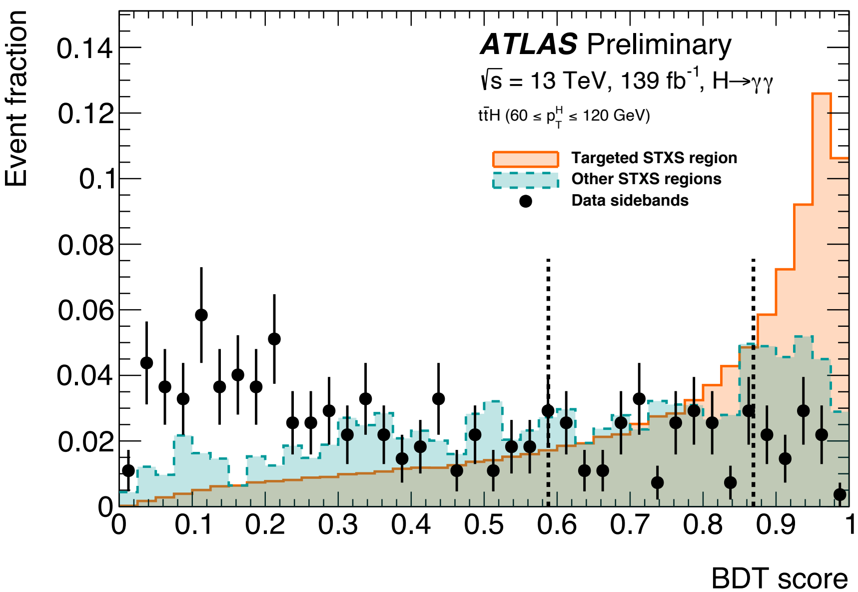

<table>
<tr><th>STXS regions</th><th>Multi-class BDT</th><th>STXS regions</th><th>Binary BDT</th></tr>
<tr><td>$gg \to H$</td><td rowspan="6">di-photon p_{T} and absolute rapidity;
di-jet p_{T}, mass, Δy, $\Delta\phi$, $\Delta\eta$ between the 2 jets;
p_{T}, mass of $\gamma\gamma + j$ and $\gamma\gamma + jj$,
Δy, $\Delta\phi$ between $\gamma\gamma$ and jj,
minimum ΔR between jets and photons,
mass of the sum of all jets;
di-lepton p_{T}, di-e or di-μ mass,
E_{T}^{miss}, p_{T} of lepton + E_{T}^{miss};
p_T, η, ϕ, mass of top candidates;
Number of jets, barrel jets ($|\eta| < 2.5$), b-jets and leptons;
leading jet p_T, sum p_{T} of all jets
$\sum E^{\mathrm{T}}$, E_{T}^{miss} significance;
Average interaction per crossing, number of primary vertices</td><td rowspan="2">individual STXS regions from $gg \to H$ or $qq' \to Hqq'$</td><td rowspan="2">Multi-class BDT variables, and
$\Delta\phi$, $\Delta\eta$ between the 2 photons ($\Delta\phi_{\gamma\gamma}$, $\Delta\eta_{\gamma\gamma}$);
Number of electrons and muons;
E_{T}^{miss}, $\sum E^{\mathrm{T}}$, E_{T}^{miss} significance, and
E_{T}^{miss} azimuthal angle computed from hardest vertex;
$\gamma\gamma$ $\vec{p}_{\mathrm{T}}$ projected to its thrust axis ($p_{\mathrm{Tt}}^{\gamma\gamma}$);
Half difference between di-photon η and sum η of leading 2 jets (η^{Zepp});
$\phi^*_{\gamma\gamma} = \tan(\frac{\pi-|\Delta\phi_{\gamma\gamma}|}{2})\sqrt{1-\tanh^2(\frac{\Delta\eta_{\gamma\gamma}}{2})}$
$\cos\theta^*_{\gamma\gamma} = |\frac{(E^{\gamma_1}+p_z^{\gamma_1})\cdot(E^{\gamma_2}-p_z^{\gamma_2})-(E^{\gamma_1}-p_z^{\gamma_1})\cdot(E^{\gamma_2}+p_z^{\gamma_2})}{m_{\gamma\gamma}+\sqrt{(m^2_{\gamma\gamma}+(p_{\mathrm{T}}^{\gamma\gamma})^2)}}|$</td></tr>
<tr><td>$qq' \to Hqq'$</td></tr>
<tr><td>$qq \to H\ell\nu$</td><td>WH STXS regions combined</td><td rowspan="2">$p_{\mathrm{T}}/m_{\gamma\gamma}$, η, ϕ of 2 leading photons;
p_{T}, η, ϕ of 2 leading leptons;
E_{T}^{miss}, E_{T}^{miss} significance, E_{T}^{miss} azimuthal angle;
Whether or not the E_{T}^{miss} built from di-photon vertex is
larger than that built from the hardest vertex by more than 30 GeV;
di-lepton mass, and transverse mass of lepton + E_{T}^{miss}</td></tr>
<tr><td>$qq \to H\ell\ell$</td><td>ZH STXS regions combined</td></tr>
<tr><td>$t\bar{t}H$</td><td>$t\bar{t}H$ STXS regions combined</td><td rowspan="2">p_{T}, η, ϕ of 2 leading photons;
p_{T}, η, ϕ and B-tagging scores of 6 leading jets;
E_{T}^{miss}, E_{T}^{miss} significance, E_{T}^{miss} azimuthal angle;
Top reconstruction BDT scores</td></tr>
<tr><td>tH</td><td>tWH, $tHqb$</td></tr>
</table>

ttH H→γγ

ATLAS-CONF-2020-026

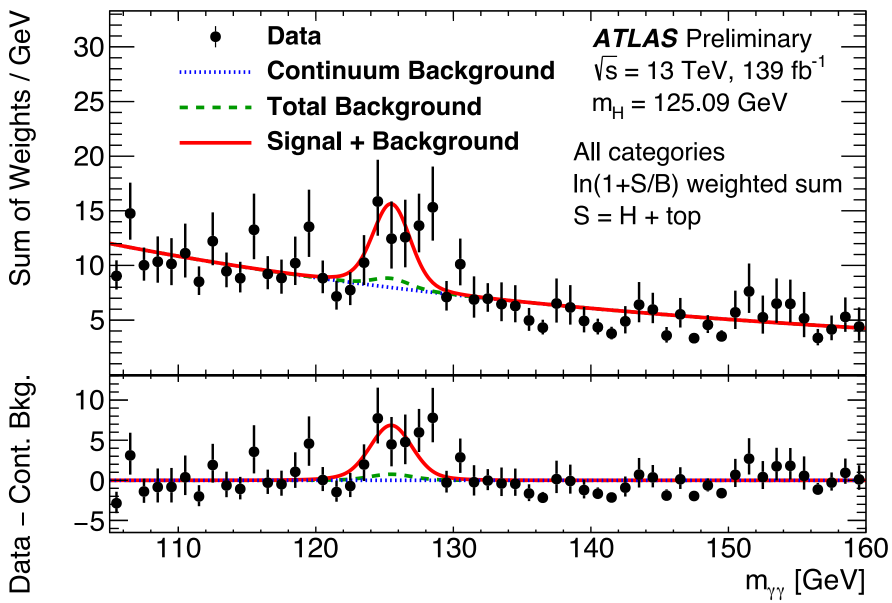

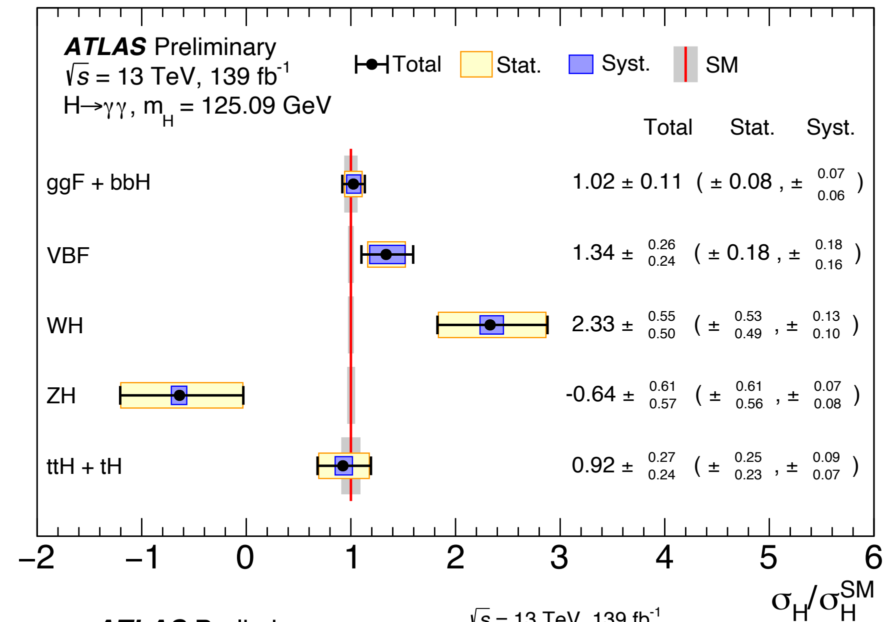

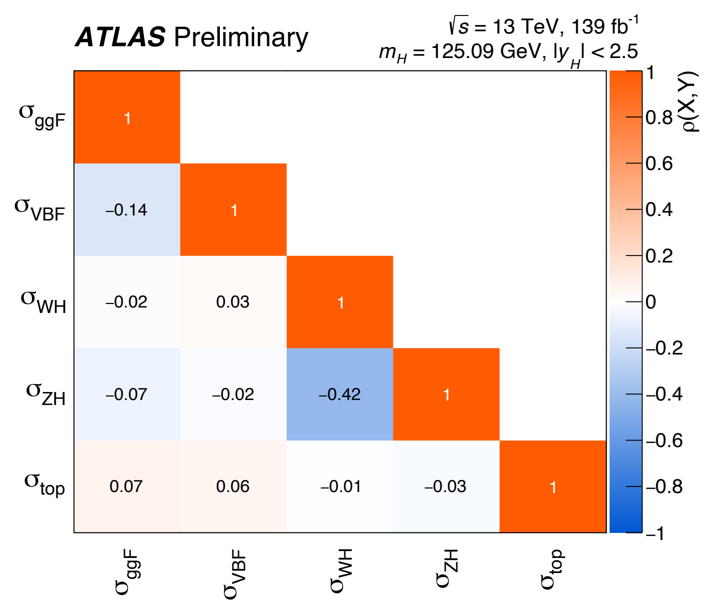

	σ_{ggF}	σ_{VBF}	σ_{WH}	σ_{ZH}	σ_{top}
σ_{ggF}	1				
σ_{VBF}	−0.14	1			
σ_{WH}	−0.02	0.03	1		
σ_{ZH}	−0.07	−0.02	−0.42	1	
σ_{top}	0.07	0.06	−0.01	−0.03	1

ttH H→γγ

ATLAS-CONF-2020-026

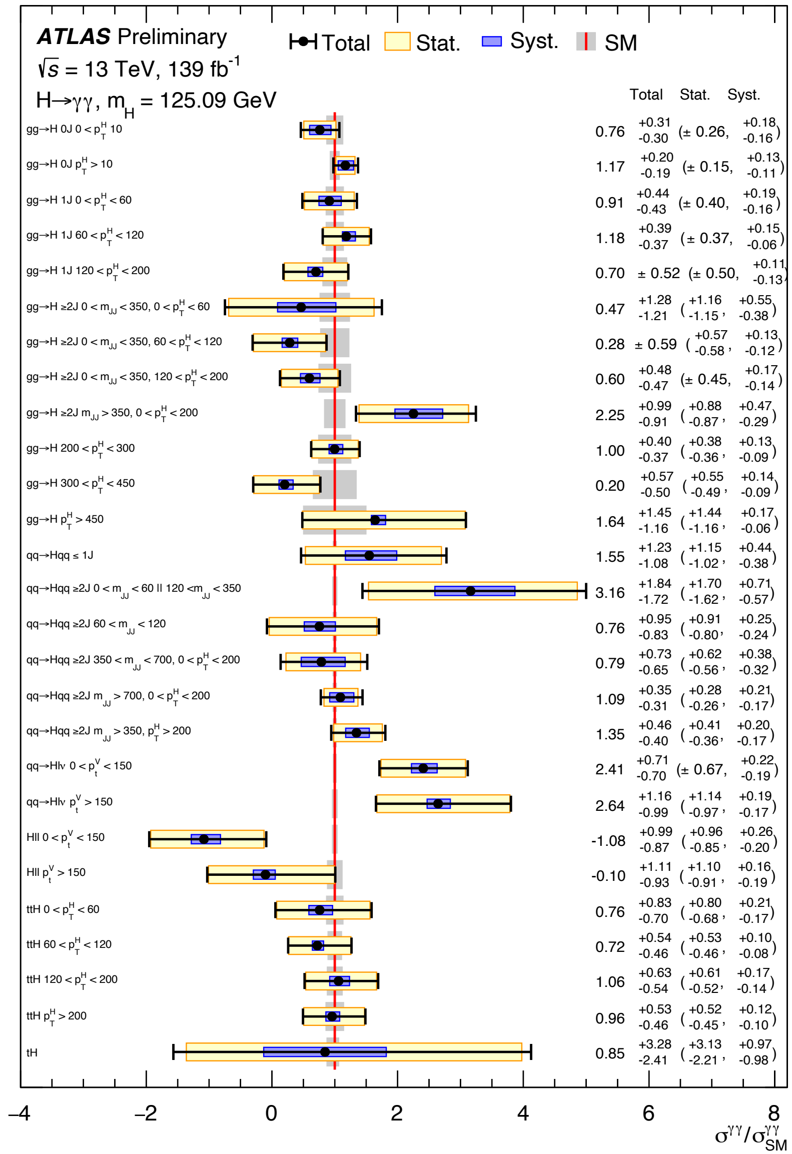

ttH H→γγ

ATLAS-CONF-2020-026

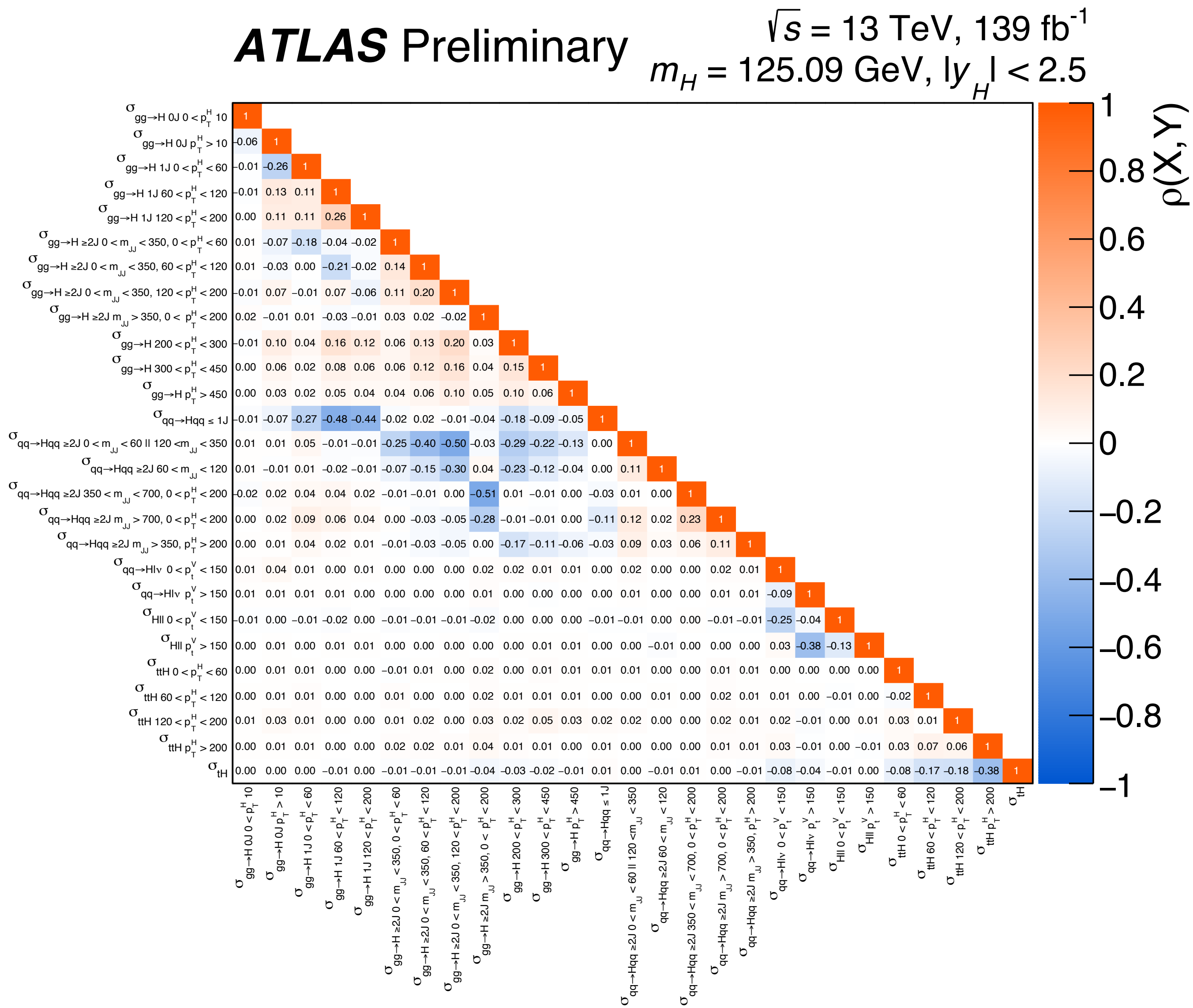

ttH H→γγ

ATLAS-CONF-2020-026

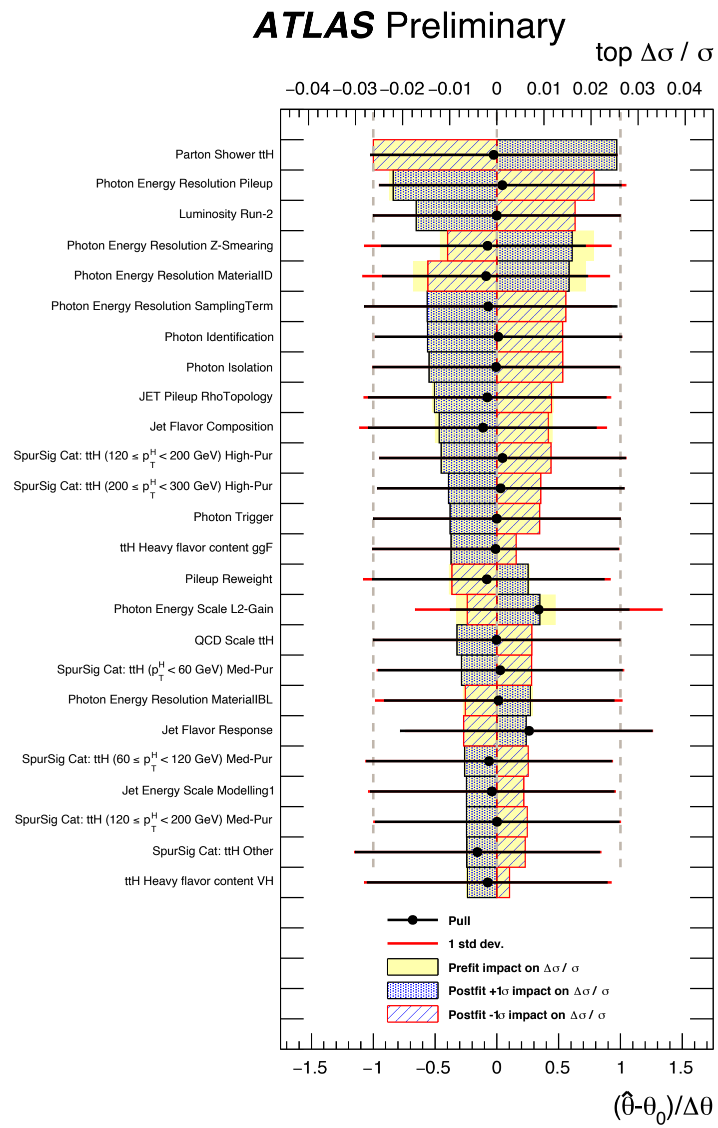

- **BDT bkg = ttH + tH vs background**
- **Top DNN = ttH vs tH**

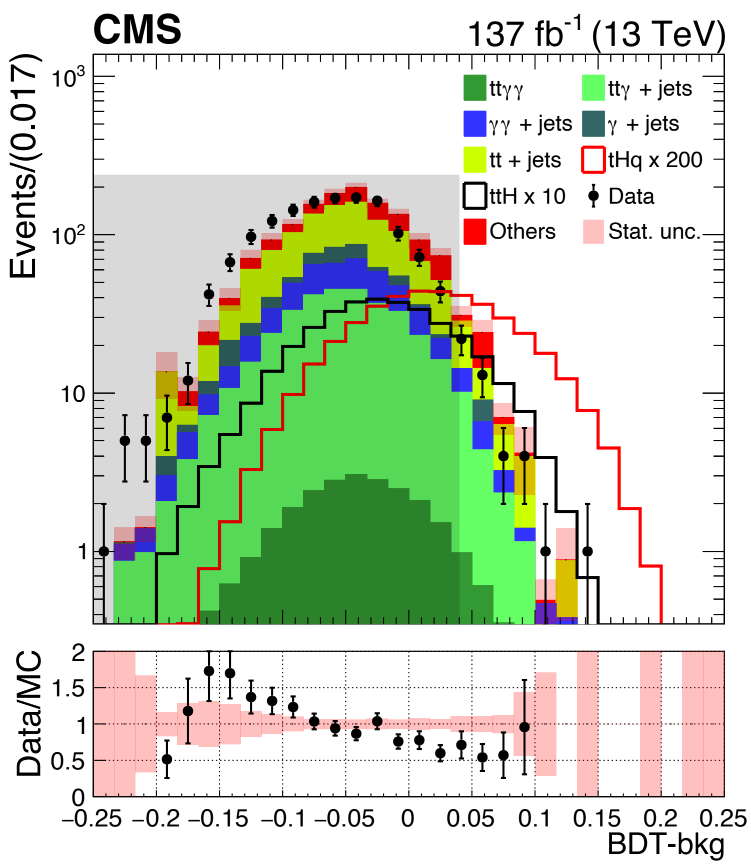

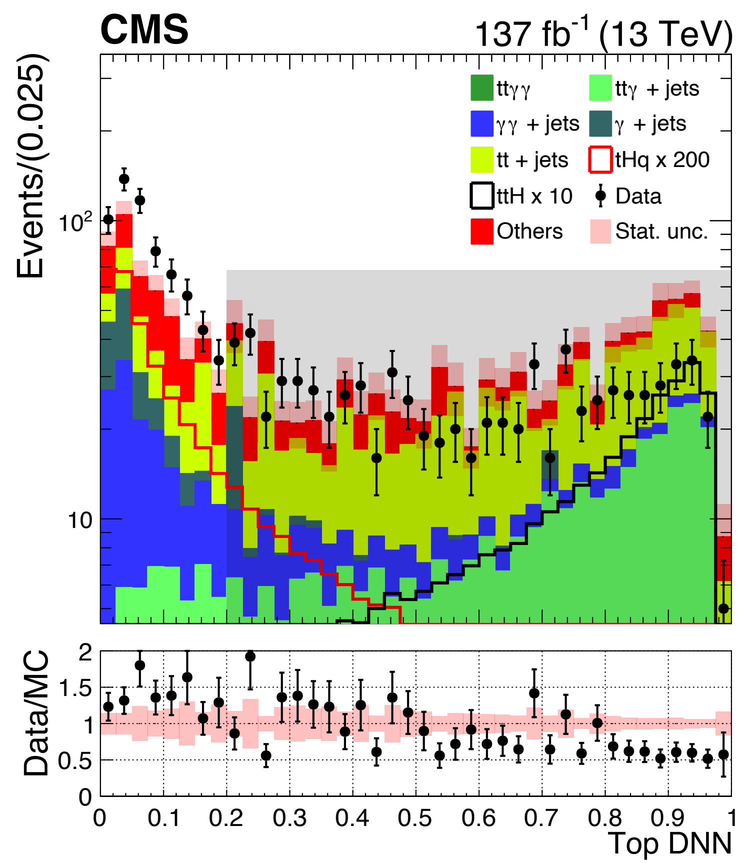

ttH leptonic　　　　*ttH hadronic*

100<m(γγ)<120 GeV
or 130<m(γγ)<190 GeV

ttZ Z→ee
control region

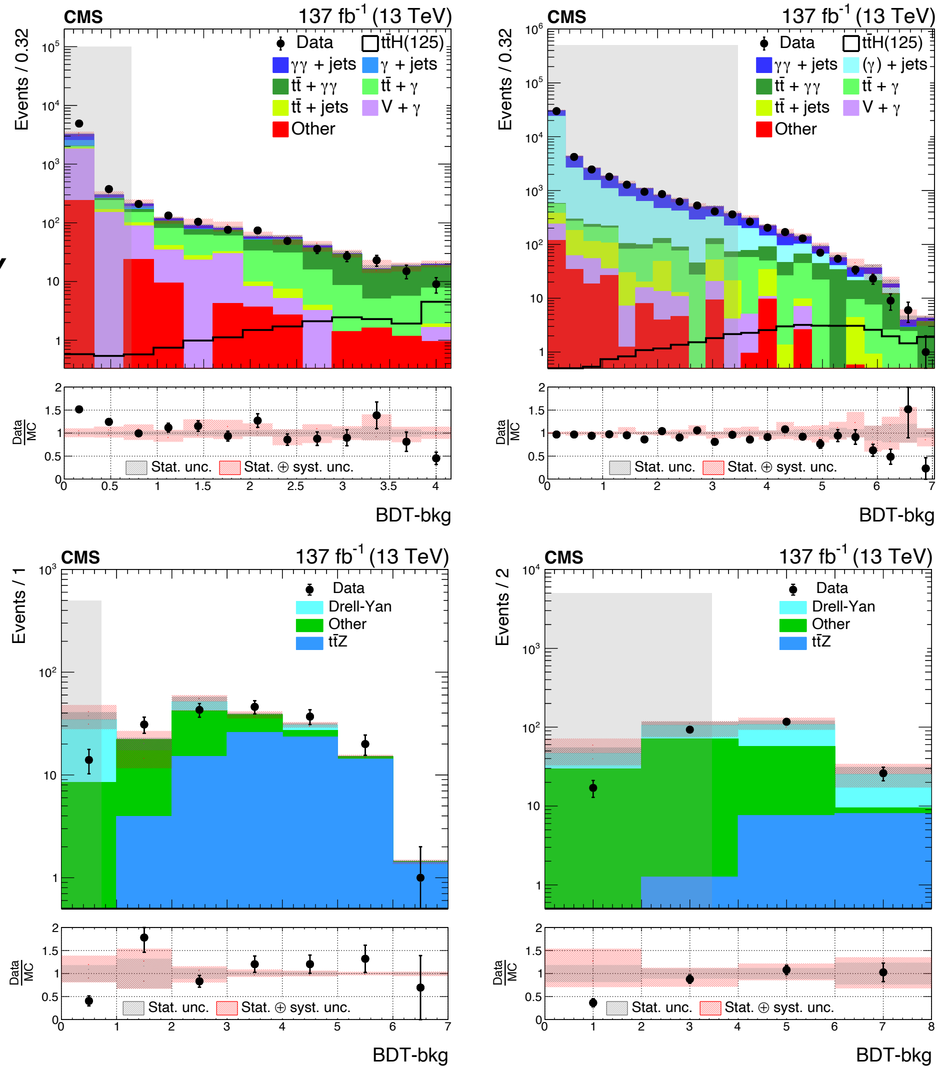

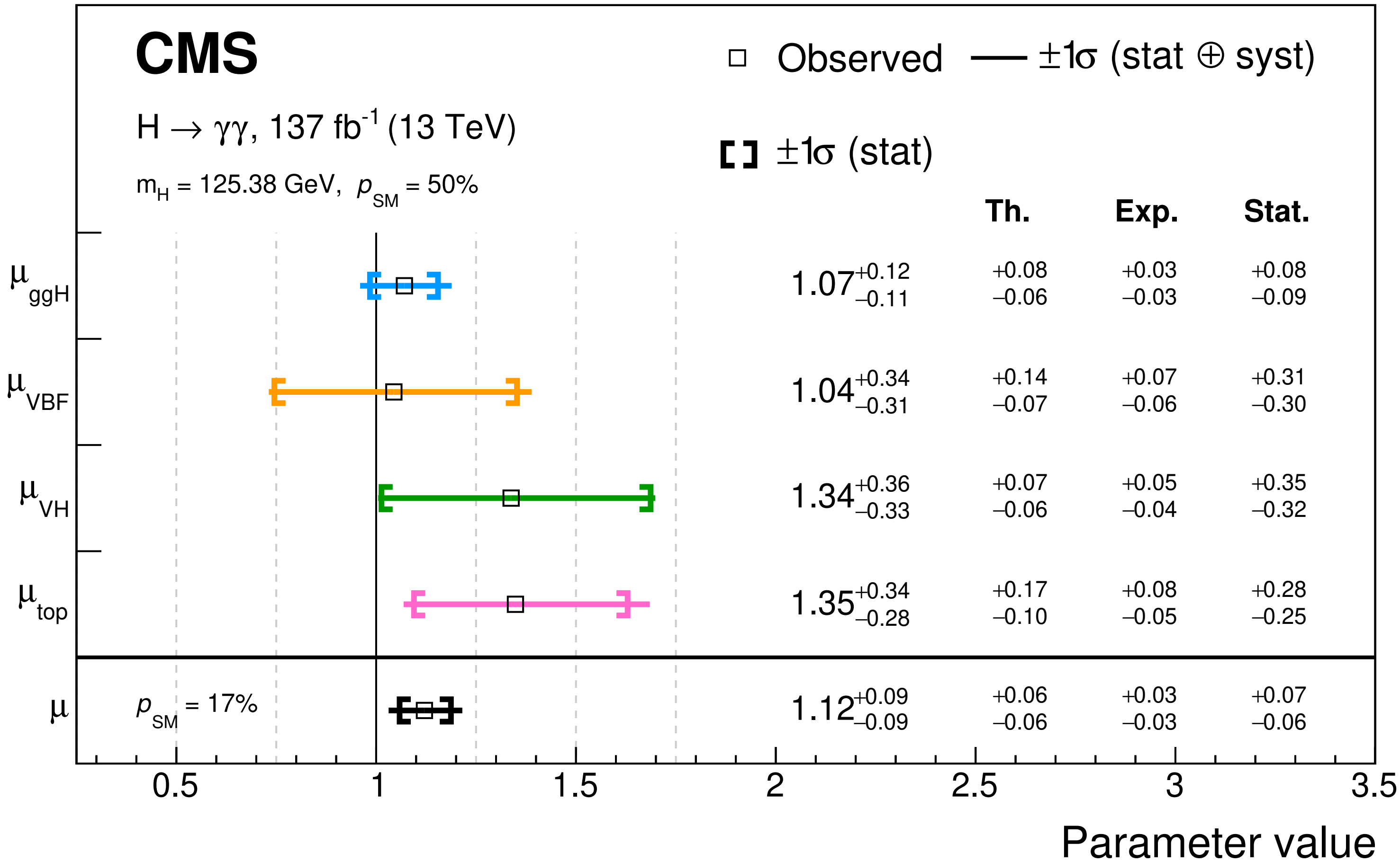
CMS
H → γγ, 137 fb-1 (13 TeV)
mH = 125.38 GeV, pSM = 50%
Observed
±1σ (stat ⊕ syst)
±1σ (stat)
Th.
Exp.
Stat.
μggH
1.07 +0.12 −0.11
+0.08 −0.06
+0.03 −0.03
+0.08 −0.09
μVBF
1.04 +0.34 −0.31
+0.14 −0.07
+0.07 −0.06
+0.31 −0.30
μVH
1.34 +0.36 −0.33
+0.07 −0.06
+0.05 −0.04
+0.35 −0.32
μtop
1.35 +0.34 −0.28
+0.17 −0.10
+0.08 −0.05
+0.28 −0.25
μ
pSM = 17%
1.12 +0.09 −0.09
+0.06 −0.06
+0.03 −0.03
+0.07 −0.06
0.5
1
1.5
2
2.5
3
3.5
Parameter value

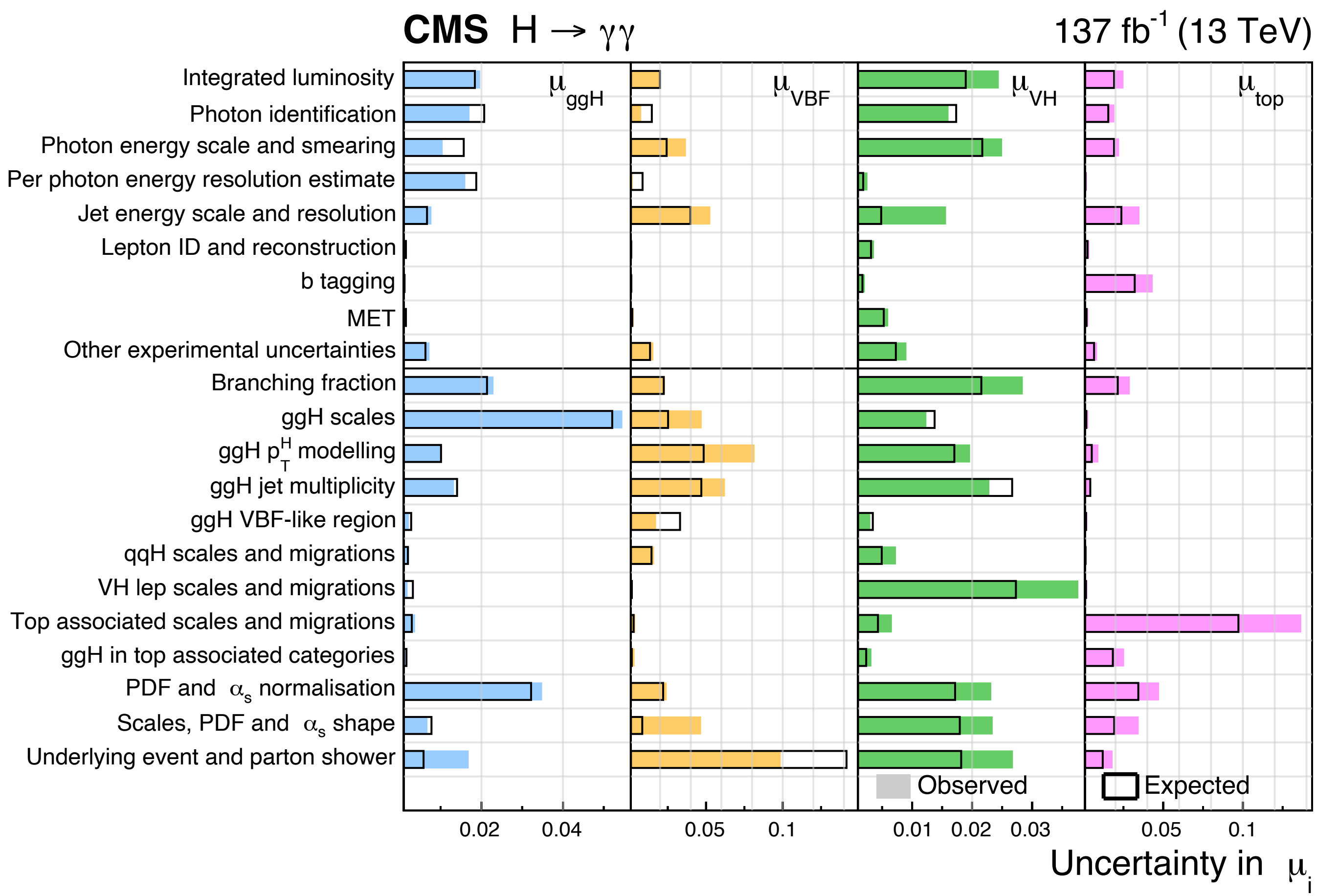

CMS H → γγ
137 fb^{-1} (13 TeV)
Integrated luminosity
Photon identification
Photon energy scale and smearing
Per photon energy resolution estimate
Jet energy scale and resolution
Lepton ID and reconstruction
b tagging
MET
Other experimental uncertainties
Branching fraction
ggH scales
ggH p_T^H modelling
ggH jet multiplicity
ggH VBF-like region
qqH scales and migrations
VH lep scales and migrations
Top associated scales and migrations
ggH in top associated categories
PDF and α_s normalisation
Scales, PDF and α_s shape
Underlying event and parton shower
μ_{ggH}
μ_{VBF}
μ_{VH}
μ_{top}
Observed
Expected
0.02 0.04
0.05 0.1
0.01 0.02 0.03
0.05 0.1
Uncertainty in μ_i

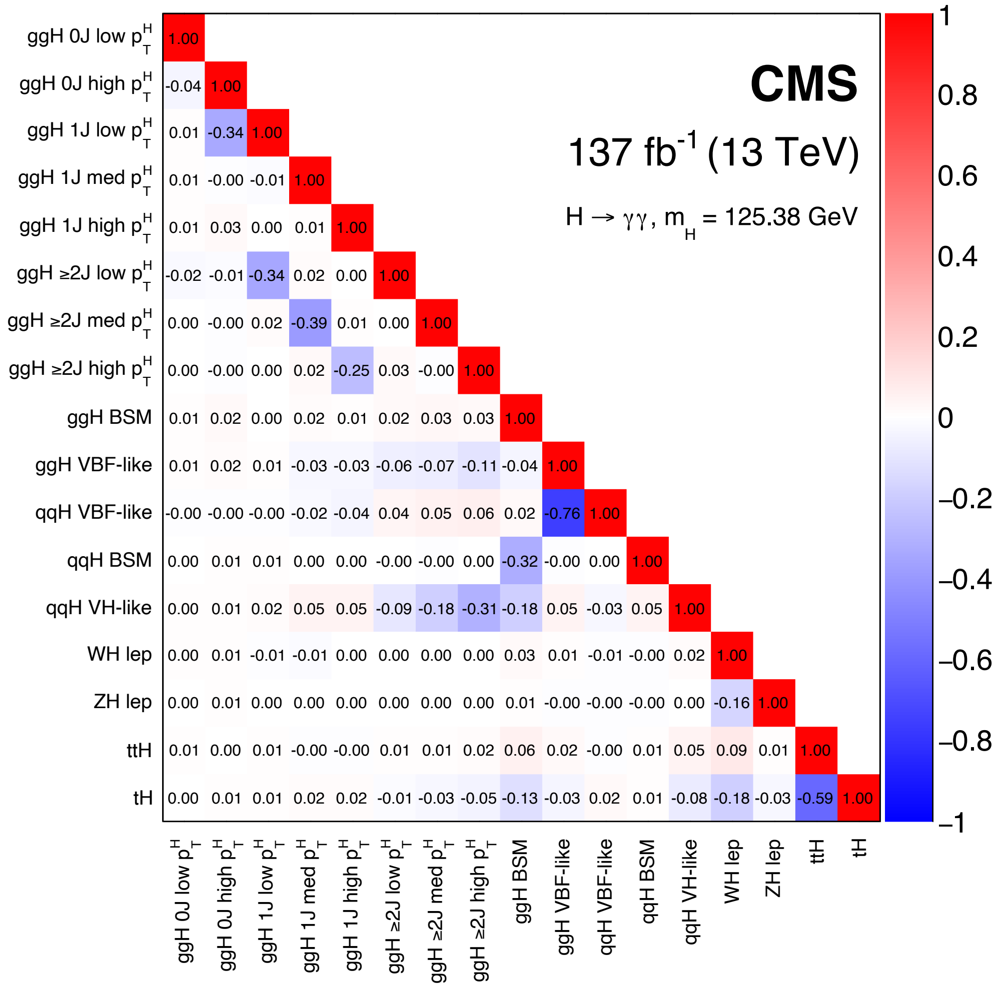
CMS
137 fb-1 (13 TeV)
H → γγ, mH = 125.38 GeV
ggH 0J low pTH: 1.00
ggH 0J high pTH: -0.04 1.00
ggH 1J low pTH: 0.01 -0.34 1.00
ggH 1J med pTH: 0.01 -0.00 -0.01 1.00
ggH 1J high pTH: 0.01 0.03 0.00 0.01 1.00
ggH ≥2J low pTH: -0.02 -0.01 -0.34 0.02 0.00 1.00
ggH ≥2J med pTH: 0.00 -0.00 0.02 -0.39 0.01 0.00 1.00
ggH ≥2J high pTH: 0.00 -0.00 0.00 0.02 -0.25 0.03 -0.00 1.00
ggH BSM: 0.01 0.02 0.00 0.02 0.01 0.02 0.03 0.03 1.00
ggH VBF-like: 0.01 0.02 0.01 -0.03 -0.03 -0.06 -0.07 -0.11 -0.04 1.00
qqH VBF-like: -0.00 -0.00 -0.00 -0.02 -0.04 0.04 0.05 0.06 0.02 -0.76 1.00
qqH BSM: 0.00 0.01 0.01 0.00 0.00 -0.00 -0.00 0.00 -0.32 -0.00 0.00 1.00
qqH VH-like: 0.00 0.01 0.02 0.05 0.05 -0.09 -0.18 -0.31 -0.18 0.05 -0.03 0.05 1.00
WH lep: 0.00 0.01 -0.01 -0.01 0.00 0.00 0.00 0.00 0.03 0.01 -0.01 -0.00 0.02 1.00
ZH lep: 0.00 0.01 0.00 0.00 0.00 0.00 0.00 0.00 0.01 -0.00 -0.00 -0.00 0.00 -0.16 1.00
ttH: 0.01 0.00 0.01 -0.00 -0.00 0.01 0.01 0.02 0.06 0.02 -0.00 0.01 0.05 0.09 0.01 1.00
tH: 0.00 0.01 0.01 0.02 0.02 -0.01 -0.03 -0.05 -0.13 -0.03 0.02 0.01 -0.08 -0.18 -0.03 -0.59 1.00
1 0.8 0.6 0.4 0.2 0 −0.2 −0.4 −0.6 −0.8 −1

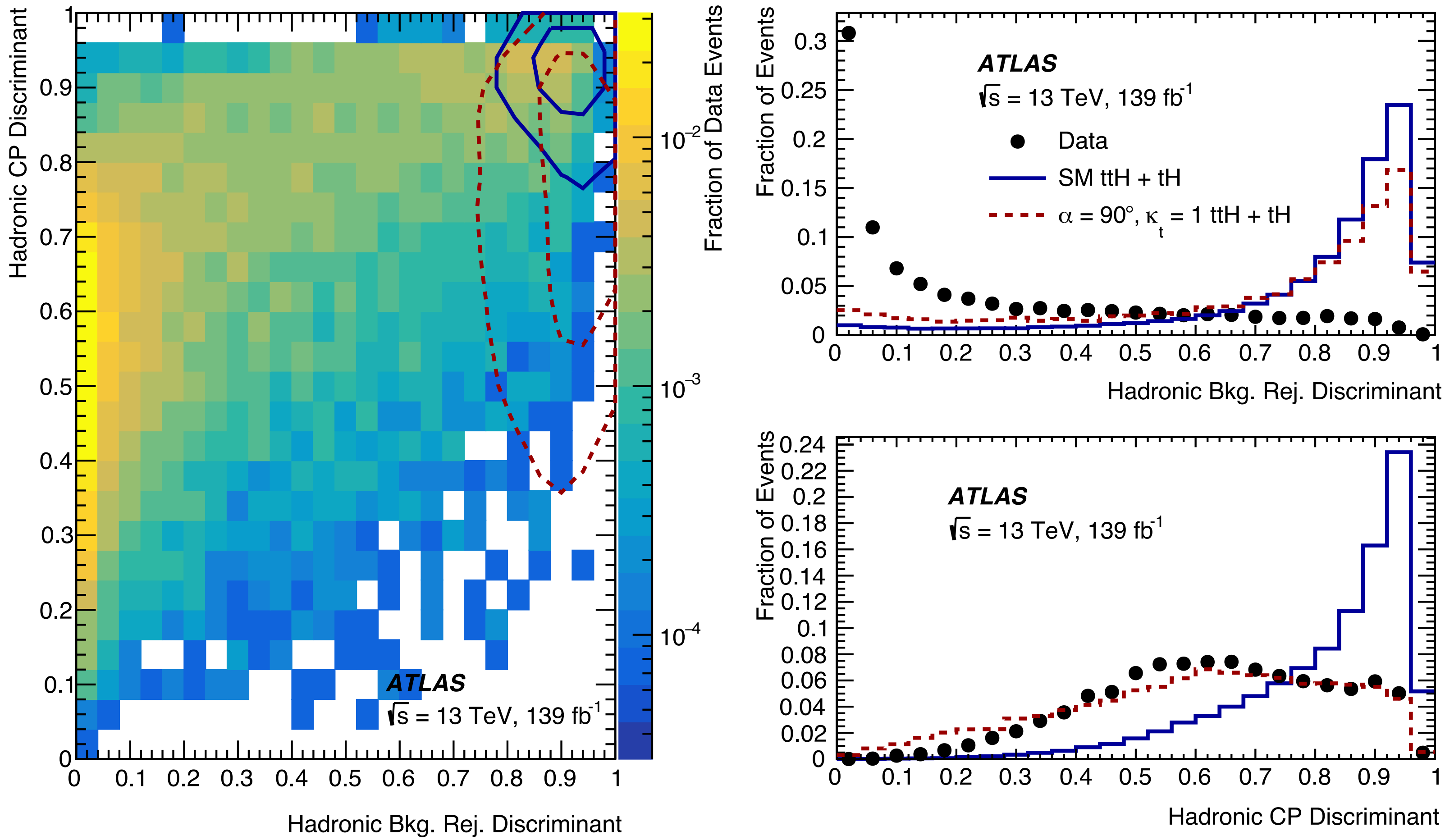

Hadronic CP Discriminant
Hadronic Bkg. Rej. Discriminant
Fraction of Data Events
ATLAS
√s = 13 TeV, 139 fb⁻¹
Fraction of Events
Data
SM ttH + tH
α = 90°, κ_t = 1 ttH + tH
Hadronic Bkg. Rej. Discriminant
ATLAS
√s = 13 TeV, 139 fb⁻¹
Fraction of Events
Hadronic CP Discriminant

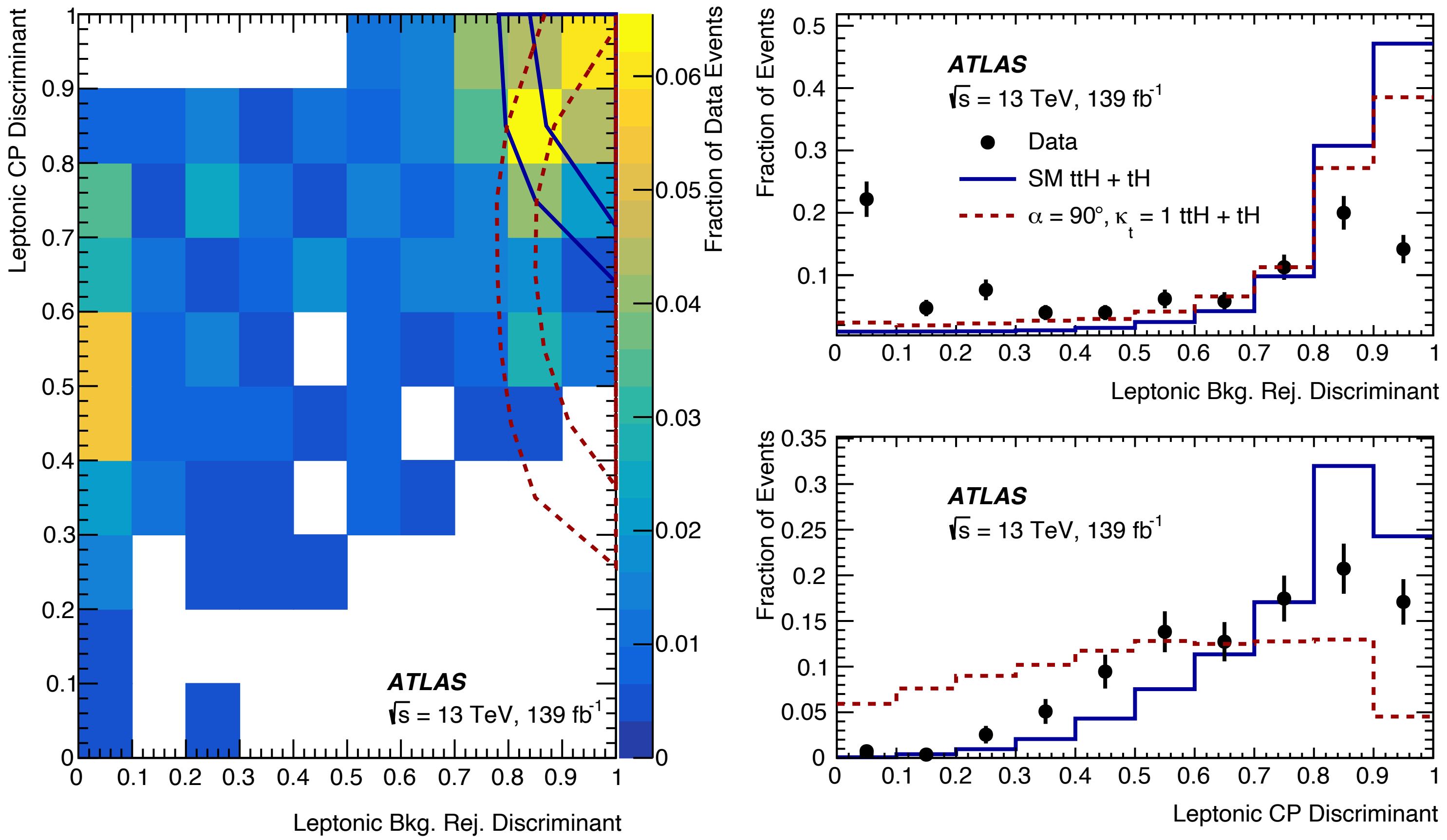

Leptonic CP Discriminant
Leptonic Bkg. Rej. Discriminant
Fraction of Data Events
ATLAS
√s = 13 TeV, 139 fb-1
Fraction of Events
Data
SM ttH + tH
α = 90°, κt = 1 ttH + tH

ttH H→γγ

ATLAS-HIGG-2019-01

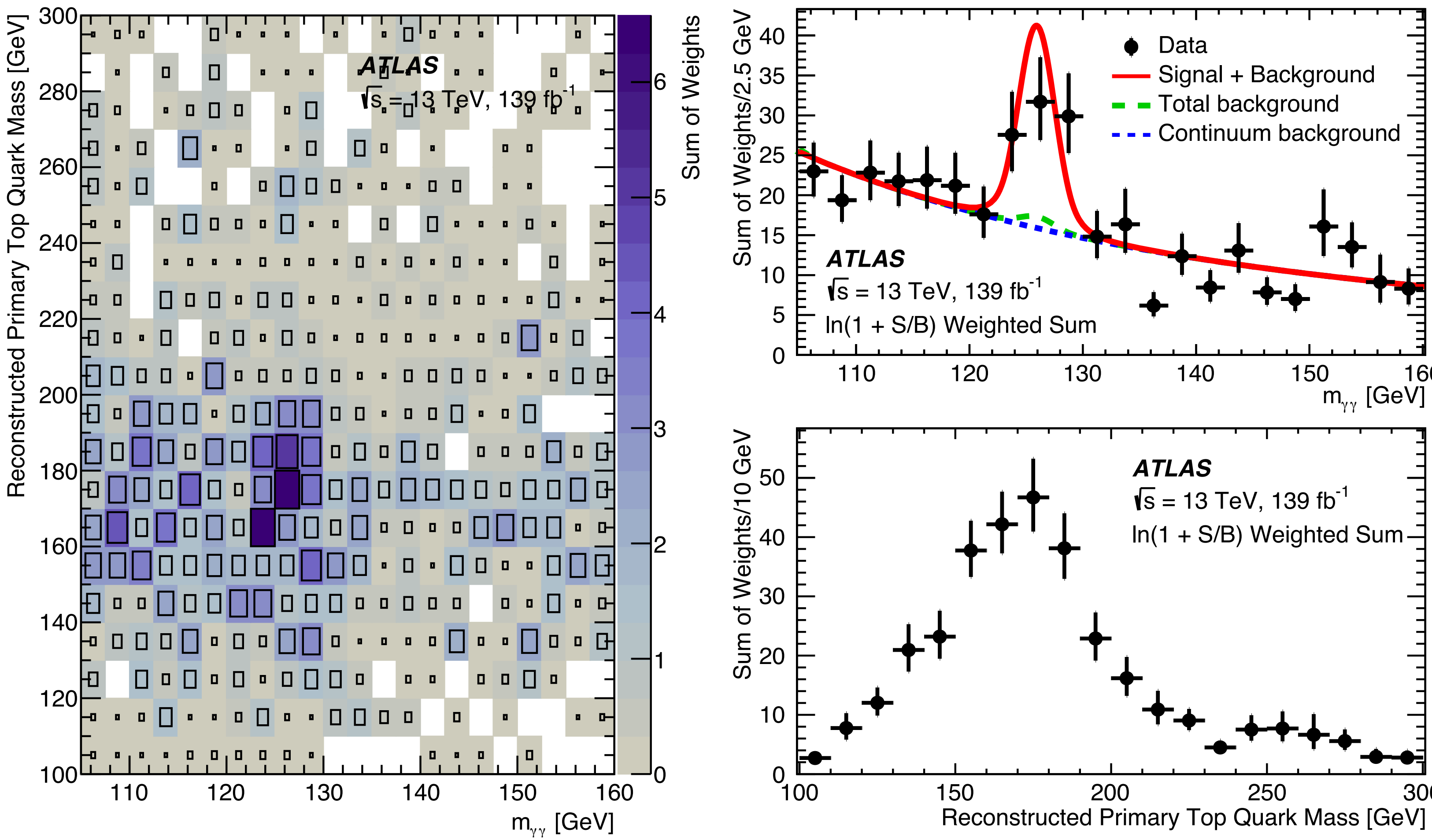

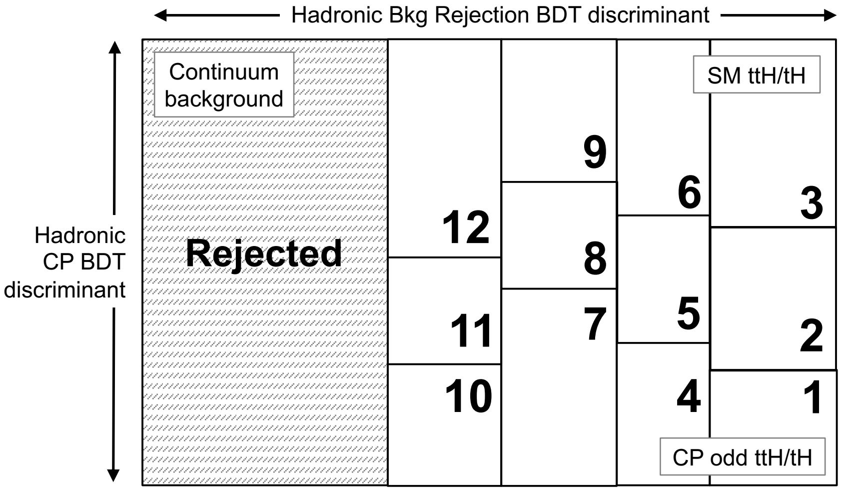
Hadronic Bkg Rejection BDT discriminant
Hadronic CP BDT discriminant
Continuum background
Rejected
SM ttH/tH
CP odd ttH/tH
12
11
10
9
8
7
6
5
4
3
2
1

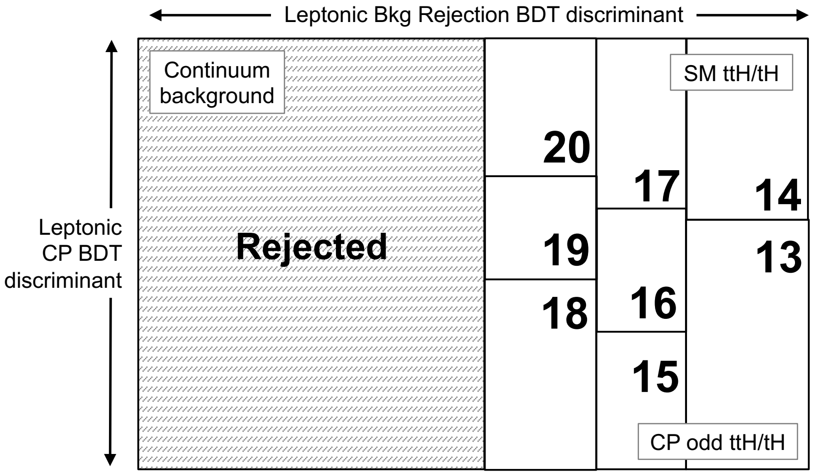
Leptonic Bkg Rejection BDT discriminant
Leptonic CP BDT discriminant
Continuum background
Rejected
SM ttH/tH
CP odd ttH/tH
20
19
18
17
16
15
14
13

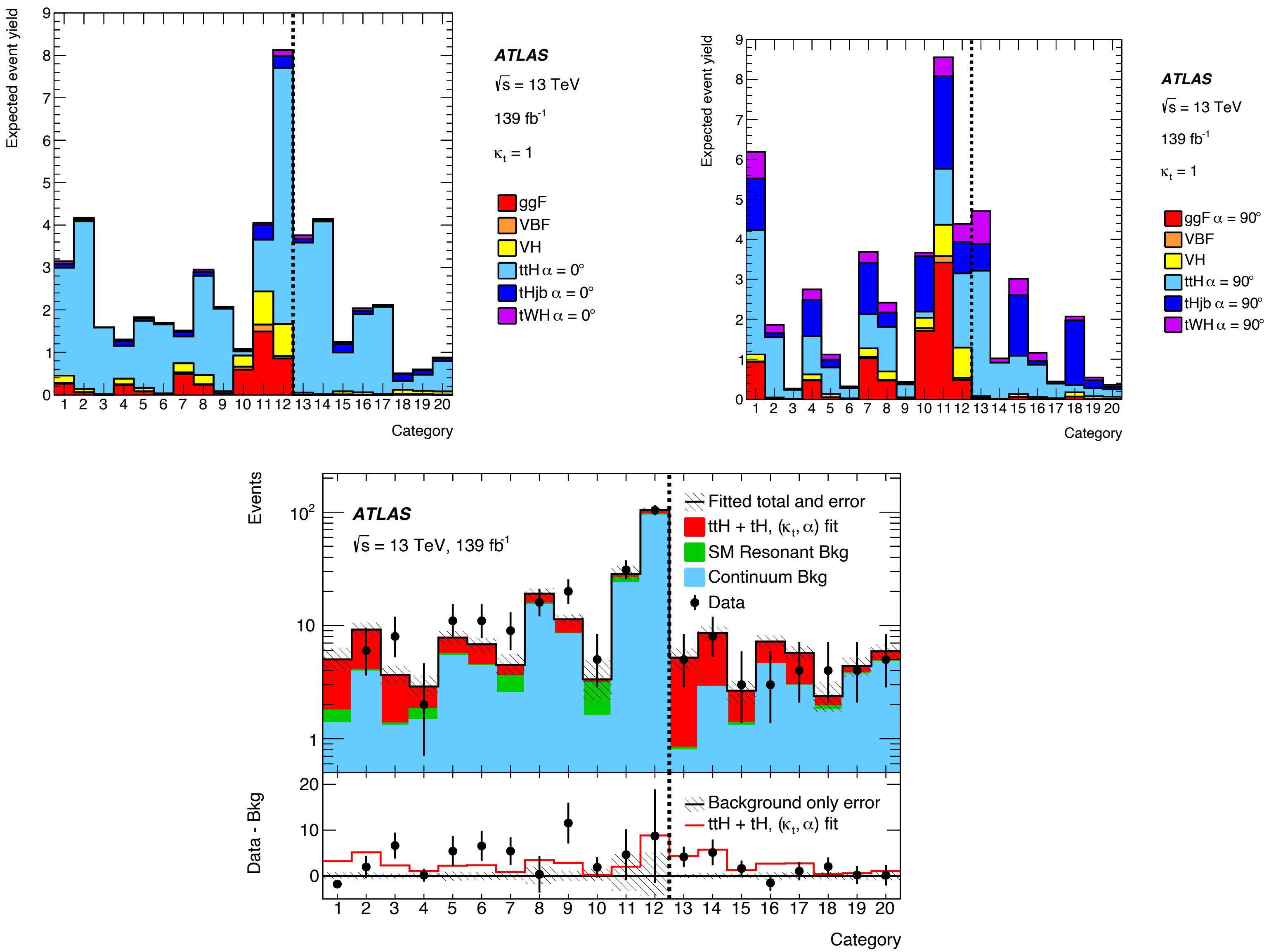

ATLAS
√s = 13 TeV
139 fb-1
κt = 1
ggF
VBF
VH
ttH α = 0°
tHjb α = 0°
tWH α = 0°
Expected event yield
Category
ATLAS
√s = 13 TeV
139 fb-1
κt = 1
ggF α = 90°
VBF
VH
ttH α = 90°
tHjb α = 90°
tWH α = 90°
Expected event yield
Category
ATLAS
√s = 13 TeV, 139 fb-1
Fitted total and error
ttH + tH, (κt, α) fit
SM Resonant Bkg
Continuum Bkg
Data
Events
Background only error
ttH + tH, (κt, α) fit
Data - Bkg
Category

ttH H→γγ

- **Gluon and photon effective Higgs couplings constrained with other H->γγ prod. modes**

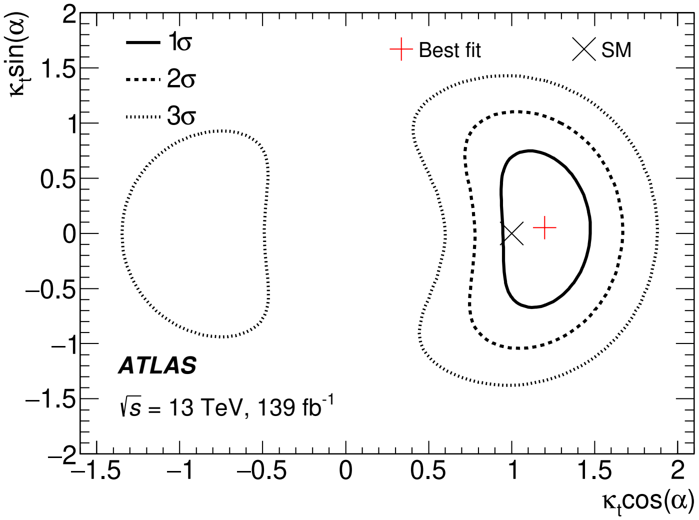

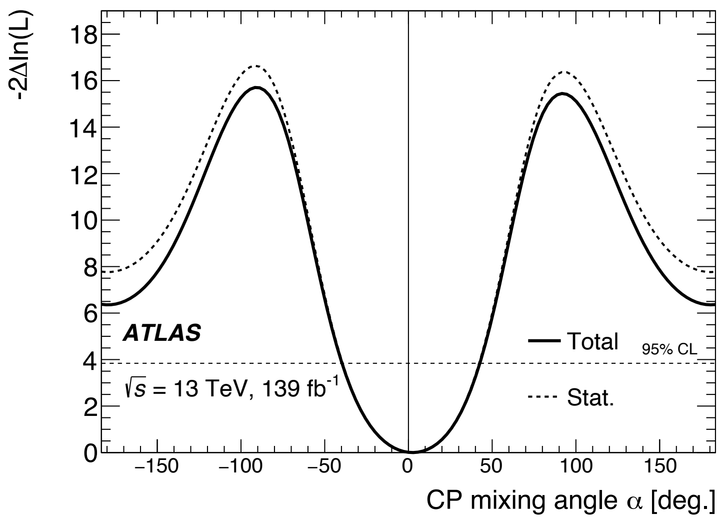

- **Gluon and photon effective Higgs couplings parametrised vs κ_t and α**

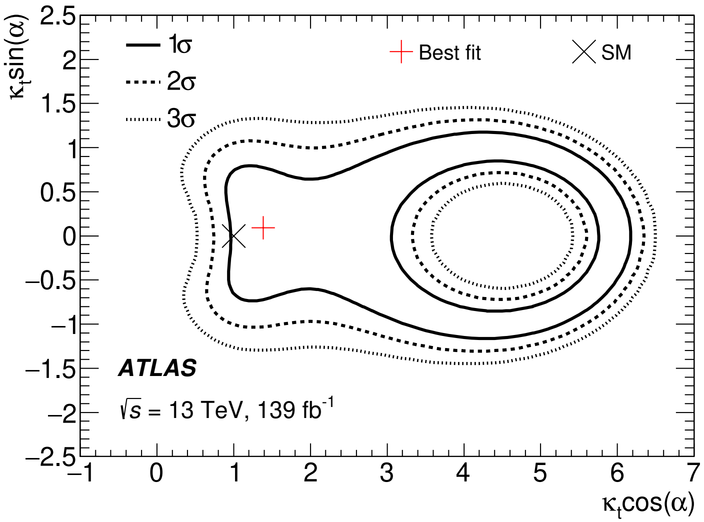

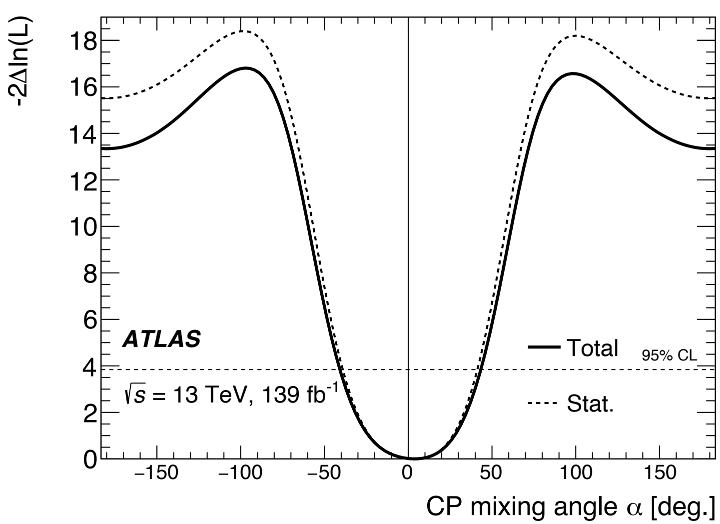

ttH H→γγ

ATLAS-HIGG-2019-01

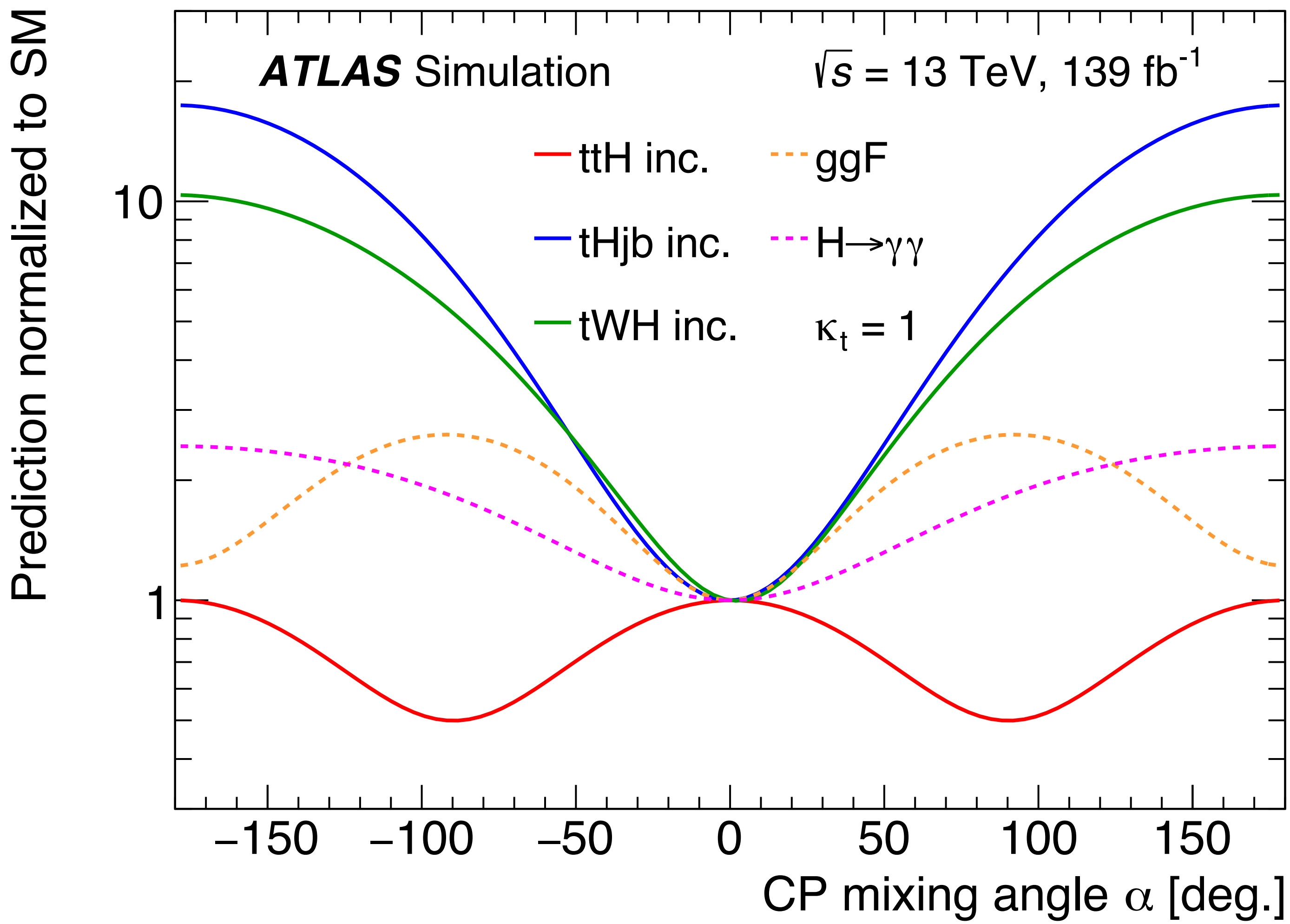

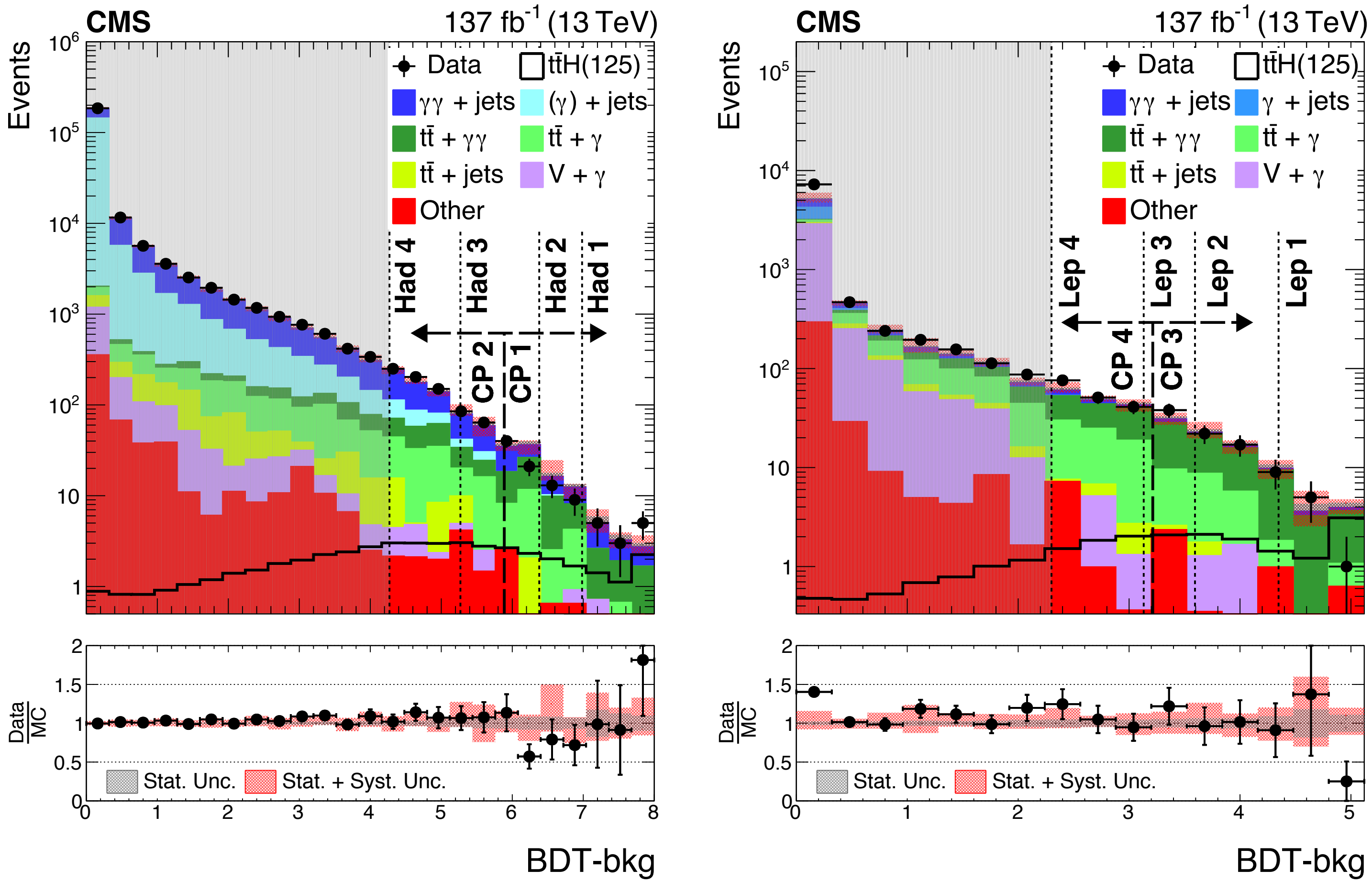
CMS
137 fb^{-1} (13 TeV)
Events
Data
t t̄ H(125)
γγ + jets
(γ) + jets
t t̄ + γγ
t t̄ + γ
t t̄ + jets
V + γ
Other
Had 4
Had 3
Had 2
Had 1
CP 2
CP 1
Data/MC
Stat. Unc.
Stat. + Syst. Unc.
BDT-bkg
CMS
137 fb^{-1} (13 TeV)
Events
Data
t t̄ H(125)
γγ + jets
γ + jets
t t̄ + γγ
t t̄ + γ
t t̄ + jets
V + γ
Other
Lep 4
Lep 3
Lep 2
Lep 1
CP 4
CP 3
Data/MC
Stat. Unc.
Stat. + Syst. Unc.
BDT-bkg

ttH H→γγ

CMS-HIG-19-013

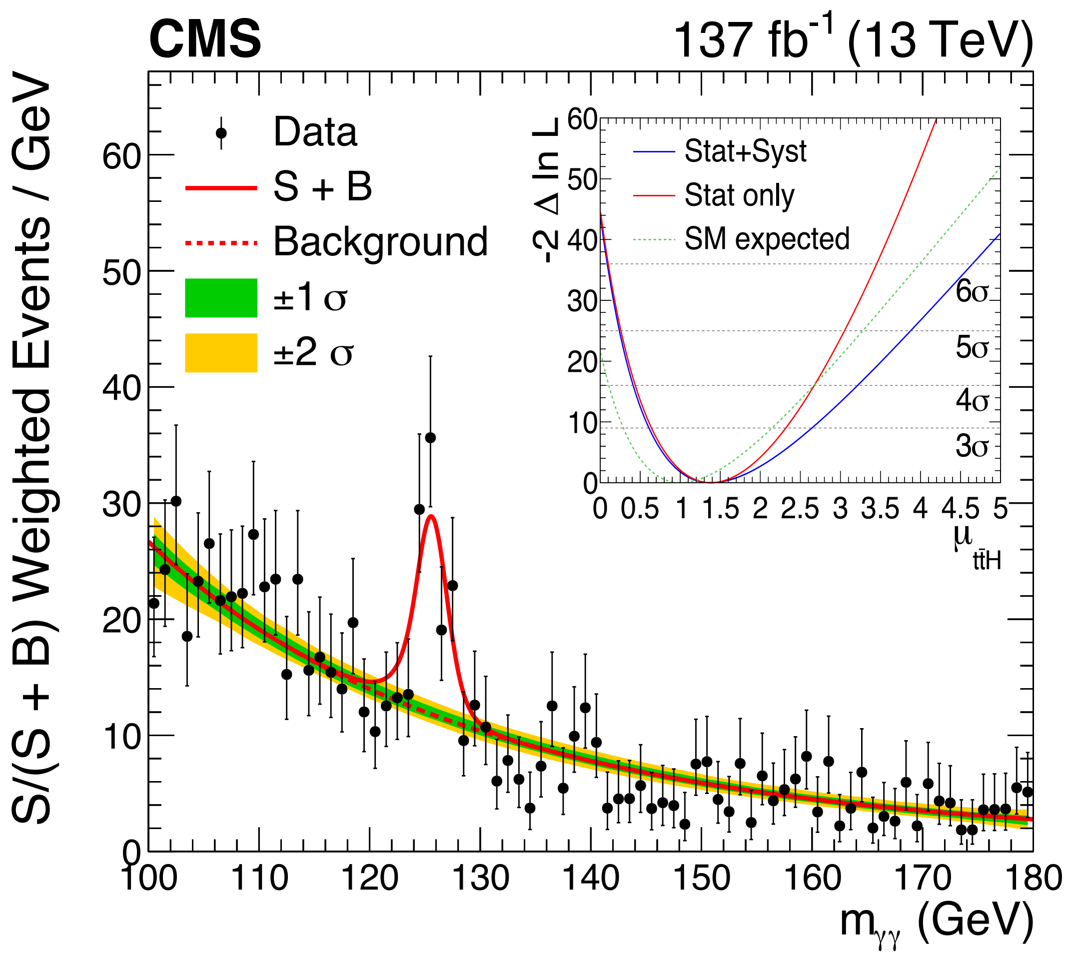

ttH H→γγ

[CMS-HIG-19-013](CMS-HIG-19-013)

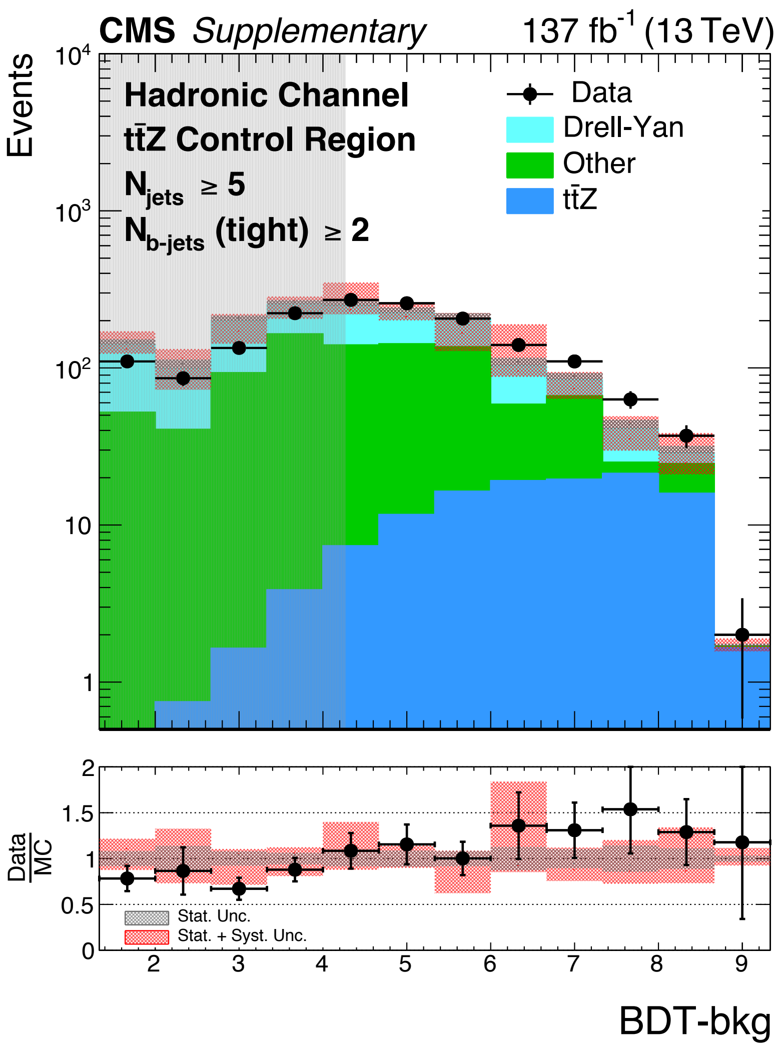

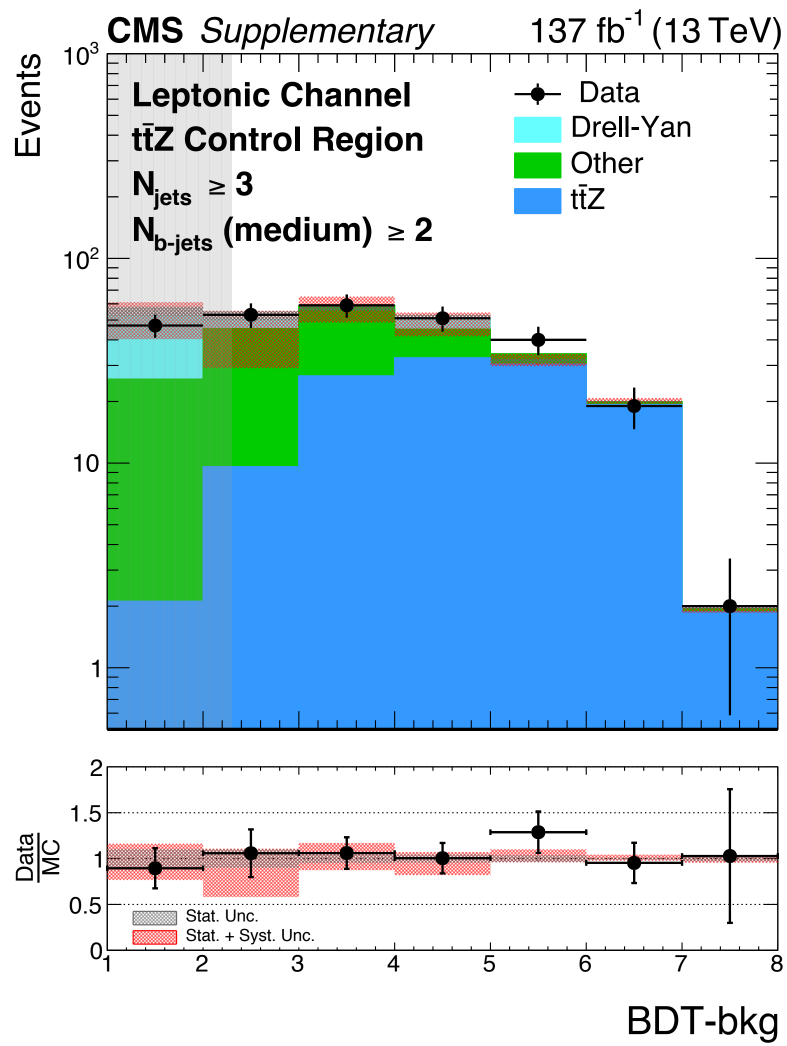

ttH H→ZZ→4l

ATLAS-HIGG-2018-28

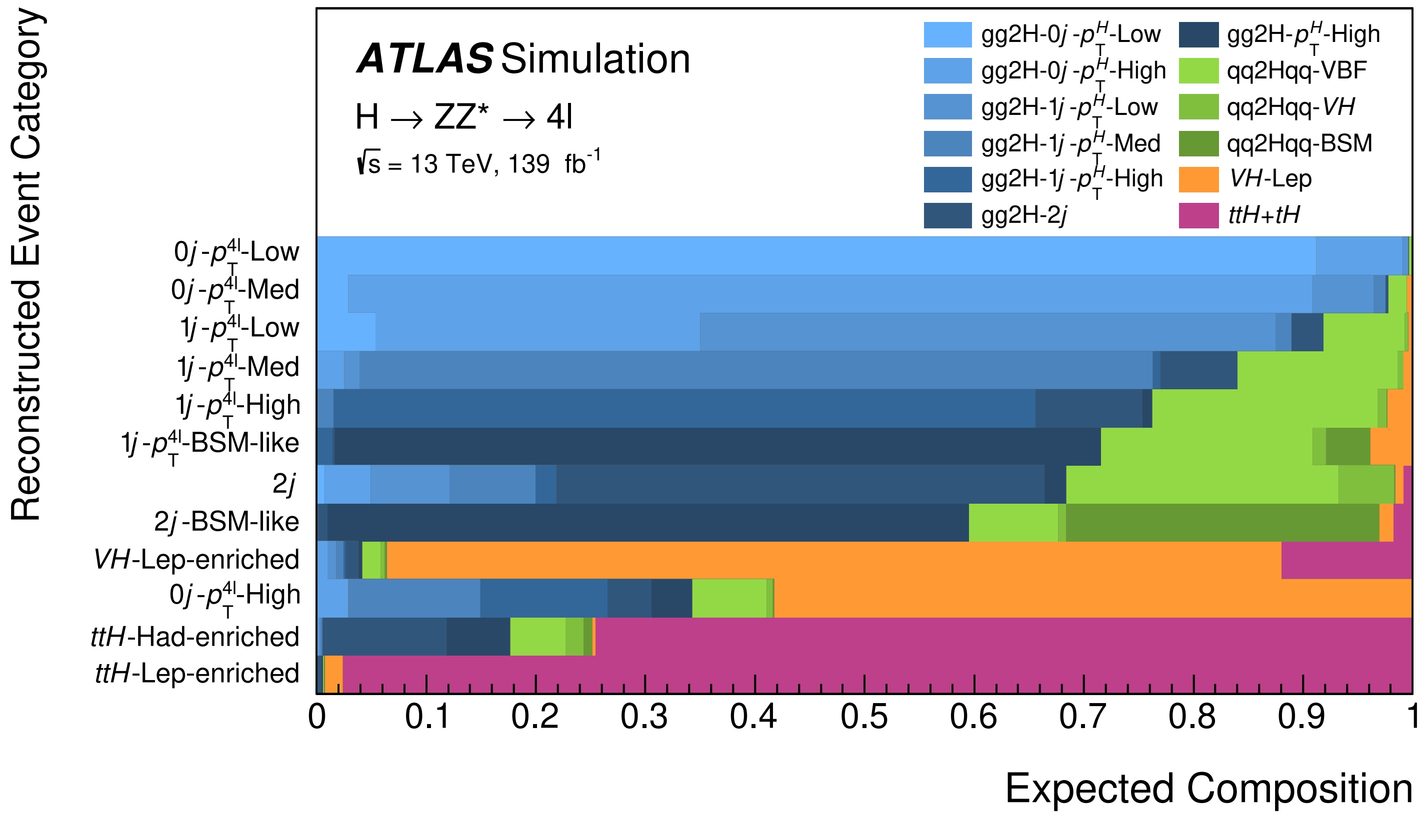

ttH H→ZZ→4l

ATLAS-HIGG-2018-28

- **NN mutli-classifier used with ggF, ttH and tXX nodes for ttH-had category**

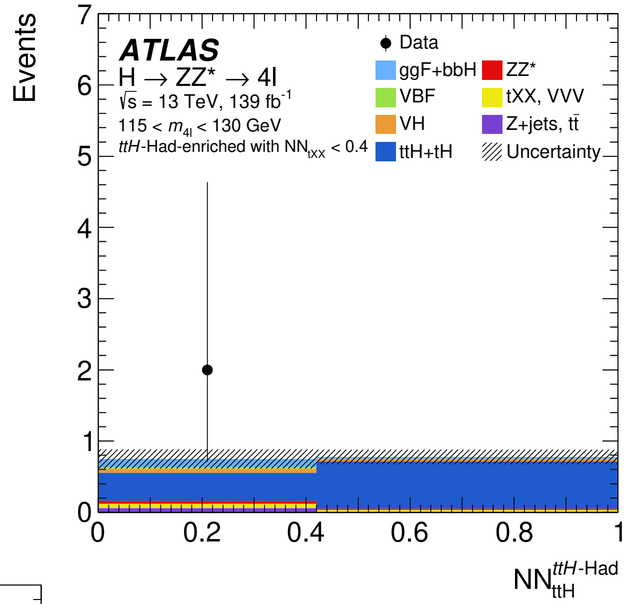

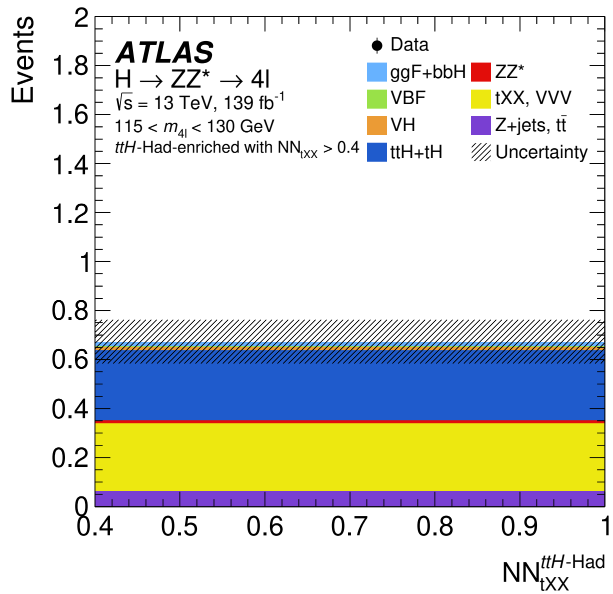

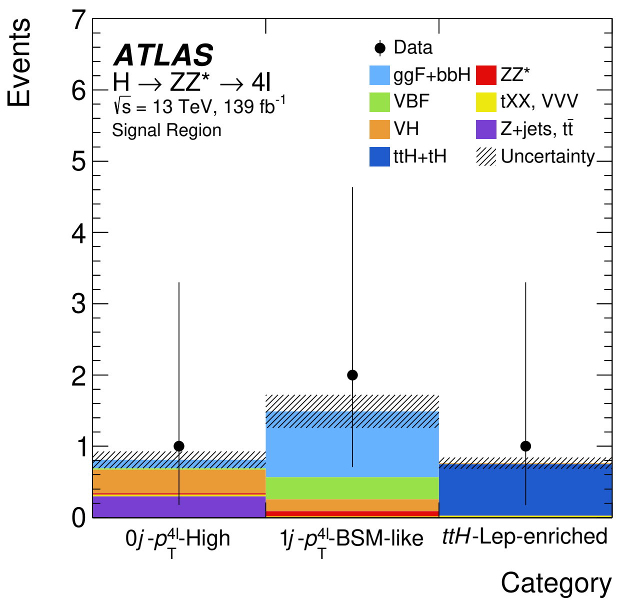

- **Cut-and-count for ttH-lep category**

ttH H→ZZ→4l

ATLAS-HIGG-2018-28

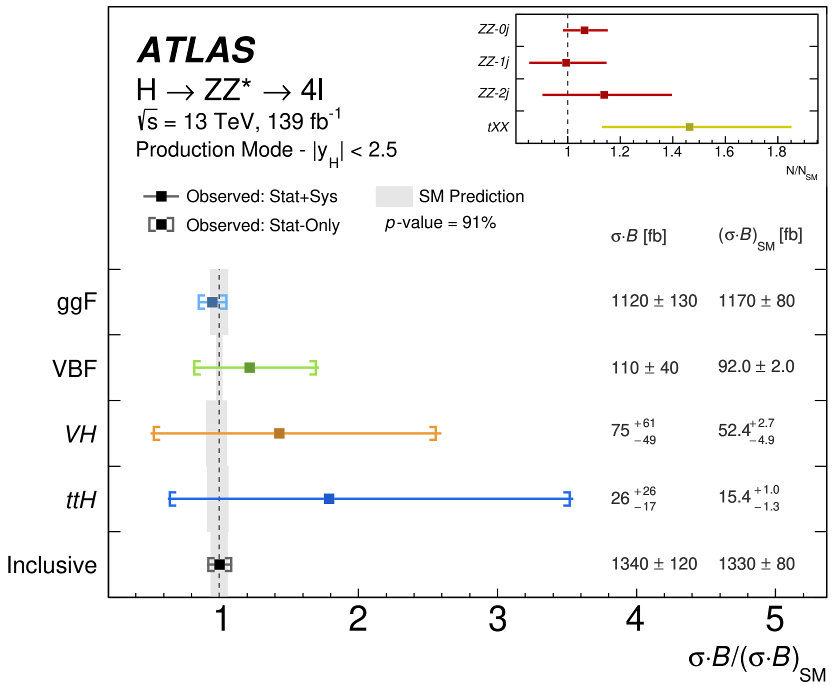

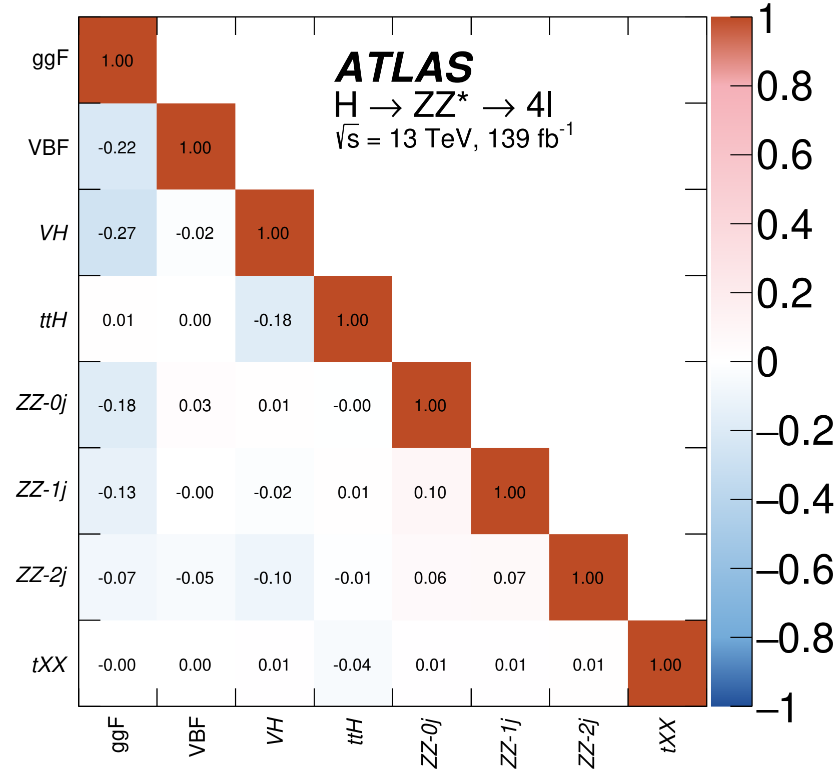

	ggF	VBF	VH	ttH	ZZ-0j	ZZ-1j	ZZ-2j	tXX
ggF	1.00							
VBF	-0.22	1.00						
VH	-0.27	-0.02	1.00					
ttH	0.01	0.00	-0.18	1.00				
ZZ-0j	-0.18	0.03	0.01	-0.00	1.00			
ZZ-1j	-0.13	-0.00	-0.02	0.01	0.10	1.00		
ZZ-2j	-0.07	-0.05	-0.10	-0.01	0.06	0.07	1.00	
tXX	-0.00	0.00	0.01	-0.04	0.01	0.01	0.01	1.00

ttH H→ZZ→4l

CMS-HIG-19-001

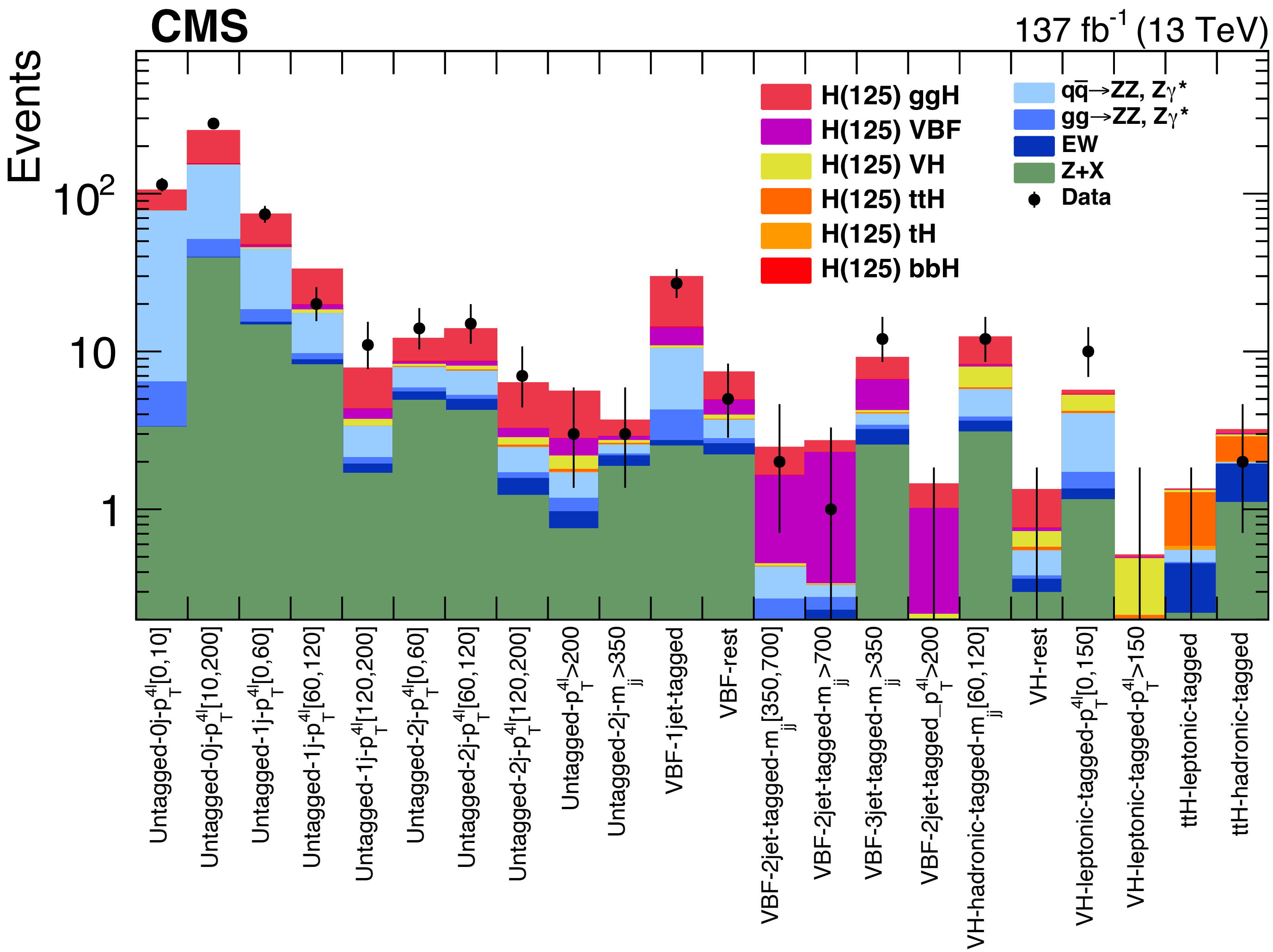

ttH H→ZZ→4l

[CMS-HIG-19-001]

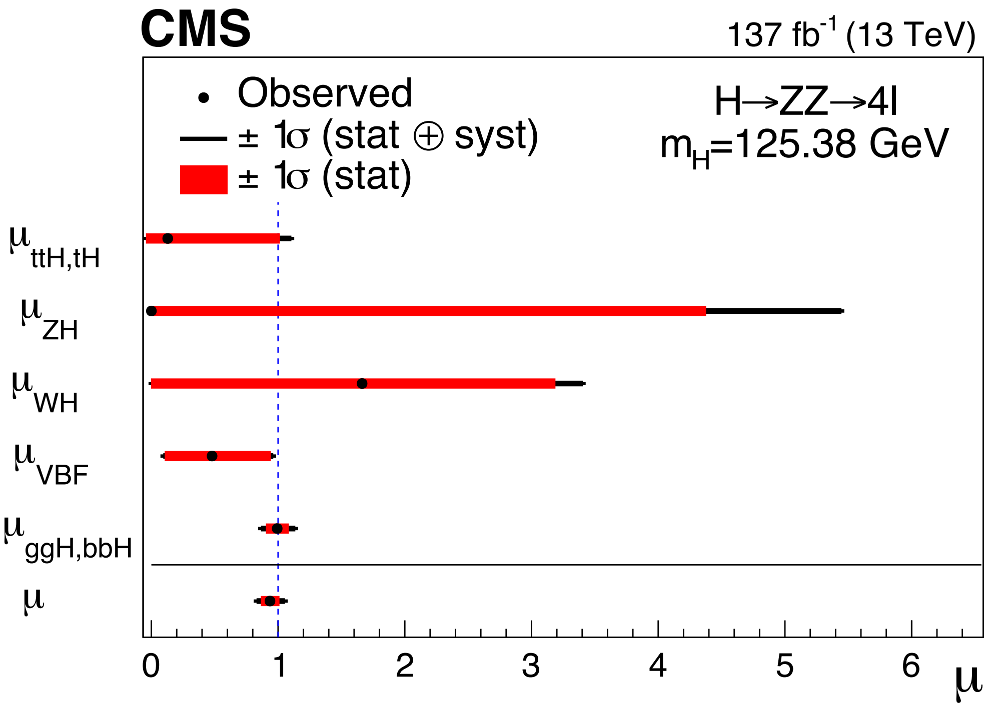

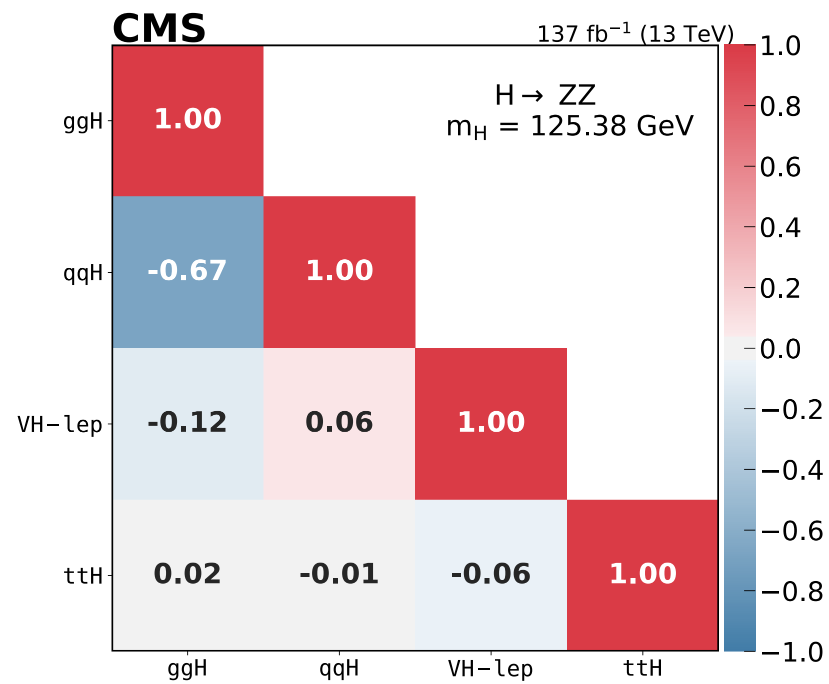

ttH H→ZZ→4l

CMS-HIG-19-001

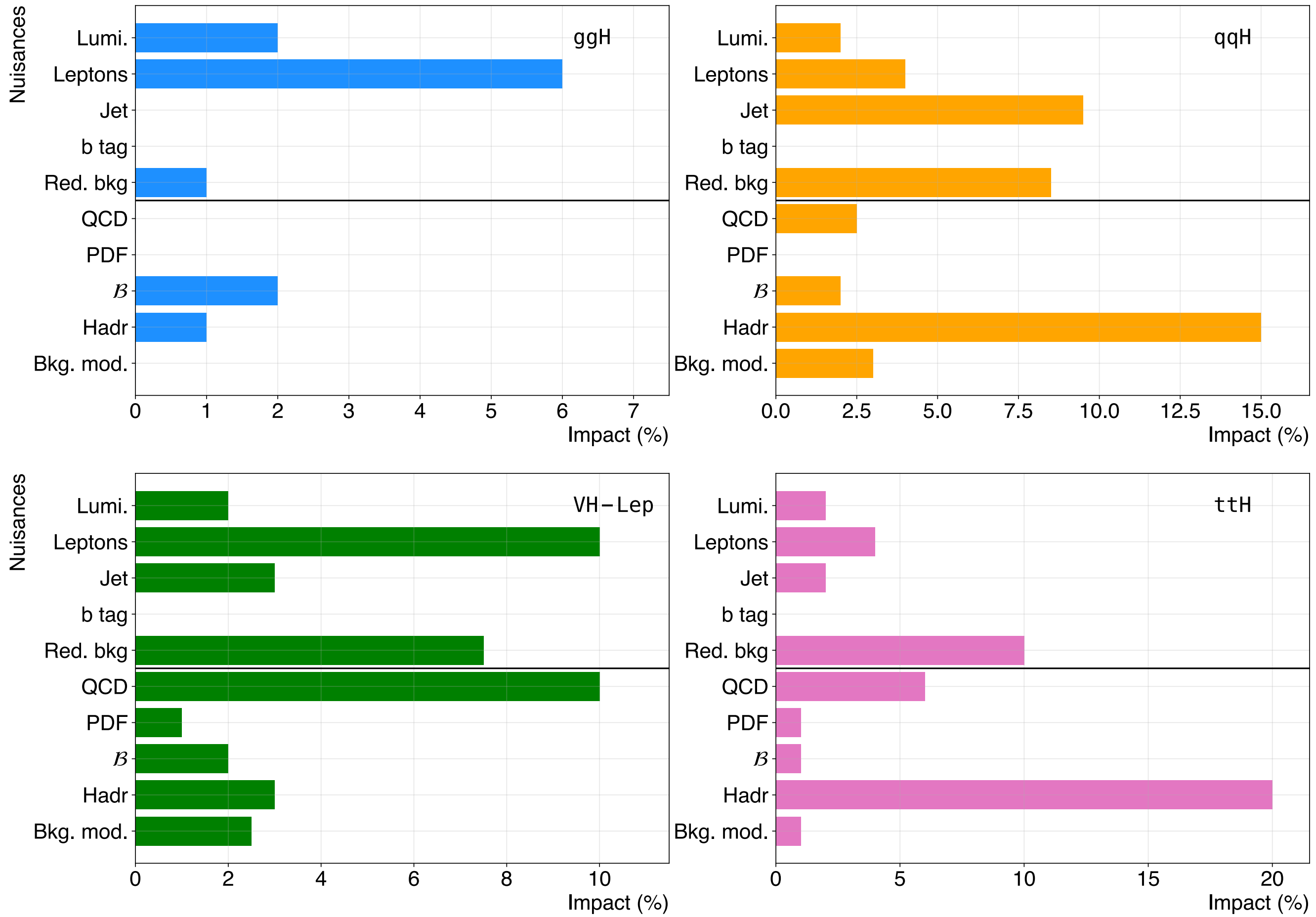

HL-LHC projections

CERN-LPCC-2018-04

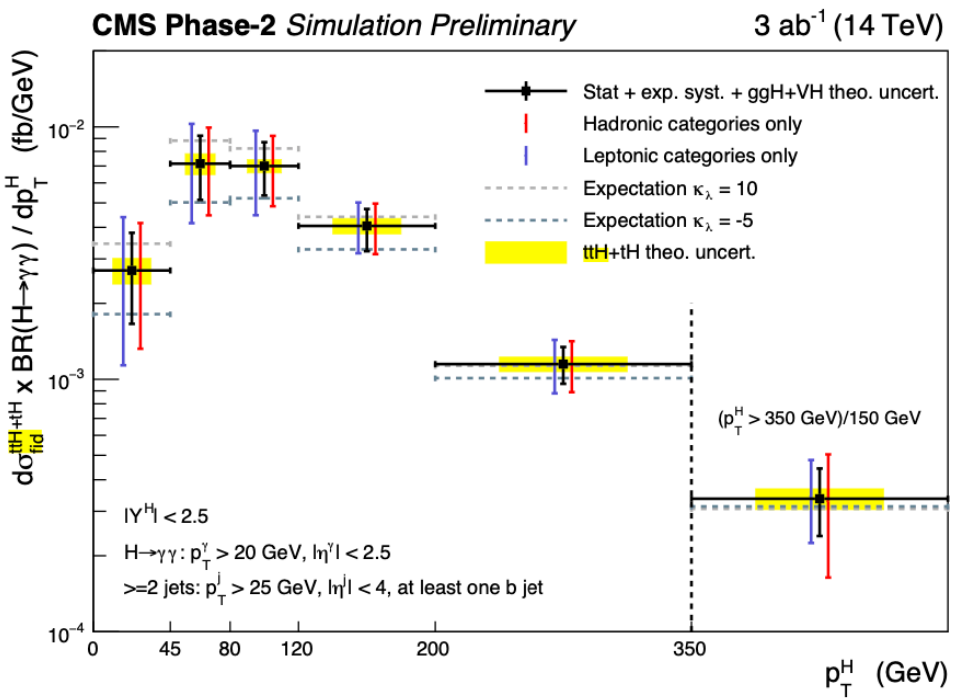

Fig. 18: The expected p_T^H differential tt̄H + tH cross sections times branching ratio, along with their uncertainties [161]. The error bars on the black points include the statistical uncertainty, the experimental systematic uncertainties and the theoretical uncertainties related to the ggH and VH contamination, which is subtracted in the fit. The cross section for $p_T{}^H > 350$ GeV is scaled by the width of the previous bin. The expected tt̄H + tH cross sections for anomalous values of the Higgs boson self-coupling ($\kappa_\lambda = 10$ and κ_λ = -5) are shown by the horizontal dashed lines.

HL-LHC projections

CERN-LPCC-2018-04

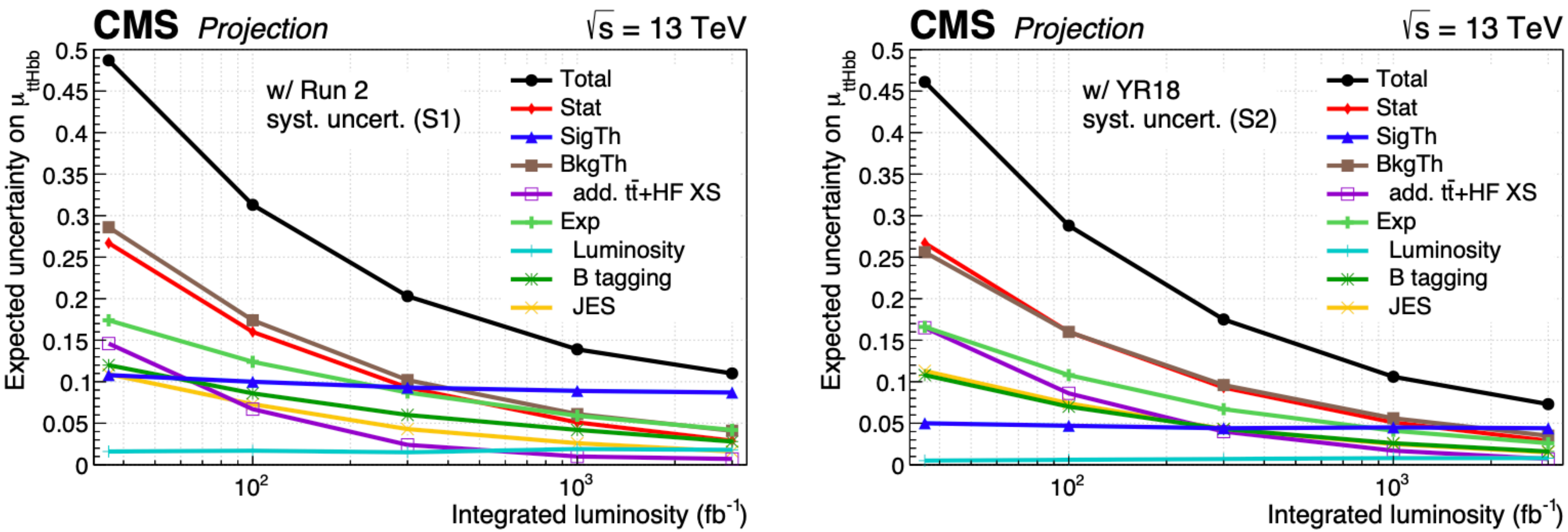

Fig. 19: Expected uncertainties on the $t\bar{t}H$ signal strength in the $H \to b\bar{b}$ channel as a function of the integrated luminosity under the S1 (left) and S2 (right) scenarios at CMS. Shown are the total uncertainty (black) and contributions of different groups of uncertainties. Results with $35.9\,\mathrm{fb}^{-1}$ are intended for comparison with the projections to higher luminosities and differ in parts from [166] for consistency with the projected results: uncertainties due to the limited number of MC events have been omitted and the assumptions in S1/S2 on the theory uncertainties are applied.

HL-LHC projections

CERN-LPCC-2018-04

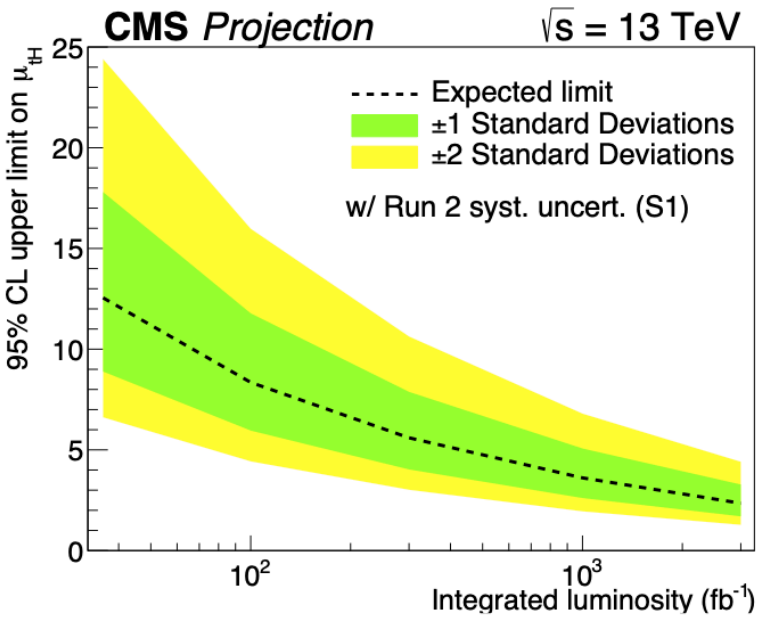

Fig. 22: The variation of expected upper limit on μ_{tH} with integrated luminosity for two projection scenarios S1 (with Run 2 systematic uncertainties [171]) and S2 (with YR18 systematic uncertainties).